



Published in final edited form as:

Prog Retin Eye Res. 2019 July ; 71: 26–56. doi:10.1016/j.preteyeres.2018.12.004.

Insights into Photoreceptor Ciliogenesis Revealed by Animal Models

Wolfgang Baehr^{*}, Christin Hanke-Gogokhia[#], Ali Sharif, Michelle Reed, Tiffanie Dahl, Jeanne M. Frederick, Guoxin Ying

Department of Ophthalmology and Visual Sciences, University of Utah Health Sciences, Salt Lake City, Utah 84132

Abstract

Photoreceptors are polarized neurons, with very specific subcellular compartmentalization and unique requirements for protein expression and trafficking. Each photoreceptor contains an outer segment, the site of photon capture that initiates vision, an inner segment that houses the biosynthetic machinery and a synaptic terminal for signal transmission to downstream neurons. Outer segments and inner segments are connected by a connecting cilium (CC), the equivalent of a transition zone (TZ) of primary cilia. The connecting cilium is part of the basal body/axoneme backbone that stabilizes the outer segment. This report will update the reader on late developments in photoreceptor ciliogenesis and transition zone formation, specifically in mouse photoreceptors, focusing on early events in photoreceptor ciliogenesis. The connecting cilium, an elongated and narrow structure through which all outer segment proteins and membrane components must traffic, functions as a gate that controls access to the outer segment. Here we will review genes and their protein products essential for basal body maturation and for CC/TZ genesis, sorted by phenotype. Emphasis is given to naturally occurring mouse mutants and gene knockouts that interfere with CC/TZ formation and ciliogenesis.

Keywords

Centrosome; mother and daughter centrioles; distal and subdistal appendages; transition zone; pericentriolar matrix; microtubules and microtubule organization center; photoreceptors; knockout mouse models

1. Introduction

A cilium serves as a cellular ‘antenna’ to sample a broad range of extracellular signals in olfaction, vision, taste and mechanosensation (Satir and Christensen, 2007; Scholey, 2013; Singla and Reiter, 2006). Primary cilia are transductive, axoneme-stabilized protrusions that elongate from the basal body of most vertebrate cell types. Primary cilia of kidney epithelia are mechanosensitive, detecting fluid flow through the tubule (Praetorius and Spring, 2003). Cilia of olfactory epithelia distinguish a large number of odorants (Kaupp, 2010), and

^{*}Corresponding author: Wolfgang Baehr, University of Utah, 65 Mario Capecchi Dr., Salt Lake City UT 84132. wbaehr@hsc.utah.edu. Phone 801-585-6643.

[#]Current address: Dyson Vision Research Institute, Weill Cornell Medical College, 1300 York Avenue, New York, NY 10065, USA

photoreceptors are able to detect light of different wavelengths and initiate vision, with single photon sensitivity (Baylor et al., 1979).

The light-sensitive rod and cone photoreceptor outer segments are regarded as modified primary cilia (Sorokin, 1968; Satir et al., 2010; Goetz and Anderson, 2010) containing massive amounts of the light sensors, rhodopsin and cone pigments, distributed over hundreds of disc membranes. Exquisitely polarized, each photoreceptor consists of an outer segment (OS), an inner segment (IS), a cell body containing the nucleus and a synaptic terminal (Fig. 1A). Inner and outer segments are connected by a narrow filament, classically termed connecting cilium (CC), approximately equivalent to the transition zone (TZ) of primary cilia (Roehlich, 1975). Rod and cone outer segments are supported by a microtubule-based axoneme backbone in which the axoneme emanates from the basal body/transition zone complex (Fig. 1B). In mouse, the axoneme consists proximally of doublet and distally mostly of singlet microtubules that extend far into the outer segment. The CC is located at the axoneme base, distal to the basal body, stabilized by doublet microtubules. The basal body is a barrel-shaped structure composed of microtubule triplets and decorated with distal and subdistal appendages. Major differences of photoreceptor sensory cilia compared to primary cilia are the very large outer segment packed with disc membranes (Fig. 1C), an extended TZ to support the outer segment, its function as a light sensor, with phagocytic renewal of the entire structure in mouse every ten days. Several comprehensive reviews on photoreceptor outer segment architecture, structural organization, disc morphogenesis and protein trafficking have been published within the last ten years (Wensel et al., 2016; Goldberg et al., 2016; Hoon et al., 2014; Pearring et al., 2013; Sung and Chuang, 2010; Nickell et al., 2007; Molday and Moritz, 2015; May-Simera et al., 2017) and the reader is invited to consult these excellent reviews for details.

This report addresses early events in photoreceptor ciliogenesis, specifically, docking of basal bodies to the inner segment cell membrane and axoneme/CC genesis. The CC is an essential structure serving as a gate that controls access to the OS. We will provide a short introduction on centrosome genesis, basal body architecture, its role as a microtubule organizing center (MTOC), and discuss details of axoneme/CC formation. Further, we will review genes and their protein products involved in formation of the centrosome, basal body and CC. The gene collection is necessarily incomplete, as the numerous genes associated with the photosensory cilium and basal body axoneme backbone have been discovered in recent years. Emphasis is given to naturally occurring mouse mutants and gene knockouts that interfere with axoneme/CC genesis and early outer segment formation, thereby providing clues as to function.

2. Mother centriole, ciliogenesis and ciliopathies.

2.1 The centrosome.

Much of our current knowledge regarding centrosomes, the basal body and ciliogenesis derives from observations of ciliated cells *in-vitro*, e.g., immortalized retinal pigment epithelial (hTert-RPE cells), Inner Medullar Collecting Duct (IMCD3) or HEK293 cells. Many interacting proteins of the centrosome-primary cilium interface have been identified by affinity proteomics coupled with mass spectroscopy analysis (Boldt et al., 2016), by

proximity-dependent biotinylation (Gupta et al., 2015) or by siRNA-based knockdown screens (Wheway et al., 2015). Primary cilia developed by these cells are small and serve very different purposes. By contrast, each mouse photoreceptor has an extended TZ, i.e., a connecting cilium that can be partitioned into proximal and distal regions (Dharmat et al., 2018). The CC stabilizes a very large primary cilium, the outer segment, dedicated entirely to light reception with generation and amplification (phototransduction) of an electrical impulse to be sent to its second-order neurons (Fu and Yau, 2007). The very different content of the photosensitive cilium predicts the requirement of modified protein sets for intraflagellar transport (IFT) and maintenance, while the basic principles of docking, axoneme extension and CC formation have been conserved.

The life of a basal body starts with centrosome formation during the cell cycle of a proliferating cell. The centrosome consists of mother and daughter centrioles; both are highly conserved, microtubule-based, barrel-shaped structures. The mother centriole is also called the microtubule organization center (MTOC) (Satir et al., 2008). The centrosome is not membrane-associated, its structure and assembly relies entirely on interactions of several hundred proteins. The mother centriole is surrounded by the pericentriolar matrix (PCM), thought to be an amorphous structure, but superresolution microscopy discovered distinct radial layers (Nigg and Holland, 2018) where PCM proteins surround the MC wall, and proteins involved in microtubule nucleation are in the outer layers (Luders, 2012). At the PCM periphery exist structures, called centriolar satellites, consisting of multiple proteins thought to be important in centrosome maintenance and ciliogenesis (Tollenaere et al., 2015; Hori and Toda, 2017; Kubo et al., 1999). At least five major PCM components (rootletin; PCM1; CEP215; MACF1; centriolin; pericentrin) have been identified, all of which contain multiple coiled-coil domains for protein interaction. Rootletin, the main component of the striated rootlet (Yang et al., 2006; Yang et al., 2002), is responsible for centrosome cohesion together with the centriolar proteins, CEP215 and CEP68 (Graser et al., 2007b). CEP215 and pericentrin are main components of the PCM and participate in microtubule nucleation and anchoring. MACF1, a member of the spectraplakins gene family, is a gigantic protein interacting with pericentrin (May-Simera et al., 2016) (see below).

Formation and maturation of both mother and daughter centrioles follow a templated pathway in which an “old” centriole serves as template for formation of a new one (Avidor-Reiss and Gopalakrishnan, 2013; Werner et al., 2017). Asymmetric inheritance of the centrosome determines if a daughter centriole stays in stem cell status (Wang et al., 2009b) and directs earlier primary ciliogenesis after cell division due to its association with remaining ciliary membrane endocytosed before entering mitosis (Paridaen et al., 2013). During S-phase, a cartwheel with nine-fold symmetry is generated from both the mother (old mother) and daughter (new mother) centriole that elongates to form a barrel in which the nine triplet MTs form the wall (procentriole assembly). In G2 and S-phases, the procentriole elongates and the new mother centriole separates from the “old” mother and acquires distal and subdistal appendages. The two centrosomes then recruit pericentriolar matrix components and undergo mitosis. Several key proteins are involved in centrosome biogenesis (Nigg and Holland, 2018; Banterle and Gonczy, 2017). A module consisting mainly of three proteins (polo like kinase 4 or PLK4, a centriolar assembly protein encoded by the STIL gene, and a spindle assembly-related protein encoded by the SAS6 gene)

appears to be the core component initiating procentriole assembly (Arquint and Nigg, 2016). Self-association of nine dimers of SAS6 provides the scaffold of the nine-fold symmetry of the cartwheel. SAS6, together with CEP135, CENPJ and γ -tubulin, form the seed of centriole growth. Microtubules nucleate from the seed followed by centriole elongation and maturation, which involves key proteins such as CP110 and CEP97 located at centriolar distal ends (Fig. 2). For more detail on centrosome genesis and maturation the reader is referred to several excellent reviews (Avidor-Reiss and Gopalakrishnan, 2013; Bettencourt-Dias et al., 2011; Bettencourt-Dias and Carvalho-Santos, 2008; Barker et al., 2014; Hoyer-Fender, 2010; Werner et al., 2017).

2.2 Basal Body.

When a cell exits the cell cycle and becomes quiescent, its mother centriole docks to the cell membrane to initiate TZ and primary cilium formation (Fig. 3). The basal body remains associated with the daughter centriole through filamentous bundles (Garcia, III and Reiter, 2016). Only the mother centriole contains distal and subdistal appendages and is capable of ciliogenesis in G1/G0 phase. Distal appendages contain multiple polypeptides, at least five of which have been identified (CEP89; CEP164; CEP83; ODF2 and SCLT1) (Tanos et al., 2013; Yang et al., 2018). These proteins contain multiple coiled-coil domains. In fact, CEP89 consists entirely of coiled-coil domains. Proteins identified to be present in subdistal appendages are CEP170 (FAM68a), NIN (ninein) and TUBE1 (ϵ -tubulin) (see below). Ultrastructural cross-sectional analysis reveals a symmetrical array of nine microtubules in a triplet arrangement (abbreviated as 9(3)+0 where 0 indicates the lack of a central microtubule filament) of A, B, and C tubules with A the most internal. C tubules are specific for the basal body, whereas A and B tubules extend into the TZ; barrel dimensions are ~400 nm in length and 200 nm wide (Li et al., 2012).

2.3 Transition zone.

The photoreceptor CC is an elongated tube of ~1.5 μ m length (0.25 μ m in primary cilia) (Gilliam et al., 2012; Wensel et al., 2016; May-Simera et al., 2017) through which all outer segment proteins and membrane components must traffic either by diffusion of soluble protein complexes (Peet et al., 2004; Slepak and Hurley, 2008), by IFT with molecular motors (Pooranachandran and Malicki, 2016; Sedmak and Wolfrum, 2011; Luby-Phelps et al., 2008; Rosenbaum and Witman, 2002), or directly by diffusion of integral membrane proteins in the periciliary plasma membrane (Nachury et al., 2010; Nachury et al., 2007). Nine-fold symmetry of the axoneme doublet structure is generated by extension of the basal body A- and B-tubules (Fig. 3) (Garcia, III and Reiter, 2016). In photoreceptors, the distal axoneme is made of MT singlets, the precise extension of which in mouse rods is unknown. In *Xenopus laevis*, the axoneme extends from the basal body into the OS to about half-length in the rod and to the cone tip (Eckmiller and Toman, 1998). The CC architecture at the base of the axoneme is characterized by Y-links connecting the MT doublet with the ciliary membrane, forming a gate and diffusion barrier. Many transition proteins have been identified, mostly belonging to two complexes, the nephrocystin (NPHP) and Meckel (MKS) complexes. The NPHP complex consists of >20 proteins, including NPHP1, NPHP3, NPHP4, IQCB1/NPHP5, CEP290/NPHP6 and RPGRIP1L (Shi et al., 2017; Sang et al., 2011; Williams et al., 2011). The MKS complex includes B9 domain proteins, Tectonics,

CC2D2A, AHI1, and several TMEM proteins localizing to the transition zone (Williams et al., 2011; Li et al., 2016a; Goncalves and Pelletier, 2017). Most of these proteins form large, interconnected complexes (Boldt et al., 2016). Interestingly, three CC proteins (SPATA7, RPGR, RPGRIP1) appear to be photoreceptor-specific and cause nonsyndromic ciliopathy when mutated. These proteins distribute to other primary cilia (Dharmat et al., 2018). Details of domain structure and possible function of these proteins in mouse photoreceptors are discussed below.

2.4 Syndromic ciliopathies

Mutations in genes encoding PCM, distal/subdistal appendages or basal body-associated proteins cause complex syndromic ciliopathies, often associated with rod/cone dystrophies such as *retinitis pigmentosa* (RP) or Leber congenital amaurosis (LCA). Syndromic ciliopathies affect multiple organs including kidney, liver, retina, brain or spermatozoa (Mockel et al., 2011). The most prominent syndromic ciliopathies affecting the retina are Joubert Syndrome (JS) (Juric-Sekhar et al., 2012), Bardet-Biedl syndrome (BBS) (Blacque and Leroux, 2006) and Senior Løken syndrome (SLS) (Ronquillo et al., 2012; Helou et al., 2007). JS is characterized by brain malfunction with molar tooth sign, kidney and liver disease, skeletal abnormalities, and including eye abnormalities. Major features of Bardet-Biedl syndrome are obesity, polydactyly, hypogonadism, renal failure and retinal degeneration (Forsythe and Beales, 2013). SLS is an autosomal recessive retina-renal ciliopathy characterized by progressive RP (Hartong et al., 2006) or LCA (den Hollander et al., 2008) with nephronophthisis (NPHP) (Otto et al., 2005; Wolf and Hildebrandt, 2011).

2.5 Photoreceptor ciliogenesis.

Most details concerning ciliogenesis in mouse photoreceptors have been derived from high resolution TEM imaging and confocal immunohistochemistry, but molecular details are far from understood. Ciliogenesis begins during pre- and postnatal photoreceptor development. Cone precursors are born during embryonic development with peak at E15 (Morrow et al., 1998; Swaroop et al., 2010), while rod progenitors are born postnatally with peak at birth. Postnatal precursors become rod photoreceptors due to the expression of NRL, a rod-specific transcription factor (Mears et al., 2001). Docking of the basal body to the cell cortex, with generation and extension of the rod axoneme, occurs in several unsynchronized postnatal steps (Sedmak and Wolfrum, 2011), as outlined in Fig. 4. Soon after birth, the distal end of the MC acquires a Golgi-derived ciliary vesicle that mediates docking to the cell membrane (Sorokin, 1962). Docking of the ciliary vesicle to the mother centriole is dependent on C2CD3, a distal appendage protein (Ye et al., 2014), and MACF1 (May-Simera et al. 2016). According to cell culture experiments, docking of the vesicle requires degradation of CP110 and CEP97, centrosomal proteins that act as negative regulators of ciliogenesis bound to the distal MC end (Spektor et al., 2007) (Fig. 2) (see par. 4.1, CP110). This *in-vitro* result however conflicts with *in-vivo* experiments which show that CP110 promotes cilia formation, acting as a positive regulator of ciliogenesis, and is required for anchoring of basal bodies to the membrane (Yadav et al., 2016), suggesting significant differences between primary cilia and photoreceptors.

The distal MC is decorated with appendages that enable membrane anchoring (Yang et al., 2018). Germline knockouts of distal appendage proteins (CEP164, C2CD3) in which basal bodies were unable to dock to cell membranes, generated syndromic ciliopathies (Siller et al., 2017; Ye et al., 2014). Further experiments are needed to verify effects of conditional DAP knockouts (CEP83, CEP89) in photoreceptors. After basal body docking to the cell membrane, A and B tubules emanate from the basal body forming the proximal axoneme which matures into the CC. Anterograde IFT of tubulin subunits by kinesin-2 extends the axoneme further (Scholey, 2013). Based on gene knockouts in mouse, a number of proteins have been identified that are essential for elongation of A and B tubules, including KIF3a, the obligatory subunit of kinesin-2 (Jiang et al., 2015b), IQCB1/NPHP5 (Ronquillo et al., 2016), ARL3-GTP (Hanke-Gogokhia et al., 2016) and ARL13b (Hanke-Gogokhia et al., 2017) (see par. 4.2). Deletion of genes encoding any of these proteins does not prevent basal body docking, but does prevent formation of an axoneme. Around P9, the first stacks of discs are assembled by evagination of the ciliary membrane (disc morphogenesis) (Ding et al., 2015; Burgoyne et al., 2015). By P21, the outer segment structure is mature.

3. Centriole and PCM components

Proteomic analysis indicates that the centrosome consists of >100 distinct proteins, most of which have unknown function (Jakobsen et al., 2011; Andersen et al., 2003). These highly interacting proteins can be subdivided into pericentriolar matrix, centrosomal, distal and subdistal appendage and CC/TZ resident proteins (Fig. 5). The corresponding genes have outstanding importance for human disease (centrosome abnormalities, cancer, syndromic ciliopathies, including retina dystrophies) (Nigg and Holland, 2018; Mockel et al., 2011). Animal models mimicking human disease based on mutations in ciliary genes (Norris and Grimes, 2012) are invaluable tools to devise strategies for gene replacement and pharmacological therapy. Below, we summarize selected proteins associated with the PCM, distal and subdistal appendages and centrioles, highlighting human retina disease when known.

3.1 Centrin (caltractins)

Centrins are small, acidic proteins that belong to the Ca²⁺ binding EF-hand protein family (50% identity with calmodulin). Also known as eukaryotic signature proteins, they are found in all eukaryotic cells from unicellular organisms (Zhang and He, 2011; Hartman and Fedorov, 2002) to mammals (Wolfrum et al., 2002). Centrins were initially identified in unicellular green algae (such as *C. reinhardtii*) as major components of several basal body-associated contractile fibers (nuclear-BB connector and distal striated fibers), and later found commonly associated with centrosomes of higher organisms and in spindle pole bodies (centrosome analog) of yeast (Salisbury, 1995; Geimer and Melkonian, 2005). Centrins are thought to play conserved roles in basal body duplication and positioning in lower eukaryotes but their function in vertebrates is largely unknown. Recessive mutations of centrin 2 cause syndromic ciliopathy in mouse (see below), but mutations causing human disease have not been identified.

Mice express four isoforms, CETN1–4, while the human genome contains only three isoform genes (CETN1–3) (Friedberg, 2006). All four mouse isoforms are expressed in the photoreceptor connecting cilium and basal body (Wolfrum and Salisbury, 1998; Trojan et al., 2008; Giessl et al., 2004). CETN1 was originally cloned from a human testis expression library (Errabolu et al., 1994) and shown to be expressed in mouse testes from the second week postnatally (Hart et al., 1999). CETN2 and CETN3 are expressed in all somatic cells and are associated with the centrosome and pericentriolar matrix (Giessl et al., 2004; Laoukili et al., 2000; Salisbury et al., 2002; Gavet et al., 2003). All centrioles feature four EF-hand high-affinity Ca²⁺ binding motifs (Trojan et al., 2008; Giessl et al., 2006; Dantas et al., 2012).

CETN1 (Centrin 1)—Centrin 1 is expressed strongly in male germ cells, in addition to other ciliated cells. Crystallography of murine CETN1 reveals a dimeric structure in which EF-hands 1/2 at the N-terminal and EF-hands 3/4 at the C-terminal are connected by a large α -helical structure, and all four EF-hand loops are occupied by Ca²⁺ (Kim et al., 2017) (Fig. 6A). In linear view, the four EF-hands are evenly distributed (Fig. 6B). In mouse, CETN1 expression is restricted to the centrioles of ciliated cells, e.g., centrioles associated with the photoreceptor connecting cilium, and is strongly expressed in sperm (Trojan et al., 2008) (Fig. 6C). The *Cetn1* gene consists of a coding exon 1 and a noncoding exon 2. Although exon 1 deletion of murine *Cetn1* produced a germline knockout (Fig. 6C and D, right panels), the deletion had no consequence on photoreceptor ciliogenesis or function, and failed to affect trafficking of OS membrane proteins (Avasthi et al., 2013). However, CETN1 deletion produced non-syndromic male infertility (the *Cetn1* gene is located on the X chromosome). *Cetn1*^{Y/-} spermatids lacked tails suggesting severe spermatogenesis defects at the late maturation phase of spermatozoa; the *Cetn1*^{Y/-} mouse revealed no other recognizable phenotype (Avasthi et al., 2013). Male infertility has been observed in other cilia-related genes that display flagellar abnormalities (Escalier, 2006).

CETN2 (Centrin 2)—Centrin 2 is expressed in ciliated cells, including retina neurons, and present at both the photoreceptor CC and centrioles (Trojan et al., 2008). CETN2 binds to the centrosomal protein SFI1 (SFI1 centrin-binding protein), a large protein participating in cell cycle progression and assembly of the mitotic spindle (Martinez-Sanz et al., 2006). Transgenically expressed EGFP-CETN2 fusion protein specifically labels both mother and daughter centrioles and CC, thus providing an excellent marker (Fig. 7) (Higginbotham et al., 2004). A germline CETN2 knockout (KO) mouse revealed syndromic ciliopathy, including dysosmia and hydrocephalus. Dysosmia resulted from olfactory cilia loss, impaired ciliary trafficking of olfactory signaling proteins, adenylate cyclase III (ACIII) and cyclic nucleotide-gated channel (CNGA2), as well as disrupted basal body apical migration in postnatal olfactory sensory neurons (OSNs). Hydrocephalus occurs due to impaired CSF flow which, in turn, results from the disrupted planar polarity of mutant ependymal cilia; transgenic expression of GFP-CETN2 rescued the *Cetn2*-deficiency phenotype (Ying et al., 2014). Only about 30% of mutants develop hydrocephalus and die within 1.5 months. However, photoreceptor ciliogenesis and function were unaffected, a phenotype that may be explained by centrin redundancy. Germline *Cetn2*^{-/-} pups were born healthy and of normal size, suggesting that CETN2 is nonessential for mouse centrosome duplication or mitotic

cell division during embryonic stages. Formations of both primary cilia (renal tubule epithelia, photoreceptors) and motile cilia (multiciliated respiratory and ependymal epithelia) occurred normally in the *Cetn2* mutants.

Our *in-vivo* result contradicts an *in-vitro* study using hTERT-RPE1 cells in a serum starvation-induced ciliogenesis assay (cell proliferation is unaffected) which showed that CRISPR/CAS9 disruption of *Cetn2* leads to dramatically reduced ciliogenesis due to impaired removal of CP110, the ciliation inhibitor located at the basal body distal end cap (Prosser and Morrison, 2015). The discrepancy between *in-vivo* and *in-vitro* data may reflect the importance of cell-cell, cell-environment interaction in ciliogenesis regulation. In view of CETN2's ubiquitous expression among adult tissues (Hart et al., 2001), it is unexpected that germline deletion of mouse CETN2 affects predominantly cilia of olfactory and ependymal epithelia. *Cetn2* mutants share significant phenotypic similarity with a mouse pericentrin (*Pctn*, a core PCM component) hypomorphic mutant (*Pctn^{ocd/ocd}*) displaying OE-specific olfactory ciliary loss.

CETN3 (Centrin 3)—CETN3 is an abundant homologue of yeast CDC31 which plays a role in centrosome duplication and separation in yeast (Middendorp et al., 2000). By RPKM (Reads Per Kilobase of transcript per Million mapped reads), CETN3 and CETN4 are most strongly expressed in mouse testes. Although CETN3 localizes to the photoreceptor CC, BB and DC, single knockout of mouse Centrin3 does not produce a detectable phenotype in retina or other tissues (GY and WB, unpublished). Notably, CETN3 overexpression can inhibit CETN2 incorporation into centrioles during S-phase procentriole assembly in mammalian cells, probably by inhibiting activity of MPS1, a kinase for both CETN2 and 3 (Sawant et al., 2015), and suggesting possible isoform interaction.

CETN4 (Centrin 4)—*Cetn4* mRNA is detected in mouse brain, kidney, lung, and ovary (Gavet et al., 2003). In brain, CETN4 is more closely related to CETN2 and is expressed exclusively in ependymal and choroidal ciliated cells where it localizes to basal bodies (Gavet et al., 2003). In human, *CETN4* is a pseudogene and a functional gene product is not expressed (Zhang et al., 2010). Thus, the functions of centrin 3 and 4 in mouse photoreceptors are unknown (Trojan et al., 2008; Giessl et al., 2006).

Summary centrin: Centrin proteins are found in the centriolar lumen, pericentriolar matrix, transition zone (TZ) of primary cilia and the photoreceptor CC, but are not known to be associated with human retina disease. Single knockouts of mouse CETN1 (male infertility) and CETN2 (dysosmia) produce specific phenotypes without impairing photoreceptor ciliogenesis; even a CETN1/CETN2 double knockout has no photoreceptor phenotype. While a mouse CETN3 single knockout again produces no recognizable phenotype, the CETN2/CETN3 double knockouts display a slowly progressing rod and cone degeneration and more severe olfactory and ependymal cilia defects than *Cetn2^{-/-}* mice (Ying, Frederick and Baehr, unpublished results). The results suggest both CETN2/CETN3 redundancy and isoform interaction in photoreceptors and other tissues. Interestingly, CETN/CETN3 double knockout mice were born in a non-Mendelian ratio, indicating that some *Cetn2^{-Y};Cetn3^{GT/GT}* male embryos fail to survive prenatal development.

3.2 Pericentriolar Matrix components

The Pericentriolar Matrix (PCM) surrounds both centrioles as an amorphous “cloud,” but recent examination by high resolution microscopy reveals the PCM as an ordered structure. Key PCM proteins are CEP135, CP110, CEPP192, CEP152, NEDD1, Cap350, CEP215, γ -tubulin, CPAP (CENPJ) and CEP215. CEPs constitute a large family of >30 centrosomal proteins, named from CEP19 to CEP350 (Kumar et al., 2013) where the numbers indicate approximate kDa. PCM proteins surround centrioles in concentric structures (Sonnen et al., 2012) with the exception of pericentrin, which spans the PCM with its C-terminal near the centrioles and N-terminal extending peripherally. While γ -tubulin forms the γ -tubulin ring complex (γ TuRC) involved in microtubule nucleation (see TUBG1 paragraph), PCM1 is present in centriolar satellites (CS), i.e., electron-dense granules seemingly scattered around centrioles (Barenz et al., 2011). Rootletin, a large striated cytoskeleton-like structure, originates from the basal body and is partially located in the PCM but is not part of the “cloud” (Yang and Li, 2006). Pericentrin, rootletin, PCM1 and Cep215 are briefly summarized below.

PCNT (Pericentrin) (Kendrin)—Pericentrin (isoform a, 2916 amino acids), the homolog of yeast Spc110p, is a protein of unknown function locating to the basal body complex of mouse photoreceptors (Muhlhans and Giessl, 2012; Muhlhans et al., 2011). PCNT is an integral component of the centrosome with numerous coiled-coil motifs (Fig. 8A) and suggested to participate in microtubule nucleation and anchoring during the cell cycle. PCNT interacts with numerous proteins including the γ -tubulin ring complex, cytoplasmic dynein, protein kinase A and PCM1 (Jurczyk et al., 2004) and CEP215 (Graser et al., 2007b). PCNT-RNA interference inhibits cilia formation by serum starvation in RPE cells (Graser et al., 2007a). Knockdown of *Pcnt* in the retina *ex-vivo* and *in-vivo* using a virus-based RNA interference approach impaired development of the photoreceptor connecting cilium and outer segment, and caused a nuclear migration defect (Falk et al., 2018).

Mutations in the human *PCNT* gene have been linked to Down syndrome (DS), primordial dwarfism and syndromic ciliopathies such as Seckel syndrome (Delaval and Doxsey, 2010; Rauch et al., 2008). Germline *Pcnt* knockout phenotype in mouse was associated with spindle misorientation, misdirected ventricular septal growth in the heart, microcephaly and decreased proliferative symmetric divisions in brain neural progenitors (Chen et al., 2014). Ninein, CEP215, and centriolin were undetectable in *Pcnt*^{-/-} mice. A hypomorphic mutant of *Pcnt* exhibited defective assembly of olfactory sensory neurons (Miyoshi et al., 2009). A frameshift mutation in the mouse pericentrin gene caused abnormal interneuron migration to the olfactory bulb (Endoh-Yamagami et al., 2010).

CROCC (ciliary rootlet coiled-coil) (Rootletin)—The photoreceptor ciliary rootlet originates at the basal body and extends to the synaptic terminal. It is composed of rootletin (2009 amino acids, isoform 1), a 220-kD protein with multiple coiled-coil domains identified first in retina (Fig. 8B) (Yang and Li, 2006; Yang et al., 2002). Rootlets are homopolymeric rootletin protofilaments bundled into variably-shaped thick filaments that connect the basal body and daughter centriole and support the slender photoreceptor cell body (Yang et al., 2002). In *Crocc* knockout mutants, ciliated cells are devoid of rootlets, but

photoreceptors develop normally and phototransduction is unaffected. However, photoreceptors degenerate over time (Yang and Li, 2006). The *CROCC* gene is not known thus far to be associated with human disease, and it is unclear whether rootletin participates in intracellular trafficking. The closest relative by sequence is C-Nap1 (CEP250), a centrosomal protein involved in centriolar cohesion. Rootletin interacts with C-Nap1 and this interaction is supported by coimmunoprecipitation from cell lysate and colocalization at the basal body/centrioles (Yang et al., 2006).

Rootletin, C-Nap1 and CEP68 were shown by STED nanoscopy to connect the two centrioles during cellular interphase to form the MTOC (Vlijm et al., 2018). STED microscopy showed that the centrosome linker complex of RPE1 cells consists of repeating rootletin units in a vast network with a C-Nap1 ring at centrioles as organizer and CEP68 as filament modulator. This coupling is important for cell migration, cilia formation and timing of mitotic spindle formation (Vlijm et al., 2018).

PCM1 (Pericentriolar Material 1)—The longest PCM1 transcript in human encodes a protein of molecular mass of ~230 kDa (human 2024 amino acids, mouse 2025). PCM1 has multiple coiled-coil domains in the N-terminal half (Fig. 8C), interacts with numerous proteins and participates in microtubule nucleation. PCM-1 is a component of centriolar satellites, characterized as electron-dense granules scattered around centrosomes (Kubo et al., 1999). PCM1 granules are distinct from pericentrin-containing granules (Kubo and Tsukita, 2003). *Pcm1*^{+/-} mice manifest neuroanatomical phenotypes with behavioral abnormalities and show significant reduction in brain volume (Zoubovsky et al., 2015). Presence of a retina phenotype was not investigated.

CDK5RAP2 (CDK5 Regulatory Subunit Associated Protein 2) (CEP215)—CEP215 (longest transcript in mouse, 1822 amino acids) is expressed widely in many tissues and localizes predominantly at the centrosome during mitosis (Ching et al., 2000). CEP215 and ninein are important for microtubule anchoring in the PCM during centrosome duplication (Chen et al., 2014). Centrosomes are held together by intercentrosomal linkers (see paragraph on rootletin, above) and dissociate during mitosis; dissociation is essential for centriole duplication. CEP215 forms a complex with CEP68 and pericentrin (PCNT) which are intercentrosomal linkers involved in centriole engagement (Pagan et al., 2015). CEP215 holds an N-terminal microtubule-association domain and multiple coiled-coil domains (Graser et al., 2007b) (Fig. 8D). CEP215 regulates mitotic spindle orientation by interacting with Cdk5 activator CDK5R1 (Ching et al., 2000). CEP215 was also found to interact with CEP152 and HSET, the minus end-directed microtubule motor protein (Firat-Karalar et al., 2014). These interactions have been shown to be essential for centrosome localization and cohesion, respectively (Chavali et al., 2016). Knockdown of CEP215 reduced centrosome cohesion and led to centrosome splitting in cultured cells suggesting that CEP215 is essential for centriole interaction and cohesion (Graser et al., 2007b). Autosomal recessive mutations of CEP215 are primarily associated with microcephaly-3, a congenital disorder identified by a substantial reduction in brain size (Sukumaran et al., 2017). A mouse model of mutant CEP215 with an in-frame deletion of exon 4 (Hertwig's anemia (an) mutant)

showed abnormal mitotic spindle orientation, and impaired centrosomal function among neuronal progenitors (Lizarraga et al., 2010).

Summary PCM proteins: The PCM assembles in the vicinity of centrioles during mitosis and expands during centrosome maturation. Providing a platform for nucleating microtubules either directly through subdistal appendages or through the γ TuRC complex, PCM functions in cilia formation/disassembly and as a docking station to distribute protein assemblies through MT transport by molecular motors (Mennella et al., 2014). Progress concerning PCM structure and visualization of PCM proteins was provided by 3D-SIM (structural illumination microscopy) (Mennella et al., 2014; Sonnen et al., 2012). The concentric structure of PCM proteins is reminiscent of the structure of the distal appendage proteins (see below). *Pcnt* germline knockout produced serious consequences associated with spindle misorientation and microcephaly (Chen et al., 2014) and a mouse model of mutant CEP215 showed impaired centrosomal function in neuronal progenitors (Lizarraga et al., 2010). Very little is known about the consequence of germline deletions of PCM proteins in retina. Knockdown of *Pcnt* in the retina *ex-vivo* and *in-vivo* via RNA interference impaired the development of the photoreceptor CC and the outer segment (Falk et al., 2018). By contrast, deletion of rootletin does not affect photoreceptor development and function, but weakens the ciliary base which eventually causes retinal degeneration (Yang et al., 2005).

3.3 Subdistal appendage proteins

Subdistal appendages (SDA) are associated with 2–3 triplet microtubules of the mother centriole, but their numbers can vary (Uzbekov and Alieva, 2018). SDAs assume a conical structure ending in a rounded head and project orthogonally from the basal body (Huang et al., 2017). Identified SDA components are ODF2/cenexin, ninein (NIN), ninein-like protein (NINL), CEP170, CEP128, centriolin (CNTRL), CCDC68, CCDC120, CC2D2A, γ -tubulin and ϵ -tubulin (reviewed in (Uzbekov and Alieva, 2018). CC2D2A is discussed in the paragraph “Gene deletions that prevent basal body docking,” whereas γ - and ϵ -tubulins are detailed in the paragraph entitled, “Microtubules.” CEP170, ninein, ninein-like protein and ODF2 are summarized briefly below.

CEP170 (centriolar protein 170) (FAM68A)—CEP170 protein consists of 1584 amino acids with a few isolated coiled-coil domains and a forkhead-associated domain (Fig. 8E), and localizes to the subdistal appendages of mature mother centrioles. During mitosis, CEP170 associates with spindle microtubules near the centrosomes. CEP170 interacts with ninein, binds microtubules at the MC subdistal appendages, is phosphorylated by polo-like kinase 1, and functions in maintaining microtubule organization and cell morphology (Guarguaglini et al., 2005).

CNTRL (Centriolin) (CEP110, FAN, CEP1)—Centriolin (2333 amino acids in mouse) is a centrosome-associated protein required for centrosome maturation. Centriolin consists nearly entirely of coiled-coil domains (Fig. 8F); it has several leucine-, glutamine- and proline-rich regions and interacts with pericentrin. Centriolin functions in mitotic cell cycle

progression (Sun et al., 2017). Depletion of centriolin by siRNA silencing leads to G₁/G₀ arrest and cytokinesis errors (Gromley et al., 2003).

NIN (Ninein) (SCKL7)—Ninein is a centrosome-specific protein consisting of two splice variants. Isoform A (2113 amino acids) has coiled-coil domains, an EF-hand, a GTP-binding site, 4 leucine-zipper domains (Fig. 8G) and localizes to the PCM (Bouckson-Castaing et al., 1996). Ninein associates with MC subdistal appendages and colocalizes with γ -tubulin (Wang et al., 2009b). Ninein is important for positioning and anchoring the microtubules minus-ends to the basal body. Localization of this protein to the basal body requires three leucine-zipper motifs in the central coiled-coil domain. Morpholino knockdown of ninein in zebrafish caused defects in the anterior neuroectoderm (Dauber et al., 2012). Compound heterozygosity for missense mutations in the NIN gene is associated with Seckel syndrome 7 (SCKL7) (Dauber et al., 2012).

NINL (Ninein-like protein) (NLP)—NINL (1394 amino acids), a Ca²⁺-binding protein with two EF-hands (Fig. 8H), is an oncogenic protein with two large CC domains. There are multiple isoforms. Isoform B is part of the Usher complex and colocalizes with USH2A and lebercilin (van Wijk E. et al., 2009). NINL colocalizes with CC2D2A at the ciliary base and *ninl* knockdown in zebrafish leads to photoreceptor outer segment loss, similar to *Cc2d2a*^{-/-} phenotypes (Bachmann-Gagescu et al., 2015). The primary function of NINL is to promote MT nucleation that contributes to centrosome maturation. Transgenic mice overexpressing NINL display spontaneous tumors (Li and Zhan, 2011). DZANK1 (Double Zink Ribbon and Ankyrin Repeat domain protein 1) and NINL interact to provide proper assembly of the cytoplasmic dynein 1 complex. Because knockdown of NINL and DZANK1 leads to vesicle accumulation in zebrafish photoreceptors, NINL and DZANK1 are thought to be required for inner segment vesicle transport (Dona et al., 2015). NLP was shown to interact with the γ -tubulin ring complex and to stimulate microtubule nucleation (Casenghi et al., 2003).

ODF2 (outer dense fiber of sperm tails 2) (cenexin)—ODF2 (longest variant, 825 amino acids) consists of multiple coiled-coil domains (Fig. 8I) and is the major protein of the sperm tail cytoskeleton (Schweizer and Hoyer-Fender, 2009). The mouse *Odf2* gene produces multiple splice variants, isoform 9 is called cenexin (Chang et al., 2013). Cenexin localizes to basal bodies of cultured mammalian cells, while ODF2 localizes along the axoneme of primary cilia. Cenexin, but not ODF2, was essential for inducing primary cilia in cell culture (Chang et al., 2013). ODF2 is located in MC subdistal appendages of somatic cells. In ODF2-deficient cells, basal bodies form neither distal appendages nor primary cilia (Ishikawa et al., 2005). The *Odf2* knockout mouse (gene trap inserted in exon 9 of the *Odf2* gene) display embryonic lethality establishing that ODF2 is required for normal embryonic development (Salmon 2006). In another line (deletion of exons 6 and 7), ciliogenesis occurs but the basal foot is missing from the basal body in multiciliated epithelial cells (and embryonic fibroblast cells), causing uncoordinated ciliary beating and primary cilium dyskinesia (Kunimoto et al., 2012). ODF2 protein localizes to photoreceptor primary cilia, and to basal bodies of ciliated cells of respiratory and kidney epithelia (Schweizer and Hoyer-Fender, 2009).

Summary of SDA proteins (SDAPs): Together with PCM components, SDAPs are essential for MT nucleation of the mother centriole. SDAs essentially form miniature centers for MT nucleation, but their role in ciliary function is unclear (Monnich et al., 2018). However, SDAPs are involved in regulation of vesicular trafficking arriving from the TGN, a function consolidated in several animal models. Knockdown of NINL and its interactant DZANK1 leads to vesicle accumulation in zebrafish photoreceptors suggesting that NINL and DZANK1 may be required for inner segment vesicular transport of membrane proteins (Dona et al., 2015). The recently identified SDA protein CEP128 regulates vesicular trafficking and targeting of Rab11 to the primary cilium (Monnich et al., 2018). In a *cc2d2a* zebrafish mutant (*sentinel* carrying W628X), mutant rods and cones formed cilia but outer segments were shortened and rhodopsin and cone pigments mislocalized. Rab8-coated vesicles accumulated at the apical inner segments suggesting CC2D2A is important for membrane protein trafficking in zebrafish (Bachmann-Gagescu et al., 2012; Mougou-Zerelli et al., 2009). Ojeda Naharros, et al., showed recently that CC2D2A plays a role in the docking of opsin-laden vesicles at the periciliary membrane (Ojeda Naharros et al., 2017). By contrast, the *Cc2d2a*^{-/-} mouse recapitulates features of Meckel syndrome with multiorgan defects (Veleri et al., 2014). Loss of CC2D2A leads to embryonic lethality; embryos did not survive past E18, often showing polydactyly, exencephaly (brain outside of skull) and *situs inversus*. Cilia are absent in *Cc2d2a*^{-/-} embryonic node and other somatic tissues.

3.4 Distal appendage proteins

Distal appendages, required for basal body docking and ciliogenesis, are described as nine-bladed pinwheel-like structures protruding from the distal end of the BB (Tanos et al., 2013). Quantitative centrosome proteomics (Tanos et al., 2013) identified five DAP components: CEP164, CEP89, CEP83, SCLT1 and FBF1 containing multiple coiled-coil domains. An additional DAP-associated protein is C2CD3 which occupies a compact region in the centriole lumen. Proteins recruited to DAPs are TTBK2 (Tau tubulin kinase 2), recycling endosome components (Rab8, Rab11), chibby (CBY1), CEP162, CP110 and CEP290 (Yang et al., 2018). In a beautiful study using direct stochastic optical reconstruction microscopy (dSTORM), DAPs were shown to form a cone-shaped architecture within a 3-dimensional megacomplex large enough to function as a gate for TM proteins (Yang et al., 2018). Core proteins of the distal appendage blades (DABs) are CEP164, SCLT1, CEP89 and CEP83, with CEP164 the outermost and CEP83 the innermost component. FBF1 locates to a space called distal appendage matrix (DAM) between DAP blades (Yang et al., 2018).

CEP164 (centrosomal protein 164) (NPHP15)—CEP164 is a centrosomal protein (1333 amino acids in mouse) with multiple coiled-coil domains involved in microtubule organization and centrosome segregation (Fig. 9A). CEP164 is required for assembly of primary cilia and localizes to the distal appendages of mature centrioles in RPE cells (Graser et al., 2007a). STED (Stimulated Emission Depletion) microscopy with a resolution of 60 nm demonstrated that CEP164 localizes to distal appendages in nine clusters spaced around a ring of ~300 nm in diameter (Lau et al., 2012). In the DAP megacomplex, CEP164 forms the outermost of several concentric rings surrounding the MC distal end (Yang et al., 2018). A major function of CEP164 is to recruit TTBK2 (Tau tubulin kinase 2) to the MC distal

end, which subsequently removes the CP110 plug to facilitate ciliogenesis. TTBK2 can also function downstream of CEP164 by increasing CEP164 (and other DA proteins) levels at distal appendages, and promote distal appendage assembly even at daughter centrioles (Cajanek and Nigg, 2014). Disruption of CEP164 in hTert-RPE1 cells blocked primary cilium formation (Daly et al., 2016; Cajanek and Nigg, 2014). CEP164 interacts with Rabin8 to activate Rab8 and may provide a molecular link between the mother centriole and the membrane biogenesis machinery that initiates cilia formation (Schmidt et al., 2012).

Recessive mutations of CEP164 are associated with nephronophthisis (NPHP15), and often with retinal degeneration (Chaki et al., 2012). CEP164 was shown to form a complex with PDE8, encoded by the *Pde6d* gene, and ARL13B, the GEF of ARL3, to traffic prenylated INPP5E to cilia of zebrafish and in cell culture, thus identifying a distinct functional network linked to JBTS and NPHP (Humbert et al., 2012). Knockdown of CEP164 in zebrafish resulted in syndromic ciliopathy with ventral body axis curvature, cell death, abnormal heart looping, pronephric tubule cysts, hydrocephalus and retinal dysplasia (Chaki et al., 2012; Slaats et al., 2014). In a conditional mouse model that lacks CEP164 in multiciliated tissues and the testis, a profound loss of airway, ependymal, and oviduct multicilia was observed, and the mutant mouse developed hydrocephalus and male infertility (Siller et al., 2017). Using tracheal multiciliated cell cultures of this mouse model, CEP164 was shown to be critical for multiciliogenesis and regulation of small vesicle recruitment, ciliary vesicle formation and basal body docking (Siller et al., 2017).

CEP83 (centrosomal protein 63) (CCDC41, NPHP18)—CEP83 (human 701, mouse 692 amino acids) localizes to the distal appendages of the mother centriole, together with CEP89 [CCDC123] and CEP164. The protein consists entirely of coiled-coil motifs, and has a large stretch of sequence rich in glutamic acid (E) (Fig. 9B). Loss of CEP83 specifically blocks centriole-to-membrane docking (Tanos et al., 2013). In addition, CEP83 colocalizes with IFT20 at the Golgi of RPE1 cells (Joo et al., 2013). Knockdown of CEP83 inhibits the recruitment of IFT20 to the centrosome, and depletion of CCDC41 or IFT20 inhibits ciliogenesis at the ciliary vesicle docking step (Joo et al., 2013). The results suggest that CEP83 collaborates with IFT20 to support the vesicle-centriole association at the onset of ciliogenesis. Mutations in CEP83 are causative of infantile nephronophthisis associated with central nervous system abnormalities (e.g., hydrocephalus) in half of the examined individuals (Failler et al., 2014). A retina degeneration phenotype was seen in several individuals.

CEP89 (centrosomal protein 89) (CCDC123, CEP123)—CEP89 (791 amino acids in mouse) consists mostly of coiled-coil domains and is one of several distal appendage proteins anchoring the mother centriole to membranes (Tanos et al., 2013). The CEP89 N-terminus carries a proline-rich region (Fig. 9G). CEP89 interacts with PCM-1, OFD1 and CEP290 and is required for primary ciliogenesis (Sillibourne et al., 2013). In the absence of CEP89 a ciliary vesicle fails to form at the distal end of the mother centriole (Sillibourne et al., 2013). Loss of CEP89 blocks centriole-to-membrane docking (Tanos et al., 2013).

SCLT1 (sodium channel and clathrin linker 1)—SCLT1 is an adaptor protein (688 amino acids in human and mouse) consisting of multiple coiled-coil domains (Fig. 9C).

Studies of a related gene in rat suggest that the encoded protein functions to link clathrin to the sodium channel protein type 10 subunit alpha protein (Liu et al., 2005). SCLT1 has also been identified as a component of centriolar distal appendages that mediates ciliogenesis (Tanos et al., 2013). Truncation mutation in SCLT1 causes a severe ciliopathy consistent with oro-facio-digital syndrome type IX (OFD9); the OFD phenotype features midline cleft, microcephaly and colobomatous microphthalmia/ anophthalmia (Adly et al., 2014).

FBF1 (Fas binding factor 1)—FBF1 was identified as a CD95-interacting protein in human cells. Fbf-1 consists of 1173 amino acids (calc. molecular weight of 130 kDa) with multiple coiled-coil domains in the C-terminal half (Fig. 9D). Expressed in a wide variety of tissues, FBF1 protein localizes in the cytoplasm (Schmidt et al., 2000). FBF1 (*dyf-19* is the *Caenorhabditis elegans* homologue of human *FBF1*) is a highly-conserved transition fiber protein and is required for the ciliary import of assembled IFT particles at the ciliary base in *C. elegans* (Wei et al., 2013). Human FBF1 shares conserved localization and function with *dyf-19*. FBF1 formed a ring-like structure around the mother centriole or at the ciliary base in IMCD3 cells. FBF1 colocalized with the DAP marker, CEP164, on mother centrioles and localized above the sub-DAP marker, ODF2 (Wei et al., 2013).

C2CD3 (C2 Ca²⁺-dependent domain containing 3) (OFD14)—C2CD3 (longest variant, 2323 amino acids in mouse) locates to the lumen of distal end centrioles (Yang et al., 2018). C2CD3 has no coiled-coil domains and appears to interact indirectly with other DAPs. It carries a nuclear localization signal at its N-terminus and contains two C2-domains in the protein's C-terminal half (Fig. 9F). C2-domains interact with membranes or proteins in a Ca²⁺-dependent manner, and are composed a β -sandwich structure consisting of a pair of four-stranded β -sheets (Pinheiro et al., 2016; Sudhof and Rizo, 1996). Hoover, *et al.* proposed that C2CD3 functions as a Ca²⁺-dependent lipid binding protein that mediates recruitment of proteins during ciliogenesis (Hoover et al., 2008). In cell culture, C2CD3 functions as a regulator of centriole elongation (Thauvin-Robinet et al., 2014). Mutations in the human *C2CD3* gene cause ciliopathy oro-facio-digital syndrome type XIV (OFD14) (Thauvin-Robinet et al., 2014). A family with novel compound heterozygous *C2CD3* mutations presented with skeletal dysplasia with no microcephaly (Cortes et al., 2016).

C2CD3 was found defective in the *hearty (hty)* mouse model which carries a splice site mutation in the *C2cd3* gene (Hoover et al., 2008). The *hty* mouse displays a syndromic ciliopathy with multiple defects, including neural tube defects, abnormal dorsal/ventral patterning of the spinal cord and severe polydactyly (up to nine digits). A gene-trapped *C2cd3* mouse model has a similar but stronger phenotype. Loss of C2CD3 results in shortened centrioles without appendages. C2CD3 associates with OFD1, the deletion of which results in centriole hyper-elongation (Thauvin-Robinet et al., 2014). Loss of C2CD3 results in failure of CP110 removal from the ciliary mother centriole, a critical step in initiating ciliogenesis. C2CD3 is also required for recruiting IFT88 and IFT52 to the mother centriole (Ye et al., 2014). Consistent with a role in distal appendage assembly, C2CD3 is essential for ciliary vesicle docking to the mother centriole. C2CD3 regulates cilium biogenesis by promoting the assembly of centriolar distal appendages critical for docking ciliary vesicles and recruiting other essential ciliogenic proteins (Ye et al., 2014).

Summary of distal appendages.: Distal appendages form a megacomplex consisting of nine conical-shaped blades (DABs) (Yang et al., 2018). The DABs are essential for docking of the mother centriole and cilia initiation. The DA matrix (DAM) contains FBF1 and IFT particles (IFT88). Germline deletion of DAP genes prevents ciliogenesis and is causative of embryonic lethality (CEP164, C2CD3). A conditional knockout of CEP164 in multiciliated tissues generated hydrocephalus and loss of multicilia (Siller et al., 2017). Distal appendage-associated proteins CP110, CEP290 (Gene deletions that prevent basal body docking) and KIF3a, ARL3, ARL13b (Gene deletions that prevent CC formation in photoreceptors) are discussed below.

3.5 Microtubules

TUBA, TUBB (α - and β -tubulins).—Microtubules are highly-conserved, cytoskeletal ~24 nm thick filaments consisting of α - and β -tubulin. Retina photoreceptors have two separate populations of microtubules: axonemal microtubules of the outer segment and cytoplasmic microtubules of the cell body (Fig. 10). Axonemal microtubules extend from the basal body distally to the outer segment. The axonemal microtubule (–) end is anchored by subdistal appendages of the basal body (Delgehyr et al., 2005) and by binding to the γ -tubulin ring complex (γ -TuRC) of the pericentriolar matrix (Doxsey et al., 1994). Microtubules comprising the rod and cone axoneme are acetylated, a posttranslational modification that provides stability (Troutt et al., 1990) and prevents breakage (Xu et al., 2017; Portran et al., 2017). Acetylated tubulin overlaps with RP1, a microtubule-associated protein (Liu et al., 2004; Hanke-Gogokhia et al., 2017). Alternatively, cytoplasmic microtubules are organized and nucleated by the basal body, oriented with (–) ends (α -tubulin) at the basal body and the (+) ends (β -tubulin) reaching toward synaptic terminals.

Photoreceptor microtubule organization serves two main purposes--to maintain the structure of the polarized cell, and provide tracks for motorized trafficking of membrane proteins. Vesicles charged with membrane proteins emerge from the trans-Golgi network (TGN) to traffic towards the PCM, and cargo is assembled for IFT through the cilium (Rosenbaum and Witman, 2002). Anterograde IFT is thought to be powered by heterotrimeric kinesin-2, a microtubule-based and plus-end oriented molecular motor (Cole et al., 1992; Scholey, 2008) associated with IFT-B particles (Pazour et al., 2002; Baker et al., 2003). Photoreceptor retrograde IFT, which recycles IFT particles back to the proximal CC, is powered by dynein-2 motors, but its need in mouse photoreceptors has not been demonstrated as the entire photosensitive cilium is replaced every ten days. IFT is important for axoneme biogenesis and maintenance. A role for kinesin-2-enabled IFT in trafficking rhodopsin through the CC has been proposed (Marszalek et al., 2000; Jimeno et al., 2006) and contested (Avasthi et al., 2009).

TUBG1 (γ -tubulin)—*TUBG1* is one of two human genes encoding γ -tubulin. *TUBG1* mutations (Leu387Pro; Tyr92Cys) cause malformations of cortical development, microcephaly and other brain malfunctions (Poirier et al., 2013). γ -tubulin is required for MT nucleation and locates to the MC of centrosomes. Antibodies directed against TUBG1 are excellent basal body markers. TUBG1 exists as an oligomer within the γ -tubulin ring complex (γ -TuRC) of higher eukaryotes, a large complex consisting of several proteins

(Aldaz et al., 2005). Laterally associated γ -tubulins in the γ -TuRC might promote microtubule nucleation by providing a template that enhances the intrinsically weak lateral interaction between α,β -tubulin heterodimers. Knockdown of *Tubg1* in mouse embryos altered cortical radial neuronal migration (Poirier et al., 2013). *Tubg1* knockout mice (*Tubg1^{-/-}*) revealed arrested development of embryos at the morula/blastocyst stages due to a characteristic mitotic arrest (Yuba-Kubo et al., 2005).

TUBD1 (δ -tubulin)—In *C. reinhardtii*, δ -tubulin is essential for the production of flagella and the production of triplet microtubules in the basal body (Garcia, III and Reiter, 2016). The precise function of δ -tubulin in mouse is unclear; it was shown to be highly expressed in testis (Smrzka et al., 2000). In somatic cell lines, mammalian δ -tubulin was both cytoplasmic and nuclear and did not colocalize with microtubules. The protein was enriched at the spindle poles during mitosis. γ -tubulin coimmunoprecipitated with δ -tubulin (Smrzka et al., 2000). δ -tubulin and ϵ -tubulin localize to the centrosome with distinct localization patterns (Chang and Stearns, 2000).

TUBE1 (ϵ -tubulin)— ϵ -Tubulin localizes to the PCM but is not part of the γ -tubulin ring complex. ϵ -Tubulin exhibits a cell cycle-specific pattern of localization, first associating with only the older centrosomes in a newly duplicated pair and later associating with both centrosomes (Chang et al., 2003; Chang and Stearns, 2000). ϵ -Tubulin localizes to the centriolar sub-distal appendages and plays a central role in microtubule organization during centriole duplication. In *C. reinhardtii*, ϵ -tubulin is required for the formation of both basal body doublet and triplet microtubules (Dutcher et al., 2002).

4. Sorting ciliopathy genes by mouse knockout phenotype

Proteins involved in basal body docking, MC maturation, CC formation and axoneme extension are usually sorted by data gleaned from immunolocalization, proteomics, bioinformatics and interacting partners (Liu et al., 2007; Sang et al., 2011; Gupta et al., 2015; Boldt et al., 2016). Jackson and collaborators used a LAP (Localization and Affinity Purification) tag strategy in which a EGFP-TEV-S-peptide construct was fused to the N-terminal of NPHP1–6, NPHP8, Joubertin and MKS1, and expressed in immortalized cell lines (NIH 3T3, IMCD3). Complexes with interacting protein were purified by affinity chromatography, and interactants identified by mass spectrometry. This technique allowed the identification of a NPHP-JBTS-MKS interaction network of numerous interacting partners and revealed an astonishing complexity of interactions. Subsequent analysis allowed a subclassification of the NPHP-JBTS-MKS proteins into three connected modules: NPHP1–4-8 localizing to cell-cell contacts and the CC (Apical Organization Module), NPHP5–6 localizing to the basal body (Cilia Integrity Module), and MKS1 linked to hedgehog signaling (Sang et al., 2011). LAP-NPHP5 and LAP-NPHP6 colocalize with the centrosomal marker pericentrin in IMCD3 cells, and LAP-NPHP5 colocalizes with NPHP6. LAP-NPHP5 co-purified with SEC3, a subunit of the exocyst, a multisubunit protein complex implicated in membrane trafficking and ciliogenesis (Sang et al., 2011).

In the following, we will attempt to group genes based upon their knockout phenotypes in photoreceptors or retina, and independent of interactions. We are aware that this grouping is

subjective as phenotypes of germline, retina- or photoreceptor-specific gene knockouts are complex, are dependent on genetic background and produce additional phenotypes in other primary cilia. We also included closely related genes that do not produce a photoreceptor phenotype (e.g., molecular motor KIF17, closely related to KIF3a). The first group describes proteins involved in basal body docking arrest, the second group discusses proteins involved in axoneme extension and CC formation. A third group involves proteins that allow CC formation but form unstable outer segments.

4.1 Gene deletions that prevent basal body docking and outer segment formation

Deletion of one of several outer segment proteins (rhodopsin, PDE6B, PRPH2) results in basal body docking to the apical inner segment cortex, elaboration of an axoneme, yet inability to form an outer segment. The genes encoding these proteins are not ciliary genes *per se*, i.e., their products are not constituents of the basal body or CC. In this paragraph, only genes associated with connecting cilium and axoneme formation or stability are discussed. Among the selected important ciliary proteins of this category are CP110, CEP97, CEP290 and CC2D2A. CP110 (centriolar coiled-coil protein 110) is recruited by CEP97 to the distal end of both centrioles, only to be removed from the distal MC as a cilium develops. CEP290 (alias NPHP6, centrosomal protein 290) is one of best characterized CEPs and interacts with numerous proteins; mutant human CEP290 is associated with ciliopathies JS, NPHP, MKS and LCA. MACF1 (microtubule-actin crosslinking factor 1) is one of the most abundant proteins of the photoreceptor proteome and associates with Parkinson's disease and cancer. CC2D2A (coiled-coil and C2-domain containing 2A) is a subdistal appendage protein (SDAP). Mutations in the human CC2D2A gene are causative of MKS, and mental retardation with RP and JS. Although germline or conditional knockouts of these genes exist, revealing many details of function, our interest focuses specifically on consequences for retina morphology, photoreceptor function and retina disease.

CP110 (centriolar coiled-coil protein 110) (CP110, CEP110)—The mouse *Ccp110* gene encodes CP110 which contains 1002 amino acids with N- and C-terminal coiled-coil (CC) domains and CaM-interacting sites (Fig. 11A). Gene expression was shown to be induced during centrosome duplication, and RNAi-mediated knockdown of CP110 suggested that CP110 plays an essential role in this process (Chen et al., 2002). Native CP110 forms large complexes with calmodulin and centrins (Tsang et al., 2006). Centrin 2 was shown recently to regulate CP100 levels and ciliogenesis in chicken lymphocytes and RPE1 cells (Prosser and Morrison, 2015). However, mouse *Cetn2* germline knockouts do not affect mouse photoreceptor and olfactory sensory neuron ciliogenesis (Ying et al., 2014).

Cell culture.: The current model of CP110 function derives from cultured cells (Tsang and Dynlacht, 2013). CEP97 recruits CP110 to the distal part of centrioles, acting as a chaperone; CP110 degradation coincides with cilia formation (Spektor et al., 2007). CP110 caps the distal end of both centrioles in non-ciliated cells. As cells begin to develop a cilium, CP110 is removed from the distal MC and degraded. CP110 binds to and antagonizes the function of CEP290, a positive regulator of ciliogenesis (Tsang et al., 2008). Loss of CEP97 and CP110 promotes primary cilia formation in growing cells, suggesting that CP110 is a

negative regulator of ciliogenesis (its presence prevents cilia formation; its absence induces cilia formation) (Spektor et al., 2007; Tsang and Dynlacht, 2013; Tsang et al., 2008). Further, CEP290 and CP110 interact with Rab8a, a small GTPase required for cilia assembly in cell culture (Tsang et al., 2008). Additional important CP110 interactors are KIF24 (Kobayashi et al., 2011) and Talpid3 (JBTS23) (Kobayashi et al., 2014). KIF24 regulates cilia assembly by remodeling of centriolar MT, and Talpid3 assembles a ring-like structure at the distal end of centrioles. Ablation of Talpid3 affects distribution of centriolar satellites which regulate protein trafficking to the centrosome.

In-vivo.: Germline *Ccp110* knockout mice die shortly after birth owing to syndromic ciliopathy defects (Yadav et al., 2016). Shh signaling is impaired in *Ccp110* null embryos and primary cilia are reduced in multiple tissues. In contrast to cell culture, CP110 promotes cilia formation *in-vivo*, and acts as a positive regulator. CP110 is required for anchoring of basal bodies to the membrane during cilia formation. CP110 loss resulted in an abnormal distribution of subdistal appendage core components (ninein, Odf2, CC2D2A), thus implicating CP110 in SDA assembly and ciliary vesicle docking, two requisite early steps in ciliogenesis (Yadav et al., 2016). In *Ccp110*^{-/-} MEFs, SDAs and DAs are not visible in the majority of basal bodies or are poorly developed and connecting cilia are compromised. The knockout phenotype is reminiscent of human short rib-polydactyly syndrome, a form of ciliopathy with a strong skeletal defect (Yadav et al., 2016).

CEP97 (centrosomal protein 97) (LRR1Q2).—CEP97 is a Ca²⁺-binding protein with a central IQ calmodulin binding motif, several small coiled-coil domains and a leucine-rich region at the N-terminal (Fig. 11B). CEP97 interacts directly with CP110 as evidenced by coimmunoprecipitation (Spektor et al., 2007). CEP97 has sequence similarity with centriolin throughout its coding sequence (Spektor et al., 2007), particularly at the N-terminal half of centriolin (23% identity by Clustal Omega alignment).

CEP290 (centrosomal protein 290) (Nphp6, BBS14, JBTS5, LCA10, MKS4, POC3, SLSN6, rd16).—CEP290 is a well-characterized centrosomal protein (Chang et al., 2006; Moradi et al., 2011; Drivas and Bennett, 2014; Rachel et al., 2012). CEP290 (in mouse 2,479 amino acids) participates in centrosomal and microtubule-associated protein complexes (Kim et al., 2008; Loktev et al., 2008). The protein has multiple domains, including CC domains, an ATP/GTP binding loop, and a C-terminal myosin-tail homology domain among other motifs (Chang et al., 2006; Moradi et al., 2011) (Fig. 11C). CEP290 binds to the cell membrane through its N-terminal domain and to MT through a domain located in the myosin-tail domain (Drivas et al., 2013). An in-frame deletion in the myosin-tail domain in mouse (*rd16* mouse, see below) produces retina degeneration. CEP290 was shown to interact with RPGR-interacting protein (RPGRIP1), dynactin subunits, kinesin-2 subunits KIF3A and KAP3, centrin-1, periciliary membrane protein 1 (PCM1) (Chang et al., 2006), ninein, RPGR, RPGRIP1, IQCB1/NPHP5 (Barbelanne et al., 2013), CP110 (Tsang et al., 2008), CC2D2A and others (Drivas et al., 2013).

While CEP290 localizes to the centrosome of dividing cells, it distributes to the CC and distal MC of postmitotic photoreceptors. Ultrastructural investigations in *C. reinhardtii* located CEP290 to the Y-shaped linkers anchoring the MT doublets to the cell membrane

(Craigie et al., 2010). In CEP290-depleted cells, Y-linkers are mostly absent, suggesting that CEP290 may function as a gate keeper controlling protein traffic to the OS. In humans, loss-of-function mutations in the *CEP290* gene have been associated with Joubert syndrome (Sayer et al., 2006; Valente et al., 2006), nephronophthisis (medullary cystic kidney disease) and Meckel syndrome (Baala et al., 2007), whereas hypomorphic mutations are associated with LCA (den Hollander et al., 2006). A compilation of *CEP290* mutations can be found at the CEP290base (Coppieters et al., 2010). Interestingly, LCA is associated with mutations throughout CEP290, while Joubert syndrome mutations are located in the C-terminal half, and Meckel syndrome mutations are in the N-terminal half (Rachel et al., 2015).

Knockout mouse models.: Several *Cep290* germline mutations have been generated (Rachel et al., 2015; Hynes et al., 2014). *Cep290* germline knockouts with deletions of exons 1–4 died before weaning due to the development of ciliopathy and hydrocephalus (Rachel et al., 2015). The phenotype of surviving mice was compatible with Joubert syndrome. *Cep290*^{-/-} photoreceptor basal bodies formed but failed to dock to the apical cell membrane, and therefore lacked a CC. A gene-trapped *Cep290* mouse line expressing the first 25 exons (gene trap placed in intron 25) produced Meckel syndrome, with most pups dying between E12–14 (Rachel et al., 2015). A second gene-trapped mouse with a gene trap in intron 23 were fertile and viable beyond one year (Hynes et al., 2014), possibly because of a partially ineffective or ‘leaky’ gene trap. The homozygous mutants exhibit a JBTS/ ciliopathy phenotype, including retinal degeneration, cerebral abnormalities and progressive cystic kidney disease consistent with the human phenotype.

The *rd16* mouse is a spontaneous *Cep290* mutant with an in-frame deletion of 299 amino acids (exons 35–39) (Fig. 11C) causing a rapidly progressing degeneration. Homozygous *rd16* mice formed CC and outer segments but these structures were unstable and disintegrated. A *rd16;Nr1*^{-/-} model (cone-only retina) showed a relatively slow ONL decline with ~80% nuclei remaining at 3 months (Cideciyan et al., 2011; Boye et al., 2014). *rd16* mice are dysosmic and show abnormal transport of G α_{olf} (GNAL) and G γ 13 (GNG13), the subunits of the olfactory G protein (McEwen et al., 2007). Zhang, *et al.* developed a miniCEP290 gene (miniCEP290(580–1180)) that delayed retinal degeneration when injected into the subretinal space of neonatal *rd16* mice. (Zhang et al., 2017).

Cep290 gene therapy.: The most frequent genetic cause of LCA is an intronic mutation in CEP290 (c.2991p1655A>G) (den Hollander et al., 2006; Garanto et al., 2013). The mutation creates a splice donor site in intron 26 producing the insertion of a pseudoexon (exon X) into CEP290 mRNA. A lentiviral vector containing CMV-driven human full-length CEP290 expressed in fibroblast cultures from CEP290-associated LCA patients carrying the exon X mutation rescued the ciliogenesis defect (Burnight et al., 2014). In an elegant study, Garanto et al. showed that naked antisense oligonucleotides (AONs) restored *Cep290* pre-mRNA splicing, rescued a ciliary phenotype present in patient-derived fibroblast cells, and reduced exon X expression in a humanized mutant *Cep290* mouse model (Collin and Garanto, 2017; Garanto et al., 2016). Similarly, treating optic cups from iPSCs with this common CEP290 mutation with an antisense morpholino effectively blocked aberrant splicing, permitted

expression of full-length CEP290, and restored normal cilia-based protein trafficking (Parfitt et al., 2016).

MACF1 (microtubule actin crosslinking factor 1)—MACF1 is a gigantic protein (5430 amino acids in human, 7355 amino acids in mouse, >500 kDa) expressed in multiple isoforms. MCAF1 is a member of the spectraplakins gene family. Spectraplakins are cytoskeletal crosslinkers with ability of interacting with all three types of cytoskeletal filaments, i.e., F-actin, microtubules and intermediate filaments (Hu et al., 2016). Whereas MACF1 assumes a key role in maintaining normal functions of many tissues (Hu et al., 2016), mutant MACF1 has been associated with Parkinson's disease (Wang et al., 2016) and cancer (Miao et al., 2017). Loss-of-function studies using knockout mouse models showed that MACF1 participates in embryo development, neurogenesis, bone formation and colonic paracellular permeability (Hu et al., 2017).

MACF1 contains numerous coiled-coil domains, several spectrin and plectin domains, and two adjacent C-terminal Ca²⁺-binding EF hands. The actin- and tubulin- interaction sites occur on either end of MACF1 (Fig. 11D). MACF1 is one of the most abundant proteins of the photoreceptor ciliary proteome (Liu et al., 2007; May-Simera et al., 2016). The predominant *Macf1a* RNA in rods peaked ~P3 when ciliogenesis initiates, and by P5, MACF1 was present at the scleral edge of the ONL. In adult retina, MACF1 colocalizes with pericentrin at the PCM and basal bodies. Germline ablation of *Macf1* is embryonically lethal (Chen et al., 2006). Six3Cre-driven excision of *Macf1* during mouse retina development affected mostly photoreceptors; retina lamination appears disrupted at P5, and ciliary rootlets appear misaligned without outer segments at P10. Ultrastructural examination revealed that basal bodies failed to acquire the ciliary vesicle necessary for docking to the cell membrane--resulting in loss of BB docking, abolished ciliogenesis and disruption of photoreceptor polarity (May-Simera et al., 2016). In mutant photoreceptors, rhodopsin and cone pigments were expressed but mislocalized in the ONL as outer segments were absent. Deletion of MACF1 in adult photoreceptors by viral expression of Cre caused reversal of basal body docking and disruption of MT anchoring surrounding the basal body (May-Simera et al., 2016).

CC2D2A (coiled-coil and C2-domain containing 2A) (JBTS9, MKS6)—CC2D2A (1643 amino acids in mouse, 1620 in human) is a subdistal appendage protein with C2 Ca²⁺ binding sites and N-terminal coiled-coil domains (Fig. 11E). In human patients, CC2D2A is associated with Meckel syndrome (MKS) (Tallila et al., 2008), mental retardation with RP (Noor et al., 2008) and Joubert syndrome (Gorden et al., 2008). CC2D2A can physically interact with NPHP6/CEP290 and Tectonic1 (TCTN1) (Veleri et al., 2014). These proteins localize within the CC and act as a barrier that prevents diffusion of transmembrane proteins between the cilia and plasma membranes. A zebrafish mutant, *sentinel* (W628X), exhibited a cystic fibrosis phenotype which was enhanced by knockdown of *Cep290* (Bachmann-Gagescu et al., 2012; Mougou-Zerelli et al., 2009). Mutant rods and cones formed cilia but outer segments were shortened and rhodopsin and cone pigments mislocalized. The stop codon truncates zebrafish CC2D2A at residue 628, but the *sentinel* mutants did not express truncated CC2D2A; therefore, the *sentinel* mutant is a CC2D2A null mutant. Rab8-coated

vesicles accumulated at the apical inner segments suggesting CC2D2A is important for membrane protein trafficking in zebrafish. In a recent paper, Ojeda Naharros, et al. show that CC2D2A plays a role in docking of opsin-carrying vesicles at the periciliary membrane (Ojeda Naharros et al., 2017).

By contrast, the *Cc2d2a*^{-/-} mouse (replacement of exons 6–8 by a lacZ/Neo cassette) recapitulates features of Meckel syndrome with multiorgan defects (Veleri et al., 2014). Loss of CC2D2A leads to embryonic lethality; embryos did not survive past E18, often showing polydactyly, exencephaly (brain outside of skull) and *situs inversus*. Cilia are absent in *Cc2d2a* embryonic node and other somatic tissues. Disruption of cilia-dependent sonic hedgehog (Shh) signaling appears to underlie exencephaly in mutant embryos. In control MEFs, CC2D2A localizes to subdistal appendages. In *Cc2d2a*^{-/-} MEFs, cilia were absent and assembly of SDAs at the mother centriole was impaired. The conclusion of the mouse CC2D2A knockout was that CC2D2A is essential for the assembly of subdistal appendages, which anchor cytoplasmic microtubules and prime the mother centriole for axoneme biogenesis (Veleri et al., 2014). The *Cc2d2a*^{-/-} mouse retina of a rare survivor shows absence of ERG responses and severe disruption of the outer nuclear layer, with poorly developed inner and outer segment structure.

Summary of gene deletions that prevent basal body docking.—CP110 caps the distal end of both centrioles and must be removed to initiate ciliogenesis. Its function as a negative regulator (in cell culture) or positive regulator of ciliogenesis is unresolved or simply represents different functions in different cells. Germline deletion of *Cp110* results in abnormal distribution of SDAPs implicating CP110 in SDA assembly and basal body docking. Germline knockouts of *Cep290* have serious consequences; mutant mice develop hydrocephalus, JS and MKS, as basal bodies failed to dock. By contrast, the *rd16* mouse with an in-frame deletion of 299 amino acids formed an unstable CC and OS, exhibiting LCA and dysosmia. Retina-specific knockout of *Macf1* affected retina lamination and rootlet alignment. The main defect appeared to be that the basal body failed to acquire the ciliary vesicle necessary for docking. In *Cc2d2a* germline knockouts, cilia were absent leading to embryonic lethality with a MKS phenotype. The main conclusion was that CC2D2A is essential for SDA assembly.

4.2 Gene deletions that prevent axoneme extension

This ensemble discusses KIF3a, the obligatory subunit of heterotrimeric kinesin-2; ARL3 and ARL13b, where ARL13b functions as the ARL3 GEF; IQCB1/NPHP5, a CEP290 interactor; and INPP5E, an inositol polyphosphate phosphatase. Kinesin-2 is an anterograde molecular motor participating in ciliary IFT, a function conserved from invertebrates (*C. elegans*, *C. reinhardtii*) to vertebrates, and including zebrafish, mouse and humans (Rosenbaum and Witman, 2002; Malicki and Avidor-Reiss, 2014; Sedmak and Wolfrum, 2011). Kinesin-2 is cytoplasmic when in its inactive state (not functioning as motor), but locates to the basal body/proximal outer segment when active in IFT (Jiang et al., 2015a; Jiang et al., 2015b). ARL3 (Arf-like protein 3) is a cytoplasmic, small GTPase located in the photoreceptor inner segment in its GDP-bound form (Hanke-Gogokhia et al., 2016). ARL13b functions a GTPase-activating protein for ARL3 and distributes exclusively in the

outer segment (Hanke-Gogokhia et al., 2017). INPP5E is a phosphatidylinositol polyphosphate phosphatase localizing to membranes of the inner segment (Golgi) and in primary cilia by means of a C-terminal lipid anchor (farnesyl) (Dyson et al., 2017; Thomas et al., 2014; Humbert et al., 2012). As a common denominator, germline or photoreceptor-specific deletions prevent CC formation possibly by interfering with IFT, i.e., trafficking of cargo from TGN to the CC, or by upsetting the function of various ciliary or centrosomal proteins.

KIF3A (kinesin family member 3A) (FLA-10, KLP-20)—KIF3a is the obligatory subunit of heterotrimeric kinesin-2 (KIF3), a molecular motor enabling anterograde IFT in ciliated cells. KIF3a was cloned from porcine brain (Kondo et al., 1994) and retina (Whitehead et al., 1999). KIF3 consists of three subunits (KIF3a, KIF3b and KAP) (Cole et al., 1992) and is present in a broad range of species, including *C. reinhardtii* (Cole et al., 1998; Kozminski et al., 1998), *C. elegans* (Signor et al., 1999) and zebrafish (Wong-Riley and Besharse, 2012; Bader et al., 2012; Rosenbaum and Witman, 2002).

KIF3a (701 amino acids in mouse, 99% identical to human) has a motor and a tail domain connected by a neck region with multiple coiled-coil domains (Fig. 12A). Germline deletion (removal of exon 2) of KIF3a, the KIF3 obligatory subunit, is embryonically lethal (Marszalek et al., 1999; Takeda et al., 1999). *Kif3a* null mice displayed a *situs inversus* phenotype; all cells of the embryonic node lacked cilia demonstrating that KIF3a is needed for the formation of embryonic cilia (Morris and Scholey, 1997). Conditional deletion of KIF3a resulted in defective bone formation and osteopenia (Qiu et al., 2012; Temiyasathit et al., 2012), male infertility (Lehti et al., 2013) and polycystic kidney disease (Lin et al., 2003). Photoreceptor-specific deletion of KIF3a with Cre drivers (cone- or rod-specific) expressing Cre post-ciliogenesis caused photoreceptor degeneration (Marszalek et al., 2000; Avasthi et al., 2009). Retina-specific deletion of KIF3a during development (Six3-Cre driver) resulted in failure of basal bodies to extend CCs and absence of outer segments (Jiang et al., 2015b). In P6 control mice, photoreceptor centrioles extended nascent CCs (Fig. 12B, left panel, shown by transgenic EGFP-CETN2 expression). MC/DC are present in knockout mice (Fig. 12B, right panel), but CCs do not form. Fully developed CCs, each paired with a daughter centriole, are present in P10 controls (Fig. 12C, left), while no similarly-labeled CCs extend from *retKif3a*^{-/-} photoreceptor apical inner segments (Fig. 12C, right).

Ultrastructure of *retKif3a*^{-/-} CCs showed that basal bodies docked at the apical IS with normal centriole appendages, but failed to extend a CC at P6 and P10 (Jiang et al., 2015b) suggesting aborted ciliogenesis in *retKif3a*^{-/-} photoreceptors and linking KIF3a to CC formation (Fig. 12E, F). Ultrastructure of synaptic terminals revealed that rod spherules and cone pedicles (including ribbon structures) formed normally. KIF3a depletion by tamoxifen-induction in adult photoreceptors resulted in progressive shortening of the OS axoneme (Jiang et al., 2015b).

In mouse MEFs, KIF3A was found to associate specifically with the MC (Kodani et al., 2013). Using *Kif3a*-deficient MEFs as a model, it was found that SDAs of MC were disorganized and consequently, MT anchoring, centriole cohesion and basal foot formation

were abrogated (Kodani et al., 2013). The dynactin subunit p150^{glued} and ninein were absent and depletion of p150^{glued} phenocopied the effects of Kif3a deletion (Kodani et al., 2013). In zebrafish, KIF3a is indispensable for ciliogenesis in organs and all cells, including photoreceptors. In *Kif3a*-deficient photoreceptors, basal bodies frequently did not dock to the cortex of the IS but associated with other membranes. Basal bodies were mispositioned suggesting a role for KIF3a in correct positioning of the basal body in zebrafish photoreceptors (Pooranachandran and Malicki, 2016).

KIF17 (kinesin family member 17) (osm-3)—Homodimeric kinesin-2 consisting of KIF17 (*osm-3*) subunits is another anterograde molecular motor involved in plus-oriented IFT in *C. elegans* and vertebrates. KIF17 transports N-methyl-D-aspartate (NMDA) receptor subunit-2B (NR2B) in neurons. Germline deletion of KIF17 in mice resulted in impaired transcription and transport of NR2B, thus regulating synaptic NR2A/2B levels, a pathway fundamental for learning and memory (Yin et al., 2011).

In ciliated cells, KIF17 and KIF3 are thought to cooperate during ciliogenesis in which KIF3 builds the axoneme core and KIF17 the axoneme distal segments (Signor et al., 1999; Pan et al., 2006; Tabish et al., 1995). However, interaction of KIF17 with KIF3 and the contribution of KIF17 to vertebrate ciliogenesis or membrane protein trafficking are unclear. KIF17 appears largely dispensable for ciliogenesis in zebrafish as *Kif17* homozygous mutant animals are viable and display subtle morphological defects of olfactory cilia only (Zhao et al., 2012). However, KIF17 appeared to play a role during early photoreceptor development of zebrafish retina (Insinna et al., 2009; Malicki and Besharse, 2012). Recent experiments performed by Dr. Besharse's group showed that zebrafish and mouse *Osm-3/Kif17* mutants display delayed onset of OS disc morphogenesis without adversely affecting the development of mature and functional photoreceptors (Lewis et al., 2017). Such results recapitulate findings of a germline deletion of KIF17 in mouse which has no effect on axoneme structure or photoreceptor function for up to two years. In mouse, KIF17 apparently is not required for anterograde IFT and CC formation (Jiang et al., 2015a).

ARL3 (ADP-ribosylation factor (Arf)-like protein 3) (RP83, JBTS35)—ARL3 is a soluble, small GTPase (182 amino acids in mouse) present in all ciliated organisms (Zhang et al., 2013). Experiments in ciliated hTert-RPE and IMCD3 cells (Wright et al., 2011), pulldowns (Linari et al., 1999; Kobayashi et al., 2003; Hanzal-Bayer et al., 2002) and crystallography (Renault et al., 2001; Veltel et al., 2008; Ismail et al., 2012; Ismail et al., 2011) identified ARL3 and its close relative, ARL2, as interactants of PDE δ and UNC119 (Schwarz et al., 2012; Ismail et al., 2011; Wright et al., 2011). ARL3 GTPase activity is regulated by the guanine nucleotide exchange factor (GEF), Arl13b (Gotthardt et al., 2015), and a GTPase activating protein (GAP), RP2 (Veltel et al., 2008) (Fig. 13A).

In photoreceptors, ARL3 localizes to the cell body, inner segment and connecting cilium (Grayson et al., 2002; Hanke-Gogokhia et al., 2016) (Fig. 13B). The active conformation of ARL3 is found to be both soluble and membrane-associated due to weak affinity to membrane (Wright et al. 2011). It appears to accumulate near the basal body, presumably in the GTP-bound form (Fig. 13B, right panel).

Arl3 germline knockouts died postnatally before day P21 (Schrack et al., 2006). The mutants exhibited abnormal development of renal, hepatic and pancreatic epithelial tubule structures and retinal degeneration reminiscent of Joubert syndrome (Schrack et al., 2006). Rod-specific knockout of ARL3 and transgenic expression of dominantly active ARL3 (ARL3-Q71L) showed that ARL3-GTP regulates trafficking of prenylated phototransduction proteins consistent with a role of ARL3-GTP as a cargo displacement factor (Hanke-Gogokhia et al., 2016; Wright et al., 2016). Retina-specific deletion of ARL3 disabled formation of connecting cilia and outer segments did not form (Fig. 13D, right panel, inset) (Hanke-Gogokhia et al., 2016). Absence of cilia in the knockout infers requirement of ARL3 for proper ciliogenesis and IFT, as shown in *C. elegans* where ARL3 was suggested to regulate IFT through a tubulin deacetylase pathway (Zhang et al., 2013; Li et al., 2010). Absence of cilia in ^{ret}*Arl3*^{-/-} photoreceptors leads to protein accumulation in the inner segment (Fig. 13E, right panel) and rapid degeneration (Fig. 13F, right panel). Ultrastructural analyses at P10 and P15 revealed normal rod photoreceptor ciliogenesis in control animals (Fig. 13G, H, left panels), and RPE, OS, IS, OLM and ONL are clearly distinguished. Basal bodies docked to the cell membrane, CCs extended and outer segment structures were elaborated. At P15, WT photoreceptor structure matures with nearly fully-developed outer segments and perfectly aligned basal bodies and CCs (Fig. 13H, left panel). By contrast, P10 ^{ret}*Arl3*^{-/-} photoreceptors revealed basal bodies docked to the cell membrane but without CCs (Fig. 13G, right panel), and similarly, P15 ^{ret}*Arl3*^{-/-} photoreceptors show ‘docked’ basal bodies with distal and subdistal appendages but no CCs (Fig. 13H, right panel).

ARL13b (ADP-ribosylation factor-like protein 13b) (JBTS8 ARL2L1, *hnn*)—

ARL13b (423 amino acids in human, 427 in mouse) is a small GTPase of the Ras superfamily (reviewed in (Zhang et al., 2013)) that is present in cilia and photoreceptor outer segments (Hanke-Gogokhia et al., 2017). ARL13b has a large G-domain, several coiled-coil domains and a C-terminal proline-rich region (Fig. 14A). Arl13b is palmitoylated at two cysteines near the N-terminal (Roy et al., 2017), a modification that is necessary for localization and stability. ARL13b was recently shown to function as a GEF for ARL3 (Gotthardt et al., 2015; Ivanova et al., 2017). The co-crystal structure of *C. reinhardtii* ARL13b and ARL3 G-domains (Fig. 14B) identifies a C-terminal helix and the switch II region (blue) as key for mediating GEF activity (Gotthardt et al., 2015).

Cilia of all mammalian tissues examined, including photoreceptors of the retina, expressed ARL13b (Higginbotham et al., 2013; Li et al., 2016b; Joiner et al., 2015; Kim et al., 2013). ARL13b mutations in the G-domain of the human *ARL13b* gene cause Joubert (Cantagrel et al., 2008; Thomas et al., 2015) and Bardet-Biedl syndromes (Fan et al., 2004). A splice-acceptor site mutation in exon 2 of mouse *Ar13b* (*hennin* mutation, Fig. 14A) was shown to be associated with defects in neural tube patterning, limbs and eyes, and homozygous mutants did not survive beyond E14.5 (Casparly et al., 2007). A kidney-specific deletion of *Ar13b* leads to kidney fibrosis (Li et al., 2016b). Zebrafish (“scorpion”) mutant *Ar13b*^{-/-} cilia showed truncated axonemes and defects in the sonic hedgehog signaling pathway suggesting a function of ARL13b in cilia formation (Sun et al., 2004; Duldulao et al., 2009; Seixas et al., 2016). Scorpion Arl13b mutants were shown to have shortened outer segments

and exhibit slowly progressing retina degeneration (Song et al., 2016). In *C. elegans*, ARL13b was implicated in the regulation of ciliary protein transport and anterograde IFT (Cevik et al., 2010; Li et al., 2010). In hTert-RPE cells, ARL13b was implicated in regulation of IFT-A mediated retrograde IFT (Nozaki et al., 2017).

In mouse photoreceptors, ARL13b is present exclusively in the outer segments (Fig. 14C), presumably anchored to discs by palmitoylation. In retina-specific deletions of ARL13b, rod and cone CCs were absent as evidenced by absence of CETN2 labeling (Fig. 14C, right panel). Rhodopsin was undetectable in mutant rods (Fig. 14D, b), but cone pigment expression persisted in the inner segments (Fig. 14D, d, f). Electron microscopy of ^{ret}*Ar113b*^{-/-} photoreceptors at P10 and P15 revealed docking of basal bodies to cell membranes and presence of distal appendages, but absence of mature CCs, axonemes and discs (Fig. 14E, b, d).

Tamoxifen-induction of Cre in the adult mouse led to impaired IFT and shortening of the axoneme, presumably by interfering with retrograde IFT (Hanke-Gogokhia et al., 2017). IFT88, an IFT-B particle required for anterograde IFT, is present at the tamoxifen-exposed ^{tam}*Ar113b*^{+/+} basal bodies (Fig. 14F, left panel, arrowheads) and proximal outer segments (Fig. 14F, arrows). However, IFT88 was significantly reduced or absent at the periciliary membrane of ^{tam}*Ar113b*^{-/-} photoreceptors (Fig. 14F, right panel, arrowheads). Quantitative evaluation (n=100) indicated 2–5-fold accumulation of IFT88 in the proximal OS in the face of a 5-fold reduction at the basal body, suggesting that IFT is impaired in the absence of ARL13b or ARL3-GTP. The connection between ARL3-GTP and IFT is unclear and remains to be elucidated, but interference with antero- and retrograde IFT could explain fully the progressive OS shortening and eventual photoreceptor degeneration in tamoxifen-induced ARL13b deletions.

IQCB1 (IQ-motif containing B1) (NPHP5, SLSN5)—IQCB1/NPHP5 (598 amino acids) has IQ calmodulin-binding motifs, central CC domains, BBSome interaction and a C-terminal CEP290 binding site (Fig. 15A) (Otto et al., 2005; Barbelanne et al., 2014; Barbelanne et al., 2013). IQCB1/NPHP5 distributes in the photoreceptor proximal outer segment (Hildebrandt et al., 1997; Ronquillo et al., 2016) (Fig. 15B) and to the basal body/CC in primary cilia of renal epithelial cells (Barbelanne et al., 2014; Barbelanne et al., 2013). IQCB1/NPHP5, calmodulin and RPGR co-precipitate, probably as a multiprotein complex (Otto et al., 2005; Murga-Zamalloa et al., 2010). IQCB1/NPHP5 interacts with RPGR indirectly (Anand and Khanna, 2012; Gerner et al., 2010) and with CEP290/NPHP6 directly (Schafer et al., 2008; Sang et al., 2011). *In-vitro* studies showed that CEP290-IQCB1/NPHP5 interaction is required for ciliogenesis (Barbelanne et al., 2013). *In-vivo*, CEP290 is undetectable in the germline *Iqcb1/Nphp5* knockout (Fig. 15C, right panel).

Mutations in the human *IQCB1/NPHP5* gene are the most common cause of SLS (Otto et al., 2005; Barbelanne et al., 2013; Halbritter et al., 2013; Chaki et al., 2011). Nephronophthisis presents with diminished kidney size, corticomedullary cysts and tubulointerstitial fibrosis (Wolf and Hildebrandt, 2011). *NPHP5* mutations have also been identified in non-syndromic LCA patients (Estrada-Cuzcano et al., 2011; Stone et al., 2011). The retina phenotype of IQCB1/NPHP5 -LCA is severe, as the outer nuclear layer (ONL) is

barely detectable in young patients (Cideciyan et al., 2011). Cone-Rod Dystrophy 2 (*crd2*) of the American Pit Bull Terrier carries a frameshift mutation in exon 10 of the canine *Iqcb1/Nphp5* gene truncating the *Iqcb1/Nphp5* gene at residue 318 (Goldstein et al., 2013). *Crd2* photoreceptors form outer segments early but are barely functioning at 6 weeks of age. By 14 weeks fewer than 10% of cones possess OS and ERGs are non-recordable (Downs et al., 2016). *Iqcb1/Nphp5* knockdown studies *in-vitro* show decreased numbers of primary cilia in hTert-RPE1 cells (Barbelanne et al., 2013; Sang et al., 2011). Morpholino-knockdown of *Iqcb1/Nphp5* in zebrafish shows development of pronephric cysts, and blocks trafficking of GFP tagged with a rhodopsin targeting signal but not GFP tagged with peripherin-2 targeting signal (Schafer et al., 2008; Zhao and Malicki, 2011). These results suggest that IQCB1/NPHP5, at least in immortalized cell lines, acts as an early positive regulator of ciliogenesis and its absence inhibits migration and/or anchoring of the basal body to the cell cortex (Barbelanne et al., 2013).

In germline *Iqcb1/Nphp5* knockout mice, photoreceptor CCs are stunted (Fig. 15B, C, D, right panels) and outer segments did not form. Knockout mice were blind at eye opening exhibiting LCA (Ronquillo et al., 2016), recapitulating the human pathology of rapid retinal degeneration. Basal bodies in *Iqcb1/Nphp5*^{-/-} photoreceptors docked to the cell membrane, but fully developed CCs did not form and outer segments failed to develop (Fig. 15D, right panel). Ultrastructure of P6 and P10 *Iqcb1/Nphp5*^{-/-} photoreceptors revealed aberrant CCs of reduced diameter. However, *Iqcb1/Nphp5*^{-/-} embryonic fibroblast (MEFs) and *Iqcb1/Nphp5*^{-/-} kidneys developed normal cilia (Ronquillo et al., 2016).

Iqcb1/Nphp5^{-/-} rod degeneration is complete at one month of age. By contrast, cone photoreceptor degeneration is delayed significantly, and cones survived in *Iqcb1/Nphp5*^{-/-}; *Nrl*^{-/-} double knockout mice up to six months. *Iqcb1/Nphp5*^{-/-}; *Nrl*^{-/-} cones expressed cone pigments and other outer segment proteins persistently in inner segments but did not degenerate. Gene replacement therapy with an scAAV8 vector expressing full length IQCB1/NPHP5 showed that connecting cilia and RP1-positive axonemes are re-formed and cone pigments and other cone outer segment proteins (cone transducin, cone PDE6) are present in the mutant cone outer segments, and rescued mutant cones exhibit a significant photopic b-wave (30% of double-het control) (Hanke-Gogokhia et al., 2018).

INPP5E (inositol polyphosphate-5-phosphatase E) (JBTS1, MORMS, Pharbin) —INPP5E (647 amino acids) is farnesylated and a peripheral membrane protein (Fig. 16A). It removes 5'-phosphates of phosphatidylinositol 3,4,5-trisphosphate (PI(3,4,5)P3) and phosphatidylinositol 3,5-bisphosphate (PI(3,4)P2) (Fig. 16B). INPP5E was shown to be located to the Golgi of COS-7 cells (Kong et al., 2000). INPP5E is present in cilia of hTert-RPE cells, mouse kidneys and cerebellum (Bielas et al., 2009), and mouse embryonic fibroblasts (MEFs) (Jacoby et al., 2009). In IMCD3 cells, targeting of INPP5E to Golgi was proposed to be PDEδ/ARL3-dependent, whereas targeting to cilia was ARL13b-dependent (Humbert et al., 2012). A three step mechanism regulating INPP5E (as an INPP5E-EGFP fusion protein) trafficking to and within IMCD3 cilia (farnesylation, PDEδ-and ARL3-dependent trafficking, and transfer to IFT cargo) has recently been postulated (Kosling et al., 2018). Presence of ciliary INPP5E replenishes PI4P in ciliary membranes; INPP5E loss-of-function replenishes PI(4,5)P2 in the plasma membrane (Phua et al., 2017).

Mutations in the human *INPP5E* gene are associated with Joubert and MORM syndromes (Bielas et al., 2009; Jacoby et al., 2009; Travaglini et al., 2013). Depletion of INPP5E in the adult mouse by tamoxifen-induction causes rapid photoreceptor degeneration. In fact, the photoreceptor layer was completely absent in tamoxifen-treated mice (Jacoby et al., 2009). Germline deletions of INPP5E are embryonically lethal (Dyson et al., 2017; Jacoby et al., 2009), and E15.5 embryos have no eyes. Conditional deletion of INPP5E in retina revealed that cilogenesis proceeds normally to P9. After P9 mutant photoreceptors rapidly degenerate (Sharif, Frederick and Baehr, unpublished).

Surprisingly, INPP5E was absent in mouse photoreceptor outer segments and localized to the proximal inner segment and Golgi (Bielas et al., 2009; Hanke-Gogokhia et al., 2016). Absence of INPP5E in the outer segment was verified by neonatal electroporation of an EGFP-INPP5E expression construct and colabeling with a Golgi marker, anti-giantin (Fig. 16C). INPP5E distributed to the perinuclear ER and Golgi apparatus (Fig. 16C, right panel), and was excluded from outer segments. This is incompatible with PDE δ -mediated trafficking of INPP5E to the OS, a pathway suggested in patients carrying a *PDE6D* null allele (Thomas et al., 2014). Presence of INPP5E in the Golgi, and its absence in the photoreceptor outer segment, implies a critical role for INPP5E in regulating Golgi-vesicular trafficking. It should be noted that when using isolated formalin-fixed rods, INPP5E was detectable strongly in the IS, but also, more weakly, in OS. Preliminary results with a photoreceptor-specific knockout of INPP5E indicate early, rapid photoreceptor degeneration with outer segment vesiculation (A. Sharif, J. Frederick, and W. Baehr, unpublished results).

4.3 Ciliary gene deletions that generate CC but fail to form OS.

This group contains two nephrocystins (NPHP1 and IQCB1/NPHP5), AHI1 (jouberin) and LCA5 (lebercilin). NPHP1, NPHP4 and LCA5 localize to the CC, and AHI1 is associated with the distal appendages of the basal body. Germline knockouts of NPHP1 and a null allele of NPHP4 cause rapid retinal degeneration, but not nephronophthisis. Germline deletion of AHI1 is associated with postnatal lethality while deletions of IQCB1/NPHP5 and LCA5 exhibit rapid LCA-like retina phenotypes.

NPHP1 (nephrocystin 1) (JBTS4)—NPHP1 (691 amino acids in mouse) is a protein with N-terminal and C-terminal coiled-coil domains, and a SH3 motif (SRC Homology 3 Domain) for protein-protein interaction (Fig. 17A). *Nphp1* was the first gene associated with nephronophthisis, discovered 20 years ago (Hildebrandt et al., 1997). Defects in the human gene are associated with Joubert and Senior-Løken syndromes. NPHP1 localizes to the TZ of renal and respiratory epithelia cilia and in photoreceptors was found in close proximity to the basal body (Fliegauf et al., 2006). In cell culture (mouse tracheal epithelial cells), high resolution STORM microscopy revealed NPHP1 is a TZ protein, arranged in a ring around the microtubule axoneme proximal to Y-links (Shi et al., 2017). Together with RFGRIPL, B9D1 and TMEM231, which form concentric rings of different diameters, NPHP1 appears to be part of the TZ gate (Shi et al., 2017). Targeted disruption of *Nphp1* in the mouse did not produce nephronophthisis, but caused male infertility and rapid retinal degeneration starting at P14-P21 (Jiang et al., 2008; Jiang et al., 2009). The *Nphp1*^{-/-} mice failed to develop normal outer segments but connecting cilia were present in the mutant

photoreceptors. Rhodopsin, transducin and other phototransduction proteins destined for the OS were predominantly located in the IS at P14, before significant degeneration of photoreceptor cells began (Jiang et al., 2008). IFT particles mislocalized along the connecting cilium. However, myosin VIIA, RPGR, KIF3A, centrin-1 and WDR19 localized normally to the connecting cilium.

AHI1 (Abelson Helper Integration site 1) (JBTS3, jouberin)—Jouberin (in human 1196 amino acids, longest transcript; in mouse, 1047 amino acids) has a weak N-terminal coiled-coil and a WD40 domain (Fig. 17B). *AHI1* gene mutations cause Joubert syndrome (Cheng et al., 2012), and missense mutations in the WD40 motif are associated with nonsyndromic *retinitis pigmentosa* (Nguyen et al., 2017). The *ahi1*lri46 mutation in zebrafish resulted in shorter cone outer segments, while the CC formed normally and CC2D2A and CEP290 localized properly (Lessieur et al., 2017). Deletion of AHI1 in mouse causes severe postnatal mortality. Photoreceptors failed to generate outer segments, but CC and axonemes were present (Louie et al., 2010; Westfall et al., 2010). AHI1 has been suggested to regulate cilium formation via its interaction with Rab8a, a small GTPase (Hsiao et al., 2009). AHI1 specifically localizes to the mother centriole, and knockdown of Ahi1 expression by shRNAi leads to impairments in ciliogenesis. Moreover, abnormal trafficking of endocytic vesicles from the plasma membrane to the Golgi were observed in Ahi1-knockdown cells (Hsiao et al., 2009). AHI1 has also been found to interact with HAP1 and NPHP1 (Tuz et al., 2013). Mutations in Ahi1 are suggested to destabilize AHI1 protein and alter cilium-mediated signaling through HAP1 and NPHP1 (Tuz et al., 2013).

NPHP4 (nephrocystin 4) (Nephroretinin) (POC10; SLSN4)—NPHP4 is a TZ protein consisting of 1425 amino acids (mouse). It does not reveal any recognizable Pfam motifs, but carries a RPGR-binding domain (RPGR-BD) and a proline-rich segment in the N-terminal half of the protein (Fig. 17C). In *C. reinhardtii*, NPHP4 is located in the distal part of the TZ, distal to CEP290, and is thought to regulate ciliary trafficking of membrane and soluble proteins (Awata et al., 2014). In mouse, NPHP4 interacts with the Retinitis GTPase Regulator (RPGR) and RPGR-Interacting Protein 1 (RPGRIP1) (Murga-Zamalloa et al., 2009; Roepman et al., 2005). Mutations in either *NPHP4* or *RPGRIP1* abolish this interaction (Roepman et al., 2005). A loss-of-function naturally occurring mouse model of *NPHP4* (*Nphp*^{nmfl92}) shows severe retinal degeneration reminiscent of LCA, with mislocalization of rhodopsin and ROM1 to the inner segment (Won et al., 2011). Connecting cilia and ribbon synapses developed normally, but outer segments failed to develop and ribbon structures eventually degenerated. However, as in *NPHP1* and *NPHP6* mouse mutants, no renal pathology was observed in the *Nphp*^{nmfl92} mouse (Chang et al., 2006; Jiang et al., 2008; Won et al., 2011).

LCA5, lebercilin (C6orf152)—Lebercilin (697 amino acids in human, 694 in mouse) is a protein with multiple coiled-coil domains in the N-terminal half (Fig. 17D) and is associated with LCA (den Hollander et al., 2007). It localizes to the CC in photoreceptors and interacts with IFT particles. Germline knockout (*Lca*^{5^{gt/gt}) showed that the basal body docked to the cell membrane and formed a CC (Boldt et al., 2011). Outer segments did not form and visual pigments in rods and cones mislocalized. Lebercilin interacted with proteins of the IFT-B}

complex and IFT140 (IFT-A complex), but localization of IFT20, IFT88 and IFT 140 was unaffected in the mutant. To date, mutations in lebercilin are only associated with LCA (non-syndromic ciliopathy phenotype).

4.4 Ciliary gene deletions that generate CC and OS, but outer segments are unstable.

This group contains mouse mutants which developed CC and OS but were unable to maintain outer segments. The mouse models are based on mutations in proteins which are selectively expressed in the retina (RPGR, RPGRIP1, SPATA7, FAM161A, PCARE and POC1b) and associated with RP and LCA. One gene, SDCCAG8 (NPHP10), is associated with syndromic ciliopathy. RPGR interacts with multiple proteins; its interaction with RPGRIP1 is essential for trafficking of RPGR to the CC (Zhao et al., 2003). RPGR cocrystallized with RPGRIP1 and PDE δ (PDE6D) (Watzlich et al., 2013; Remans et al., 2014). It likely serves as a docking station for PDE δ /lipidated protein/ARL3-GTP complexes, a key step in trafficking of lipidated proteins in rod and cone photoreceptors (see paragraph ARL3). SPATA7 interacts with NPHP4, NPHP1, AHI1, RPGR and RPGRIP1 and appears to be a key organizer of proteins associated with the photoreceptor-specific distal CC (Dharmat et al., 2018). In the absence of SPATA7, the MT structure of the distal CC spreads and falls apart, followed by retinal degeneration. FAM161A is strongly expressed in retina inner segments and the connecting cilium, and is thought to be involved in membrane protein trafficking from the Golgi to the CC (Karlstetter et al., 2014). PCARE is expressed in inner segments and the CC, its function is unknown. SDCCAG8 has been shown to interact with multiple proteins shown to be causative in inherited retinal degeneration, such as RPGRIP1, RPGR and NPHP4. However its function is controversial, as germline knockouts displayed multiple phenotypes ranging from embryonic and postnatal lethality to long-term survival (see paragraph SDCCAG8).

RPGR (*retinitis pigmentosa* GTPase regulator) (RP3, *rd9*)—RPGR is expressed as two major variants, the constitutive form (90 kDa) containing all exons 1–19 and the RPGR-Orf15 variant in which exon 15 is extended due to a splice donor mutation. RPGR carries an RCC1 domain and a CAAX motif at the C-terminus (Fig. 17E). The CAAX motif signals farnesylation and membrane attachment as a peripheral membrane protein. ORF15 contains repetitive Q- and G-rich regions and a basic domain (BD) at the C-terminus. The physiological function of RPGR is still unclear. The RLD domain (residues 1–392) was cocrystallized with RPGR-interacting domain (RID) of RPGRIP1 (Fig. 17K) and with PDE δ , the chaperone of lipidated proteins in photoreceptors (Watzlich et al., 2013; Remans et al., 2014). Interaction of RPGR with RPGRIP1 is essential for trafficking of RPGR to the CC (Zhao et al., 2003). RPGR is thought to function together with RPGRIP1 and CEP290 as a “ciliary gate” (Megaw et al., 2015), regulating trafficking through the “gate” and CC. Cocrystallization of RPGR with PDE δ suggests that RPGR may function as a docking station for lipidated cargo bound to PDE δ (Watzlich et al., 2013).

Mutations in the N-terminal RCC1 domain and in ORF15 in human are associated with classical XLRP, cone dystrophy, cone-rod dystrophy, and ciliopathy, also termed “RPGR disease” (reviewed in (Megaw et al., 2015; Shu et al., 2007)). RPGR is located to the CC by binding to RPGRIP1, a photoreceptor-specific protein (Zhao et al., 2003) and has multiple

binding partners, including PDE δ , NPHP4, CEP290, KIF3A and ARL3 (Megaw et al., 2015). Germline deletion of RPGR in mouse (exon 4–6 deletion) (Hong et al., 2000) and conditional exon 1 deletion (Huang et al., 2012) did not affect ciliogenesis. Mutant photoreceptors developed normally, but mutant discs are disorganized. Phototransduction component levels in the Hong knockout (Hong et al., 2000) are basically unaltered (Rao et al., 2015). A naturally occurring knockout mouse (*rd9*) with a 32 bp ORF15 duplication exhibited an even slower degeneration, starting around two months postnatally (Thompson et al., 2012). *Rd9* M-opsin mislocalized as early as at 2M postnatally, but S-opsin and rhodopsin localizations were normal. Two naturally occurring dog models, XLPRA1 and XLPRA2, have been reported (Guyon et al., 2007; Acland et al., 1994). XLPRA1 dogs carry a stop codon in the RPGR exon ORF15 associated with late onset XLRP. XLPRA2 dogs carry a frame-shift mutation in ORF15 causing a much more severe degeneration, starting a few weeks after birth (Zhang et al., 2002; Beltran et al., 2012).

RPGRIP1 (RPGR-interacting protein 1)—RPGRIP1 (Boylan and Wright, 2000) is a 144 kDa protein (1286 amino acids in human, 1331 in mouse) that interacts with the RCC1 domain of RPGR (Fig. 17K). Both human and mouse proteins colocalize to the photoreceptor CC. Null mutations in the human RPGRIP1 gene were found associated with recessive LCA (Dryja et al., 2001). RPGRIP1 contains three predicted coiled-coil domains, a C2-domain and a RPGR-interacting domain (RID) at the C-terminal region (Arts et al., 2009) (Fig. 17F). The interaction between RPGR and RPGRIP1 was impaired *in-vivo* by RP3-associated mutations in RPGR (Roepman et al., 2000). RPGRIP1 interacts with NPHP4 through the C2-domain, and their interaction is disrupted by LCA mutations in RPGRIP1 and by nephronophthisis mutations in NPHP4 (Roepman et al., 2005). Crystal structure of the complex between a RID fragment of RPGRIP1 and a RCC1 domain of RPGR (Fig. 17K) showed that the RID domain has a canonical β -sandwich structure consistent with a C2-domain. The RID β -sandwich does not bind Ca^{2+} and/or phospholipids and thus constitutes a unique type of protein-protein interaction module (Remans et al., 2014).

Rpgrip1 knockout mice (*Rpgrip1*^{-/-} or *Rpgrip1*^{tm1Tili}) (Zhao et al., 2003), truncated after exon 14 or after 500 residues) elaborate oversized and distorted outer segment discs, but ciliogenesis in mutant mice appears to be normal (Zhao et al., 2003; Won et al., 2009). Mice lacking RPGRIP1 and RPGR are phenotypically indistinguishable from mice lacking RPGRIP1s alone (Zhao et al., 2003). RPGR is absent in the CC of *Rpgrip1* knockout mice, but not vice versa (Zhao et al., 2003). AAV-mediated RPGRIP1 gene replacement preserved photoreceptor structure and function (Pawlyk et al., 2005) and restored the normal localization of RPGR (Pawlyk et al., 2010). An ENU-induced mouse model carrying a splice-acceptor site mutation in *Rpgrip1* (*Rpgrip1*^{nmf247}), resulting in deletion of exon 7 and a frame-shift, have a more severe phenotype and do not elaborate rod outer segments (Won et al., 2009). *Rpgrip1*^{nmf247} mice lack NPHP4 and RPGR in photoreceptor cilia (Patil et al., 2012). RPGRIP1 loss in photoreceptors shifts the subcellular partitioning of SDCCAG8/ NPHP10 and NPHP4 to the ER membrane (Patil et al., 2012). In an ENU-induced zebrafish model, rod outer segments were absent but cone outer segments developed (Raghupathy et al., 2017). A naturally occurring dog model (frame-shift in exon 2 of the *Rpgrip1* gene), by

contrast, developed rod and cone outer segments and displayed variable retina degeneration phenotypes (Mellersh et al., 2006).

SPATA7 (spermatogenesis-associated protein 7) (LCA3, HSD3)—The *SPATA7* gene was first identified in human spermatocytes, predicted to be involved in chromatin preparation in early meiotic prophase nuclei (Zhang et al., 2003). *SPATA7* is an acidic protein of 599 amino acids (582 in mouse), with N-terminal coiled-coil and C-terminal RPGRIP1-interacting domains (Fig. 17G). Homozygous nonsense and frame-shift mutations in *SPATA7* are associated with rod-cone dystrophy (Perrault et al., 2010; Wang et al., 2009a). *SPATA7* is a ciliary protein, localizes to the photoreceptor CC and interacts with RPGRIP1 (Eblimit et al., 2015). In *Spata7* knockout mice, ciliogenesis is normal but rhodopsin significantly mislocalizes to the ONL as early as P15. RPGRIP1 also mislocalizes supporting the idea that *SPATA7* is essential for RPGRIP1 localization to the CC. By contrast, PRPH2 localized normally to the OS, consistent with a trafficking pathway of PRPH2 distinct from rhodopsin (Tian et al., 2014). The knockout mouse phenotype is a juvenile recessive RP (Eblimit et al., 2015). By ultrastructure, OS are shortened at P15 and discs are disorganized. AAV8-based gene therapy ameliorated rod and cone photoreceptor loss in *Spata7*^{-/-} mice, but the treated retina still degenerated (Zhong et al., 2015). In *Spata7*^{-/-} mice, RPGRIP1 levels at the CC are reduced suggesting that *SPATA7* may be required for the stable assembly of the ciliary RPGRIP1 protein complex (Eblimit et al., 2015). Further analysis revealed that *SPATA7* together with RPGR and RPGRIP1 maintains the structure of the distal connecting cilium (DCC), a region specific for photoreceptors (Dharmat et al., 2018).

FAM161A (family with sequence similarity 161 member A) (RP28)—FAM161A (in human 716 amino acids, in mouse 700 (isoform x1)) is expressed predominantly in the retina. FAM161A homozygous nonsense mutations were found to be associated with RP28 (Langmann et al., 2008). Fam161a has multiple coiled-coil domains (Fig. 17H), localizes to photoreceptor cells during development and in the adult retina, is present in the inner segment and outer plexiform layer (Langmann et al., 2008). Immunofluorescence and immune-EM located FAM161A to the connecting cilium and centrioles (Zach et al., 2012). FAM161a directly interacts through its C-terminal moiety with lebercilin, CEP290, OFD1 and SDCCAG8 (Di Gioia et al., 2012). Interactions were also reported with POC1B associated with recessive cone-rod dystrophy (Roosing et al., 2014). Interactome analysis revealed that FAM161A is a member of a Golgi-centrosomal network interconnecting Golgi maintenance, intracellular transport and centrosome organization. (Di Gioia et al., 2015). In *Fam161a*^{GT/GT} mice, connecting cilia were shortened, photoreceptor outer segments were disorganized and the outer retina was completely absent at 6 months (Karlstetter et al., 2014). Centrin 3 was reduced and targeting of the Fam161a interactors, lebercilin and CEP290, was impaired. Outer segment cargo proteins, opsin and peripherin 2, were misrouted (Karlstetter et al., 2014).

PCARE (photoreceptor cilium actin regulator) (C2orf71, RP54)—PCARE is a large ciliary protein consisting of 1288 amino acids in human (1279 amino acids in mouse). PCARE carries a MGC amino terminus and a myristoylation consensus sequence; it is likely

myristoylated at glycine-2 and palmitoylated at C3 (Nishimura et al., 2010). The protein does not contain coiled-coil domains or other recognizable motifs of the Pfam protein families database (Finn et al., 2016). The amino acid sequence reveals Pro-rich (at position 1015–1067) and Ser-rich regions (at positions 1077–1133). Nonsense and missense mutation in the human *PCARE* gene are associated with non-syndromic RP (Audo et al., 2011; Gerth-Kahlert et al., 2017; Collin et al., 2010). PCARE is expressed in zebrafish photoreceptor connecting cilia (Corral-Serrano et al., 2015). Knockdown *C2orf71* expression in zebrafish results in visual defects (Nishimura et al., 2010). Loss of the *Pcare* gene in mouse caused severe degeneration as early as 3 weeks (Kevany et al., 2015). In *Pcare*^{-/-} mice, connecting cilia and disorganized outer segments were present at three weeks of age. In Gordon and Irish setter dogs with late on-set retinal atrophy, a novel PRA (progressive retina atrophy) locus was identified, termed rod–cone degeneration 4 (*rcd4*), in which a frame-shift mutation (C1051VfsX90) truncates PCARE (Downs et al., 2013). A stable *pcare1* mutant zebrafish model generated by CRISPR/CAS9 was recently generated (Corral-Serrano et al., 2018). Retinas of both embryonic (5 dpf) and adult (6 mpf) *pcare1* mutant zebrafish display disorganization of photoreceptor outer segments, resembling the phenotype observed in *Pcare*^{-/-} mice (Kevany et al., 2015).

C8ORF37 (RP64, BBS21, CORD16, smalltalk)—C8ORF37 (in human 207 amino acids, in mouse 209) is expressed ubiquitously. It has a Retinal Maintenance motif (RMP) covering most of its sequence, but its function is unknown (Estrada-Cuzcano et al., 2012). C8ORF37 is a cytoplasmic protein present in rod and cone inner segments (Sharif et al., 2018). Immunostaining using C8ORF37 antibodies suggested that C8ORF37 may be a ciliary protein as it localizes to the basal body (van Huet et al., 2013; Estrada-Cuzcano et al., 2012; Heon et al., 2016). Autosomal recessive mutations in C8ORF37 have been linked to *retinitis pigmentosa* (RP64), cone-rod dystrophy (CORD16) and Bardet-Biedl syndrome (BBS21) (Heon et al., 2016). Gene knockdown in zebrafish resulted in impaired visual behavior and defects in the formation of Kupffer’s vesicle (Heon et al., 2016). CRISPR/CAS9 knockout mouse models of *C8orf37* exhibit progressive and simultaneous degeneration of rod and cone photoreceptors (Sharif et al., 2018). The major ultrastructural feature of *C8orf37* knockout photoreceptors was disorganization of the outer segment discs which appear misaligned at the onset of disc morphogenesis; levels of OS-specific membrane proteins, including proteins involved in membrane disc organization, were reduced (Sharif et al., 2018). Extra-ocular phenotypes such as obesity and polydactyly were not observed. Considering the distribution of wildtype C8ORF37 throughout the photoreceptor cell body and its absence in the OS, the normal structure of the KO photoreceptor connecting cilium, and absence of defects in other ciliary organs of the KO mice, C8ORF37 may participate in the secretory pathway of membrane proteins destined for the OS (Sharif et al., 2018).

SDCCAG8 (serologically-defined colon cancer antigen 8) (NPHP10, BBS16, CCCAP, SLSN7)—SDCCAG8 is a centrosomal and TZ protein consisting of 713 amino acids in mouse. It was first cloned and characterized as a coiled-coil domain centrosome associated protein CCCAP (Kenedy et al., 2003). The C-terminal region allows for homodimerization of SDCCAG8 (Kenedy et al., 2003). SDCCAG8 also contains an N-

terminal globular domain that is connected to the coiled-coiled domains via a short helical sequence (Fig. 17I). Many mutations in the human *SDCCAG8* have been linked to syndromic ciliopathy with kidney and retinal dystrophies (Otto et al., 2010) and Bardet-Biedl syndrome (Schaefer et al., 2011). Most currently identified human patient mutations in *SDCCAG8* resulting in BBS occur within the first 7 of 8 coiled-coiled domains, transcribed from exons 4–16 (Otto et al., 2010). *SDCCAG8* has been shown to interact with multiple proteins causing inherited retinal degeneration, such as RPGRIP1, RPGR and NPHP4 (Patil et al., 2012).

An *Sdccag8* knockout mouse model carrying gene-trap cassette in intron 1 blocked expression of the 78 kDa and 83 kDa *SDCCAG8* protein isoforms in the retina (Airik et al., 2014). *Sdccag8* knockout mice were viable and photoreceptor outer segment shortening was observed at postnatal day 30 through immunohistochemistry, and loss of photoreceptor function was measured as a decrease in photopic electroretinogram (ERG) amplitude at postnatal day 100. Nephronophthisis was also observed (Airik et al., 2014). A second *Sdccag8* knockout mouse model was created by insertion of a gene-trap in intron 6 of the *Sdccag8* gene, resulting in polydactyly and early postnatal fatality (Insolera et al., 2014). Both models apparently eliminated expression of *SDCCAG8*, yet the viability phenotypes differ drastically. A third mouse model (*Sdccag8*^{SBT}) exhibiting hind limb polydactyly with very poor viability harbors a mutation created by random insertion of the pT2-BART3 transposon (Dharmat et al., 2018; Weihbrecht et al., 2018). Our lab created an *SDCCAG8* knockout mouse using CRISPR/CAS9 technology to create a 5bp deletion in exon 7 (Reed M and Baehr W, unpublished), resulting in a frame-shift. Early lethality, polydactyly and organ underdevelopment were observed, similar to the second gene-trap model (Insolera et al., 2014).

POC1B (POC1 centriolar protein B) (CORD20)—Proteome of the centriole (POC) 1 is a highly conserved centriole/basal body component that is involved in the assembly/stability of the centriole/basal body as well as ciliogenesis (Hames et al., 2008; Keller et al., 2009; Pearson and Winey, 2009). POC1 proteins have two functional domains connected by a spacer sequence (Fig. 17J). The N-terminal WD40 domain forms a 7-bladed β -propeller which is required for centrosome targeting (Hames et al., 2008; Keller et al., 2009). The C-terminal coiled-coil allows POC1 to interact with other proteins (Hames et al., 2008; Roosing et al., 2014). In vertebrates a gene duplication of POC1 resulted in two paralogues, POC1A and POC1B (previously called Pix2 and Pix1) (Keller et al., 2009). Human patient mutations in *POC1A* have been shown to be causative for a ciliopathy characterized by primordial dwarfism termed SOFT syndrome (short stature, onychodysplasia, facial dysmorphism, and hypotrichosis) (Shaheen et al., 2012; Sarig et al., 2012). A LINE-1 retrotransposon-mediated insertion into the mouse *Poc1a* gene resulted in mice with impaired cilia formation, multipolar spindles, growth insufficiency, and male infertility (Geister et al., 2015). A homozygous POC1B missense mutation p.Arg106Pro that prevents the formation of the third WD40 repeat of POC1B was found in affected individuals in a consanguineous family with a high incidence of LCA, Joubert syndrome and polycystic kidney disease (Beck et al., 2014). Knockdown of *Poc1b* in zebrafish using morpholino injection resulted in shortened and disorganized photoreceptors (Roosing et al., 2014; Zhang

et al., 2015). Another study found that the number and length of connecting cilia, as well as inner segment length, is also reduced in morphant larvae (Beck et al., 2014).

5. Epilogue

The centrosome and basal body are the major microtubule-organizing centers of dividing and postmitotic cells, respectively. Complexity of their biogenesis, duplication and maintenance is astounding: numerous genes and proteins with largely unknown function are necessary to build these cytoplasmic structures. This report reviews select centrosomal and CC/TZ-associated genes to highlight their importance for centrosome biogenesis and early events of ciliogenesis. As we selected a limited number of genes, the functions of which are poorly understood or completely unknown, the selection is necessarily subjective and thus incomplete. Another intent was to examine individual components through the eyes of a biochemist and to dissect protein domain structures augmented by crystallography, if available.

Progress in ciliary gene identification, propelled by sophisticated protein interaction methods and proteomics, has been explosive over the last decade. Much progress is based on tissue culture experiments with IMCD3, RPE or immortalized tumor cells. Primary cilia of cultured cells, however, are distinct from primary cilia *in-vivo*, e.g., cilia of olfactory sensory neurons or photoreceptors. Such cilia have precise functions (olfaction and vision) and have adapted through millennia of evolution to current conditions. While many cellular functions, such as centrosome formation, microtubule organization and IFT have been conserved throughout evolution, individual cilia have adapted pathways according to their specialized sensory loads.

The light-sensitive cilium of photoreceptors, consisting of an outer segment, CC and the basal body/axoneme backbone, is a highly specialized primary cilium. The outer segment which performs photoreception and transduction, has a much larger volume than primary cilia of kidney epithelial or RPE cells. The CC can be divided into proximal and distal parts (Dharmat et al., 2018), where the distal part is photoreceptor-specific. The outer segment has a very high concentration of rhodopsin and its chromophore, 11-cis retinal (3–8 mM). Photolysis of retinal during photoreception generates toxic adducts which must be removed. Outer segment membrane is replaced every 10 days, requiring highly active membrane protein transport. Renewal is achieved by disc assembly/morphogenesis at the proximal end of the outer segment with concomitant disc shedding distally, with phagocytosis of shed disc membrane mediated by RPE apical processes. Daily renewal of 10% (~100 discs) of the outer segment membrane requires very active metabolism, i.e., persisting high rate of biosynthesis to replace OS proteins, with reliable transport and targeting pathways. Therefore, it is unsurprising that photoreceptors during their long evolution have optimized tools (proteins) to generate and maintain cilia, and develop specific trafficking pathways for membrane-bound and soluble proteins.

We emphasize here some differences between primary cilia and photoreceptor cilia, focusing on CETN2, CP110 and CC2D2A. Mouse CETN2 (see chapter on centrins) is nonessential for ciliogenesis as formations of both primary cilia (renal tubule epithelia, photoreceptors)

and motile cilia (multiciliated respiratory epithelia, ependymal epithelia) proceed normally in *Cetn2* germline knockouts (Ying, et al, 2014). However, the *in-vivo* result contradicts an *in-vitro* study showing that CRISPR/CAS9 disruption of *Cetn2* in hTERT-RPE1 cells leads to dramatically reduced ciliogenesis due to impaired removal of CP110 (a known basal body distal end cap and ciliation inhibitor) assayed via serum starvation-induced ciliogenesis. Also in cell culture, loss of CEP97 and CP110 promotes primary cilia formation in growing cells, suggesting that CP110 is a negative regulator of ciliogenesis (its presence prevents cilia formation; its absence induces cilia formation) (see CP110 paragraph). By contrast, photoreceptor CP110 is required for basal body anchoring to the plasma membrane and promotes cilia formation, acting as a positive regulator.

In a zebrafish *Cc2d2a* null mutant (see CC2D2A paragraph), *sentinel* (W628X), (Bachmann-Gagescu et al., 2012; Mougou-Zerelli et al., 2009), mutant rods and cones formed cilia but outer segments were shortened and rhodopsin and cone pigments mislocalized. Rab8-coated vesicles accumulated at the apical inner segments suggesting CC2D2A is important for membrane protein trafficking in zebrafish. In a recent paper, Naharros et al show that CC2D2A plays a role in docking of opsin-carrying vesicles at the periciliary membrane (Ojeda Naharros et al., 2017). By contrast, the *Cc2d2a*^{-/-} mouse recapitulates features of Meckel syndrome with multiorgan defects (Veleri et al., 2014). Loss of CC2D2A leads to embryonic lethality; embryos often show polydactyly, exencephaly and *situs inversus*. Cilia are absent in *Cc2d2a* embryonic node and other somatic tissues. The conclusion of the mouse CC2D2A knockout was that CC2D2A is essential for the assembly of subdistal appendages, which anchor cytoplasmic microtubules and prime the mother centriole for axoneme biogenesis (Veleri et al., 2014).

Future directions

From a photoreceptor development and disease perspective, germline knockouts using CRISPR/CAS9 and conditional knockouts of BB- and CC/TZ-associated genes (using one of various retina-, rod-, cone-, or RPE-specific Cre drivers) remain promising, as the mouse knockout phenotype provides important clues of wildtype gene function. Mutant mice with floxed genes can be generated relatively easily from commercially-available ESC lines carrying gene traps with conditional possibilities. Recent developments using CRISPR/CAS9 to ‘knock in’ exons with flanking loxP sites for conditional deletion are quite exciting but of poor efficiency. However, technology such as Easi-CRISPR (“efficient additions with single-stranded DNA inserts”) promises to be much more efficient, thus reducing the cost of generating conditional knockouts (Miura et al., 2018; Quadros et al., 2017). We anticipate that research focusing on centrioles, CC/TZ and syndromic/non-syndromic ciliopathies will continue to expand in view of the importance of untreatable human disease. Further, gene mutations introduced into animal models by gene editing (DiCarlo et al., 2018; DiCarlo et al., 2017) will provide cornerstones toward understanding disease mechanisms and developing gene replacement therapy.

Acknowledgements.

This work was supported in part by NIH grants EY08123, EY019298 (WB); unrestricted grants to the University of Utah Department of Ophthalmology from Research to Prevent Blindness (RPB; New York). WB is the recipient of

an RPB Senior Investigator award, a RPB Nelson Trust Award, and an award from the Retina Research Foundation (Alice McPherson, MD), Houston. Michelle Reed and Tiffanie Dahl were stipend recipients from the T32 training grant in 2016 and 2017, respectively.

Abbreviations

BB	basal body
BBS	Bardet-Biedl syndrome
CC	connecting cilium
CD	coiled-coil domain
C2	C2 domain for protein-protein or protein membrane interaction
DA	distal appendages
DC	daughter centriole
ER	endoplasmic reticulum
IS	inner segment
LCA	Leber congenital amaurosis
IFT	intraflagellar transport
JS	Joubert syndrome
MC	mother centriole
MKS	Meckel syndrome
MT	microtubules
MTOC	microtubule organization center
NPHP	nephronophthisis
PCM	pericentriolar matrix
OFD	orofacioidigital syndrome
OS	outer segment
RP	retinitis pigmentosa
SLS	Senior Løken syndrome
SDA	subdistal appendages
TZ	transition zone

Reference List

1. Acland GM, Blanton SH, Hershfield B, and Aguires GD (1994). XLPPRA: a canine retinal degeneration inherited as an X-linked trait. *Am. J. Med. Genet* 52, 27–33. [PubMed: 7977457]
2. Adly N, Alhashem A, Ammari A, and Alkuraya FS (2014). Ciliary genes TBC1D32/C6orf170 and SCLT1 are mutated in patients with OFD type IX. *Hum. Mutat* 35, 36–40. [PubMed: 24285566]
3. Airik R, Slaats GG, Guo Z, Weiss AC, Khan N, Ghosh A, Hurd TW, Bekker-Jensen S, Schroder JM, Elledge SJ, Andersen JS, Kispert A, Castelli M, Boletta A, Giles RH, and Hildebrandt F (2014). Renal-retinal ciliopathy gene Sdccag8 regulates DNA damage response signaling. *J. Am. Soc. Nephrol* 25, 2573–2583. [PubMed: 24722439]
4. Aldaz H, Rice LM, Stearns T, and Agard DA (2005). Insights into microtubule nucleation from the crystal structure of human gamma-tubulin. *Nature* 435, 523–527. [PubMed: 15917813]
5. Anand M and Khanna H (2012). Ciliary transition zone (TZ) proteins RPGR and CEP290: role in photoreceptor cilia and degenerative diseases. *Expert. Opin. Ther. Targets* 16, 541–551. [PubMed: 22563985]
6. Andersen JS, Wilkinson CJ, Mayor T, Mortensen P, Nigg EA, and Mann M (2003). Proteomic characterization of the human centrosome by protein correlation profiling. *Nature* 426, 570–574. [PubMed: 14654843]
7. Arquint C and Nigg EA (2016). The PLK4-STIL-SAS-6 module at the core of centriole duplication. *Biochem. Soc. Trans* 44, 1253–1263. [PubMed: 27911707]
8. Arts HH, Cremers FP, Knoers NV, and Roepman R (2009). Focus on molecules: RPEGRIPI. *Exp. Eye Res* 88, 332–333. [PubMed: 18538322]
9. Audo I, Lancelot ME, Mohand-Said S, Antonio A, Germain A, Sahel JA, Bhattacharya SS, and Zeitz C (2011). Novel C2orf71 mutations account for approximately 1% of cases in a large French arRP cohort. *Hum. Mutat* 32, E2091–E2103. [PubMed: 21412943]
10. Avasthi P, Scheel JF, Ying G, Frederick JM, Baehr W, and Wolfrum U (2013). Germline deletion of *Cetn1* causes infertility in male mice. *J. Cell Sci* 126, 3204–3213. [PubMed: 23641067]
11. Avasthi P, Watt CB, Williams DS, Le YZ, Li S, Chen CK, Marc RE, Frederick JM, and Baehr W (2009). Trafficking of membrane proteins to cone but not rod outer segments is dependent on heterotrimeric kinesin-II. *J. Neurosci* 29, 14287–14298. [PubMed: 19906976]
12. Avidor-Reiss T and Gopalakrishnan J (2013). Building a centriole. *Curr. Opin. Cell Biol* 25, 72–77. [PubMed: 23199753]
13. Awata J, Takada S, Standley C, Lehtreck KF, Bellve KD, Pazour GJ, Fogarty KE, and Witman GB (2014). NPHP4 controls ciliary trafficking of membrane proteins and large soluble proteins at the transition zone. *J. Cell Sci* 127, 4714–4727. [PubMed: 25150219]
14. Baala L, Audollent S, Martinovic J, Ozilou C, Babron MC, Sivanandamoorthy S, Saunier S, Salomon R, Gonzales M, Rattenberry E, Esculpavit C, Toutain A, Moraine C, Parent P, Marcocelles P, Dauge MC, Roume J, Le MM, Meiner V, Meir K, Menez F, Beaufriere AM, Francannet C, Tantau J, Sinico M, Dumez Y, Macdonald F, Munnich A, Lyonnet S, Gubler MC, Genin E, Johnson CA, Vekemans M, Encha-Razavi F, and Attie-Bitach T (2007). Pleiotropic effects of CEP290 (NPHP6) mutations extend to Meckel syndrome. *Am. J. Hum. Genet* 81, 170–179. [PubMed: 17564974]
15. Bachmann-Gagescu R, Dona M, Hetterschijt L, Tonnaer E, Peters T, de VE, Mans DA, van Beersum SE, Phelps IG, Arts HH, Keunen JE, Ueffing M, Roepman R, Boldt K, Doherty D, Moens CB, Neuhauss SC, Kremer H, and van WE (2015). The Ciliopathy Protein CC2D2A Associates with NINL and Functions in RAB8-MICAL3-Regulated Vesicle Trafficking. *PLoS. Genet* 11, e1005575. [PubMed: 26485645]
16. Bachmann-Gagescu R, Ishak GE, Dempsey JC, Adkins J, O'Day D, Phelps IG, Gunay-Aygun M, Kline AD, Szczaluba K, Martorell L, Alswaid A, Alrasheed S, Pai S, Izatt L, Ronan A, Parisi MA, Mefford H, Glass I, and Doherty D (2012). Genotype-phenotype correlation in CC2D2A-related Joubert syndrome reveals an association with ventriculomegaly and seizures. *J. Med. Genet* 49, 126–137. [PubMed: 22241855]
17. Bader JR, Kusik BW, and Besharse JC (2012). Analysis of KIF17 distal tip trafficking in zebrafish cone photoreceptors. *Vision Res* 75, 37–43. [PubMed: 23099049]

18. Baker SA, Freeman K, Luby-Phelps K, Pazour GJ, and Besharse JC (2003). IFT20 links kinesin II with a mammalian intraflagellar transport complex that is conserved in motile flagella and sensory cilia. *J. Biol. Chem* 278, 34211–34218. [PubMed: 12821668]
19. Banterle N and Gonczy P (2017). Centriole Biogenesis: From Identifying the Characters to Understanding the Plot. *Annu. Rev. Cell Dev. Biol* 33, 23–49. [PubMed: 28813178]
20. Barbelanne M, Hossain D, Chan DP, Peranen J, and Tsang WY (2014). Nephrocystin proteins NPHP5 and Cep290 regulate BBSome integrity, ciliary trafficking and cargo delivery. *Hum. Mol. Genet*
21. Barbelanne M, Song J, Ahmadzai M, and Tsang WY (2013). Pathogenic NPHP5 mutations impair protein interaction with Cep290, a prerequisite for ciliogenesis. *Hum. Mol. Genet* 22, 2482–2494. [PubMed: 23446637]
22. Barenz F, Mayilo D, and Gruss OJ (2011). Centriolar satellites: busy orbits around the centrosome. *Eur. J. Cell Biol* 90, 983–989. [PubMed: 21945726]
23. Barker AR, Renzaglia KS, Fry K, and Dawe HR (2014). Bioinformatic analysis of ciliary transition zone proteins reveals insights into the evolution of ciliopathy networks. *BMC. Genomics* 15, 531. [PubMed: 24969356]
24. Baylor DA, Lamb TD, and Yau KW (1979). Responses of retinal rods to single photons. *J Physiol* 288, 613–634. [PubMed: 112243]
25. Beck BB, Phillips JB, Bartram MP, Wegner J, Thoenes M, Pannes A, Sampson J, Heller R, Gobel H, Koerber F, Neugebauer A, Hedergott A, Nurnberg G, Nurnberg P, Thiele H, Altmuller J, Toliat MR, Staubach S, Boycott KM, Valente EM, Janecke AR, Eisenberger T, Bergmann C, Tebbe L, Wang Y, Wu Y, Fry AM, Westerfield M, Wolfrum U, and Bolz HJ (2014). Mutation of POC1B in a severe syndromic retinal ciliopathy. *Hum. Mutat* 35, 1153–1162. [PubMed: 25044745]
26. Beltran WA, Cideciyan AV, Lewin AS, Iwabe S, Khanna H, Sumaroka A, Chiodo VA, Fajardo DS, Roman AJ, Deng WT, Swider M, Aleman TS, Boye SL, Genini S, Swaroop A, Hauswirth WW, Jacobson SG, and Aguirre GD (2012). Gene therapy rescues photoreceptor blindness in dogs and paves the way for treating human X-linked retinitis pigmentosa. *Proc. Natl. Acad. Sci. U. S. A* 109, 2132–2137. [PubMed: 22308428]
27. Bettencourt-Dias M and Carvalho-Santos Z (2008). Double life of centrioles: CP110 in the spotlight. *Trends Cell Biol* 18, 8–11. [PubMed: 18068367]
28. Bettencourt-Dias M, Hildebrandt F, Pellman D, Woods G, and Godinho SA (2011). Centrosomes and cilia in human disease. *Trends Genet* 27, 307–315. [PubMed: 21680046]
29. Bielas SL, Silhavy JL, Brancati F, Kisseleva MV, Al-Gazali L, Sztriha L, Bayoumi RA, Zaki MS, Abdel-Aleem A, Rosti RO, Kayserili H, Swistun D, Scott LC, Bertini E, Boltshauser E, Fazzi E, Travaglini L, Field SJ, Gayral S, Jacoby M, Schurmans S, Dallapiccola B, Majerus PW, Valente EM, and Gleeson JG (2009). Mutations in INPP5E, encoding inositol polyphosphate-5-phosphatase E, link phosphatidyl inositol signaling to the ciliopathies. *Nat. Genet* 41, 1032–1036. [PubMed: 19668216]
30. Blacque OE and Leroux MR (2006). Bardet-Biedl syndrome: an emerging pathomechanism of intracellular transport. *Cell Mol. Life Sci* 63, 2145–2161. [PubMed: 16909204]
31. Boldt K, Mans DA, Won J, van RJ, Vogt A, Kinkl N, Letteboer SJ, Hicks WL, Hurd RE, Naggert JK, Texier Y, den Hollander AI, Koenekoop RK, Bennett J, Cremers FP, Gloeckner CJ, Nishina PM, Roepman R, and Ueffing M (2011). Disruption of intraflagellar protein transport in photoreceptor cilia causes Leber congenital amaurosis in humans and mice. *J. Clin. Invest* 121, 2169–2180. [PubMed: 21606596]
32. Boldt K, van RJ, Lu Q, Koutroumpas K, Nguyen TM, Texier Y, van Beersum SE, Horn N, Willer JR, Mans DA, Dougherty G, Lamers IJ, Coene KL, Arts HH, Betts MJ, Beyer T, Bolat E, Gloeckner CJ, Haidari K, Hettterschijt L, Iaconis D, Jenkins D, Klose F, Knapp B, Latour B, Letteboer SJ, Marcelis CL, Mitic D, Morleo M, Oud MM, Riemersma M, Rix S, Terhal PA, Toedt G, van Dam TJ, de VE, Wissinger Y, Wu KM, Apic G, Beales PL, Blacque OE, Gibson TJ, Huynen MA, Katsanis N, Kremer H, Omran H, van WE, Wolfrum U, Kepes F, Davis EE, Franco B, Giles RH, Ueffing M, Russell RB, and Roepman R (2016). An organelle-specific protein landscape identifies novel diseases and molecular mechanisms. *Nat. Commun* 7, 11491. [PubMed: 27173435]

33. Bouckson-Castaing V, Moudjou M, Ferguson DJ, Mucklow S, Belkaid Y, Milon G, and Crocker PR (1996). Molecular characterisation of ninein, a new coiled-coil protein of the centrosome. *J. Cell Sci* 109 (Pt 1), 179–190. [PubMed: 8834802]
34. Boye SE, Huang WC, Roman AJ, Sumaroka A, Boye SL, Ryals RC, Olivares MB, Ruan Q, Tucker BA, Stone EM, Swaroop A, Cideciyan AV, Hauswirth WW, and Jacobson SG (2014). Natural history of cone disease in the murine model of Leber congenital amaurosis due to CEP290 mutation: determining the timing and expectation of therapy. *PLoS. ONE* 9, e92928. [PubMed: 24671090]
35. Boylan JP and Wright AF (2000). Identification of a novel protein interacting with RPGR. *Hum. Mol. Genet* 9, 2085–2093. [PubMed: 10958647]
36. Burgoyne T, Meschede IP, Burden JJ, Bailly M, Seabra MC, and Futter CE (2015). Rod disc renewal occurs by evagination of the ciliary plasma membrane that makes cadherin-based contacts with the inner segment. *Proc. Natl. Acad. Sci. U. S. A* 112, 15922–15927. [PubMed: 26668363]
37. Burnight ER, Wiley LA, Drack AV, Braun TA, Anfinson KR, Kaalberg EE, Halder JA, Affatigato LM, Mullins RF, Stone EM, and Tucker BA (2014). CEP290 gene transfer rescues Leber congenital amaurosis cellular phenotype. *Gene Ther* 21, 662–672. [PubMed: 24807808]
38. Cajanek L and Nigg EA (2014). Cep164 triggers ciliogenesis by recruiting Tau tubulin kinase 2 to the mother centriole. *Proc. Natl. Acad. Sci. U. S. A* 111, E2841–E2850. [PubMed: 24982133]
39. Cantagrel V, Silhavy JL, Bielas SL, Swistun D, Marsh SE, Bertrand JY, Audollent S, Attie-Bitach T, Holden KR, Dobyns WB, Traver D, Al-Gazali L, Ali BR, Lindner TH, Caspary T, Otto EA, Hildebrandt F, Glass IA, Logan CV, Johnson CA, Bennett C, Brancati F, Valente EM, Woods CG, and Gleeson JG (2008). Mutations in the cilia gene ARL13B lead to the classical form of Joubert syndrome. *Am. J. Hum. Genet* 83, 170–179. [PubMed: 18674751]
40. Casenghi M, Meraldi P, Weinhart U, Duncan PI, Korner R, and Nigg EA (2003). Polo-like kinase 1 regulates Nlp, a centrosome protein involved in microtubule nucleation. *Dev. Cell* 5, 113–125. [PubMed: 12852856]
41. Caspary T, Larkins CE, and Anderson KV (2007). The graded response to Sonic Hedgehog depends on cilia architecture. *Dev. Cell* 12, 767–778. [PubMed: 17488627]
42. Cevik S, Hori Y, Kaplan OI, Kida K, Toivenon T, Foley-Fisher C, Cottell D, Katada T, Kontani K, and Blacque OE (2010). Joubert syndrome Arl13b functions at ciliary membranes and stabilizes protein transport in *Caenorhabditis elegans*. *J. Cell Biol* 188, 953–969. [PubMed: 20231383]
43. Chaki M, Airik R, Ghosh AK, Giles RH, Chen R, Slaats GG, Wang H, Hurd TW, Zhou W, Cluckey A, Gee HY, Ramaswami G, Hong CJ, Hamilton BA, Cervenka I, Ganji RS, Bryja V, Arts HH, van RJ, Oud MM, Letteboer SJ, Roepman R, Husson H, Ibraghimov-Beskrovnaya O, Yasunaga T, Walz G, Eley L, Sayer JA, Schermer B, Liebau MC, Benzing T, Le CS, Drummond I, Janssen S, Allen SJ, Natarajan S, O'Toole JF, Attanasio M, Saunier S, Antignac C, Koenekoop RK, Ren H, Lopez I, Nayir A, Stoetzel C, Dollfus H, Massoudi R, Gleeson JG, Andreoli SP, Doherty DG, Lindstrad A, Golzio C, Katsanis N, Pape L, Abboud EB, Al-Rajhi AA, Lewis RA, Omran H, Lee EY, Wang S, Sekiguchi JM, Saunders R, Johnson CA, Garner E, Vanselow K, Andersen JS, Shlomag J, Nurnberg G, Nurnberg P, Levy S, Smogorzewska A, Otto EA, and Hildebrandt F (2012). Exome capture reveals ZNF423 and CEP164 mutations, linking renal ciliopathies to DNA damage response signaling. *Cell* 150, 533–548. [PubMed: 22863007]
44. Chaki M, Hoefele J, Allen SJ, Ramaswami G, Janssen S, Bergmann C, Heckenlively JR, Otto EA, and Hildebrandt F (2011). Genotype-phenotype correlation in 440 patients with NPHP-related ciliopathies. *Kidney Int* 80, 1239–1245. [PubMed: 21866095]
45. Chang B, Khanna H, Hawes N, Jimeno D, He S, Lillo C, Parapuram SK, Cheng H, Scott A, Hurd RE, Sayer JA, Otto EA, Attanasio M, O'Toole JF, Jin G, Shou C, Hildebrandt F, Williams DS, Heckenlively JR, and Swaroop A (2006). In-frame deletion in a novel centrosomal/ciliary protein CEP290/NPHP6 perturbs its interaction with RPGR and results in early-onset retinal degeneration in the rd16 mouse. *Hum. Mol. Genet* 15, 1847–1857. [PubMed: 16632484]
46. Chang J, Seo SG, Lee KH, Nagashima K, Bang JK, Kim BY, Erikson RL, Lee KW, Lee HJ, Park JE, and Lee KS (2013). Essential role of Cenexin1, but not Odf2, in ciliogenesis. *Cell Cycle* 12, 655–662. [PubMed: 23343771]
47. Chang P, Giddings TH Jr., Winey M, and Stearns T (2003). Epsilon-tubulin is required for centriole duplication and microtubule organization. *Nat. Cell Biol* 5, 71–76. [PubMed: 12510196]

48. Chang P and Stearns T (2000). Delta-tubulin and epsilon-tubulin: two new human centrosomal tubulins reveal new aspects of centrosome structure and function. *Nat. Cell Biol* 2, 30–35. [PubMed: 10620804]
49. Chavali PL, Chandrasekaran G, Barr AR, Tatrai P, Taylor C, Papachristou EK, Woods CG, Chavali S, and Gergely F (2016). A CEP215-HSET complex links centrosomes with spindle poles and drives centrosome clustering in cancer. *Nat. Commun* 7, 11005. [PubMed: 26987684]
50. Chen CT, Hehnlly H, Yu Q, Farkas D, Zheng G, Redick SD, Hung HF, Samtani R, Jurczyk A, Akbarian S, Wise C, Jackson A, Bober M, Guo Y, Lo C, and Doxsey S (2014). A unique set of centrosome proteins requires pericentrin for spindle-pole localization and spindle orientation. *Curr. Biol* 24, 2327–2334. [PubMed: 25220058]
51. Chen HJ, Lin CM, Lin CS, Perez-Olle R, Leung CL, and Liem RK (2006). The role of microtubule actin cross-linking factor 1 (MACF1) in the Wnt signaling pathway. *Genes Dev* 20, 1933–1945. [PubMed: 16815997]
52. Chen Z, Indjeian VB, McManus M, Wang L, and Dynlacht BD (2002). CP110, a cell cycle-dependent CDK substrate, regulates centrosome duplication in human cells. *Dev. Cell* 3, 339–350. [PubMed: 12361598]
53. Cheng YZ, Eley L, Hynes AM, Overman LM, Simms RJ, Barker A, Dawe HR, Lindsay S, and Sayer JA (2012). Investigating embryonic expression patterns and evolution of AHI1 and CEP290 genes, implicated in Joubert syndrome. *PLoS. ONE* 7, e44975. [PubMed: 23028714]
54. Ching YP, Qi Z, and Wang JH (2000). Cloning of three novel neuronal Cdk5 activator binding proteins. *Gene* 242, 285–294. [PubMed: 10721722]
55. Cideciyan AV, Rachel RA, Aleman TS, Swider M, Schwartz SB, Sumaroka A, Roman AJ, Stone EM, Jacobson SG, and Swaroop A (2011). Cone photoreceptors are the main targets for gene therapy of NPHP5 (IQCB1) or NPHP6 (CEP290) blindness: generation of an all-cone Nphp6 hypomorph mouse that mimics the human retinal ciliopathy. *Hum. Mol. Genet* 20, 1411–1423. [PubMed: 21245082]
56. Cole DG, Cande WZ, Baskin RJ, Skoufias DA, Hogan CJ, and Scholey JM (1992). Isolation of a sea urchin egg kinesin-related protein using peptide antibodies. *J Cell Sci* 101 (Pt 2), 291–301. [PubMed: 1629246]
57. Cole DG, Diener DR, Himelblau AL, Beech PL, Fuster JC, and Rosenbaum JL (1998). Chlamydomonas kinesin-II-dependent intraflagellar transport (IFT): IFT particles contain proteins required for ciliary assembly in *Caenorhabditis elegans* sensory neurons. *J Cell Biol* 141, 993–1008. [PubMed: 9585417]
58. Collin RW and Garanto A (2017). Applications of antisense oligonucleotides for the treatment of inherited retinal diseases. *Curr. Opin. Ophthalmol* 28, 260–266. [PubMed: 28151748]
59. Collin RW, Safieh C, Littink KW, Shalev SA, Garzosi HJ, Rizel L, Abbasi AH, Cremers FP, den Hollander AI, Klevering BJ, and Ben-Yosef T (2010). Mutations in C2ORF71 cause autosomal-recessive retinitis pigmentosa. *Am. J. Hum. Genet* 86, 783–788. [PubMed: 20398884]
60. Coppieters F, Lefever S, Leroy BP, and De BE (2010). CEP290, a gene with many faces: mutation overview and presentation of CEP290base. *Hum. Mutat* 31, 1097–1108. [PubMed: 20690115]
61. Corral-Serrano JC, Letteboer S, Garanto A, and Roepman R (2015). Investigating the role of C2orf71 in the pathogenesis of retinitis pigmentosa. *IOVS* 56, 4643.
62. Corral-Serrano JC, Messchaert M, Dona M, Peters TA, Kamminga LM, van WE, and Collin RWJ (2018). C2orf71/pcare1 is important for photoreceptor outer segment morphogenesis and visual function in zebrafish. *Sci. Rep* 8, 9675. [PubMed: 29946172]
63. Cortes CR, McInerney-Leo AM, Vogel I, Rondon Galeano MC, Leo PJ, Harris JE, Anderson LK, Keith PA, Brown MA, Ramsing M, Duncan EL, Zankl A, and Wicking C (2016). Mutations in human C2CD3 cause skeletal dysplasia and provide new insights into phenotypic and cellular consequences of altered C2CD3 function. *Sci. Rep* 6, 24083. [PubMed: 27094867]
64. Craige B, Tsao CC, Diener DR, Hou Y, Lechtreck KF, Rosenbaum JL, and Witman GB (2010). CEP290 tethers flagellar transition zone microtubules to the membrane and regulates flagellar protein content. *J. Cell Biol* 190, 927–940. [PubMed: 20819941]

65. Daly OM, Gaboriau D, Karakaya K, King S, Dantas TJ, Lalor P, Dockery P, Kramer A, and Morrison CG (2016). CEP164-null cells generated by genome editing show a ciliation defect with intact DNA repair capacity. *J. Cell Sci* 129, 1769–1774. [PubMed: 26966185]
66. Dantas TJ, Daly OM, and Morrison CG (2012). Such small hands: the roles of centrins/caltractins in the centriole and in genome maintenance. *Cell Mol. Life. Sci* 69, 2979–2997. [PubMed: 22460578]
67. Dauber A, Lafranchi SH, Maliga Z, Lui JC, Moon JE, McDeed C, Henke K, Zonana J, Kingman GA, Pers TH, Baron J, Rosenfeld RG, Hirschhorn JN, Harris MP, and Hwa V (2012). Novel microcephalic primordial dwarfism disorder associated with variants in the centrosomal protein ninein. *J. Clin. Endocrinol. Metab* 97, E2140–E2151. [PubMed: 22933543]
68. Delaval B and Doxsey SJ (2010). Pericentrin in cellular function and disease. *J. Cell Biol* 188, 181–190. [PubMed: 19951897]
- Delgehyr N, Sillibourne J, Bornens M 2005 Microtubule nucleation and anchoring at the centrosome are independent processes linked to ninein function. *J. Cell. Sci* 118 (Pt 8), 1565–1575. [PubMed: 15784680]
69. den Hollander AI, Koenekoop RK, Mohamed MD, Arts HH, Boldt K, Towns KV, Sedmak T, Beer M, Nagel-Wolfrum K, McKibbin M, Dharmaraj S, Lopez I, Iivings L, Williams GA, Springell K, Woods CG, Jafri H, Rashid Y, Strom TM, van der Zwaag B, Gosens I, Kersten FF, van WE, Veltman JA, Zonneveld MN, van Beersum SE, Maumenee IH, Wolfrum U, Cheetham ME, Ueffing M, Cremers FP, Inglehearn CF, and Roepman R (2007). Mutations in LCA5, encoding the ciliary protein lebercilin, cause Leber congenital amaurosis. *Nat. Genet* 39, 889–895. [PubMed: 17546029]
70. den Hollander AI, Koenekoop RK, Yzer S, Lopez I, Arends ML, Voeseke KE, Zonneveld MN, Strom TM, Meitinger T, Brunner HG, Hoyng CB, Van den Born LI, Rohrschneider K, and Cremers FP (2006). Mutations in the CEP290 (NPHP6) gene are a frequent cause of Leber congenital amaurosis. *Am. J Hum. Genet* 79, 556–561. [PubMed: 16909394]
71. den Hollander AI, Roepman R, Koenekoop RK, and Cremers FP (2008). Leber congenital amaurosis: genes, proteins and disease mechanisms. *Prog. Retin. Eye Res* 27, 391–419. [PubMed: 18632300]
72. Dharmat R, Eblimit A, Robichaux MA, Zhang Z, Nguyen TT, Jung SY, He F, Jain A, Li Y, Qin J, Overbeek P, Roepman R, Mardon G, Wensel TG, and Chen R (2018). SPATA7 maintains a novel photoreceptor-specific zone in the distal connecting cilium. *J. Cell Biol* 217, 2851–2865. [PubMed: 29899041]
73. Di Gioia SA, Farinelli P, Letteboer SJ, Arsenijevic Y, Sharon D, Roepman R, and Rivolta C (2015). Interactome analysis reveals that FAM161A, deficient in recessive retinitis pigmentosa, is a component of the Golgi-centrosomal network. *Hum. Mol. Genet* 24, 3359–3371. [PubMed: 25749990]
74. Di Gioia SA, Letteboer SJ, Kostic C, Bandah-Rozenfeld D, Hettterschijt L, Sharon D, Arsenijevic Y, Roepman R, and Rivolta C (2012). FAM161A, associated with retinitis pigmentosa, is a component of the cilia-basal body complex and interacts with proteins involved in ciliopathies. *Hum. Mol. Genet* 21, 5174–5184. [PubMed: 22940612]
75. DiCarlo JE, Mahajan VB, and Tsang SH (2018). Gene therapy and genome surgery in the retina. *J. Clin. Invest* 128, 2177–2188. [PubMed: 29856367]
76. DiCarlo JE, Sengillo JD, Justus S, Cabral T, Tsang SH, and Mahajan VB (2017). CRISPR-Cas Genome Surgery in Ophthalmology. *Transl. Vis. Sci. Technol* 6, 13.
77. Ding JD, Salinas RY, and Arshavsky VY (2015). Discs of mammalian rod photoreceptors form through the membrane evagination mechanism. *J. Cell Biol* 211, 495–502. [PubMed: 26527746]
78. Dona M, Bachmann-Gagescu R, Texier Y, Toedt G, Hettterschijt L, Tonnaer EL, Peters TA, van Beersum SE, Bergboer JG, Horn N, de VE, Slijkerman RW, van RJ, Flik G, Keunen JE, Ueffing M, Gibson TJ, Roepman R, Boldt K, Kremer H, and van WE (2015). NINL and DZANK1 Co-function in Vesicle Transport and Are Essential for Photoreceptor Development in Zebrafish. *PLoS. Genet* 11, e1005574. [PubMed: 26485514]
79. Downs LM, Bell JS, Freeman J, Hartley C, Hayward LJ, and Mellersh CS (2013). Late-onset progressive retinal atrophy in the Gordon and Irish Setter breeds is associated with a frameshift mutation in C2orf71. *Anim Genet* 44, 169–177. [PubMed: 22686255]

80. Downs LM, Scott EM, Cideciyan AV, Iwabe S, Dufour V, Gardiner KL, Genini S, Marinho LF, Sumaroka A, Kosyk MS, Swider M, Aguirre GK, Jacobson SG, Beltran WA, and Aguirre GD (2016). Overlap of abnormal photoreceptor development and progressive degeneration in Leber congenital amaurosis caused by NPHP5 mutation. *Hum. Mol. Genet* 25, 4211–4226. [PubMed: 27506978]
81. Drivas TG and Bennett J (2014). CEP290 and the primary cilium. *Adv Exp Med Biol* 801, 519–525. [PubMed: 24664739]
82. Drivas TG, Holzbaier EL, and Bennett J (2013). Disruption of CEP290 microtubule/membrane-binding domains causes retinal degeneration. *J. Clin. Invest* 123, 4525–4539. [PubMed: 24051377]
83. Dryja TP, Adams SM, Grimsby JL, McGee TL, Hong DH, Li T, Andreasson S, and Berson EL (2001). Null RPGRIP1 alleles in patients with Leber congenital amaurosis. *Am. J. Hum. Genet* 68, 1295–1298. [PubMed: 11283794]
84. Duldulao NA, Lee S, and Sun Z (2009). Cilia localization is essential for in vivo functions of the Joubert syndrome protein Arl13b/Scorpion. *Development* 136, 4033–4042. [PubMed: 19906870]
85. Dutcher SK, Morrissette NS, Preble AM, Rackley C, and Stanga J (2002). Epsilon-tubulin is an essential component of the centriole. *Mol. Biol. Cell* 13, 3859–3869. [PubMed: 12429830]
86. Dyson JM, Conduit SE, Feeney SJ, Hakim S, DiTommaso T, Fulcher AJ, Sriratanana A, Ramm G, Horan KA, Gurung R, Wicking C, Smyth I, and Mitchell CA (2017). INPP5E regulates phosphoinositide-dependent cilia transition zone function. *J. Cell Biol* 216, 247–263. [PubMed: 27998989]
87. Eblimit A, Nguyen TM, Chen Y, Esteve-Rudd J, Zhong H, Letteboer S, van RJ, Simons DL, Ding Q, Wu KM, Li Y, van BS, Moayed Y, Xu H, Pickard P, Wang K, Gan L, Wu SM, Williams DS, Mardon G, Roepman R, and Chen R (2015). Spata7 is a retinal ciliopathy gene critical for correct RPGRIP1 localization and protein trafficking in the retina. *Hum. Mol. Genet* 24, 1584–1601. [PubMed: 25398945]
88. Eckmiller MS and Toman A (1998). Association of kinesin with microtubules in diverse cytoskeletal systems in the outer segments of rods and cones. *Acta Anat. (Basel)* 162, 133–141. [PubMed: 9831760]
89. Endoh-Yamagami S, Karkar KM, May SR, Cobos I, Thwin MT, Long JE, Ashique AM, Zarbalis K, Rubenstein JL, and Peterson AS (2010). A mutation in the pericentrin gene causes abnormal interneuron migration to the olfactory bulb in mice. *Dev. Biol* 340, 41–53. [PubMed: 20096683]
90. Errabolu R, Sanders MA, and Salisbury JL (1994). Cloning of a cDNA encoding human centrin, an EF-hand protein of centrosomes and mitotic spindle poles. *J. Cell Sci* 107 (Pt 1), 9–16. [PubMed: 8175926]
91. Escalier D (2006). Knockout mouse models of sperm flagellum anomalies. *Hum. Reprod. Update* 12, 449–461. [PubMed: 16565154]
92. Estrada-Cuzcano A, Koenekoop RK, Coppieters F, Kohl S, Lopez I, Collin RW, De Baere EB, Roeleveld D, Marek J, Bernd A, Rohrschneider K, Van den Born LI, Meire F, Maumenee IH, Jacobson SG, Hoyng CB, Zrenner E, Cremers FP, and den Hollander AI (2011). IQCB1 mutations in patients with leber congenital amaurosis. *Invest Ophthalmol. Vis. Sci* 52, 834–839. [PubMed: 20881296]
93. Estrada-Cuzcano A, Neveling K, Kohl S, Banin E, Rotenstreich Y, Sharon D, Falik-Zaccai TC, Hipp S, Roepman R, Wissinger B, Letteboer SJ, Mans DA, Blokland EA, Kwint MP, Gijsen SJ, van Huet RA, Collin RW, Scheffer H, Veltman JA, Zrenner E, den Hollander AI, Klevering BJ, and Cremers FP (2012). Mutations in C8orf37, encoding a ciliary protein, are associated with autosomal-recessive retinal dystrophies with early macular involvement. *Am. J. Hum. Genet* 90, 102–109. [PubMed: 22177090]
94. Failler M, Gee HY, Joo K, Halbritter J, Belkacem L, Filhol E, Porath JD, Braun DA, Schueler M, Frigo A, Alibeu O, Masson C, Brochard K, Hurault de LB, Novo R, Pietrement C, Kayserili H, Salomon R, Gubler MC, Otto EA, Antignac C, Kim J, Benmerah A, Hildebrandt F, and Saunier S (2014). Mutations of CEP83 cause infantile nephronophthisis and intellectual disability. *Am. J. Hum. Genet* 94, 905–914. [PubMed: 24882706]
95. Falk N, Kessler K, Schramm SF, Boldt K, Becirovic E, Michalakis S, Regus-Leidig H, Noegel AA, Ueffing M, Thiel CT, Roepman R, Brandstatter JH, and Giessel A (2018). Functional analyses of Pericentrin and Syne-2 interaction in ciliogenesis. *J. Cell Sci* 131.

96. Fan Y, Esmail MA, Ansley SJ, Blacque OE, Boroevich K, Ross AJ, Moore SJ, Badano JL, May-Simera H, Compton DS, Green JS, Lewis RA, van Haelst MM, Parfrey PS, Baillie DL, Beales PL, Katsanis N, Davidson WS, and Leroux MR (2004). Mutations in a member of the Ras superfamily of small GTP-binding proteins causes Bardet-Biedl syndrome. *Nat. Genet* 36, 989–993. [PubMed: 15314642]
97. Finn RD, Coghill P, Eberhardt RY, Eddy SR, Mistry J, Mitchell AL, Potter SC, Punta M, Qureshi M, Sangrador-Vegas A, Salazar GA, Tate J, and Bateman A (2016). The Pfam protein families database: towards a more sustainable future. *Nucleic Acids Res* 44, D279–D285. [PubMed: 26673716]
98. Firat-Karalar EN, Rauniyar N, Yates JR III, and Stearns T (2014). Proximity interactions among centrosome components identify regulators of centriole duplication. *Curr. Biol* 24, 664–670. [PubMed: 24613305]
99. Fliegau M, Horvath J, von SC, Olbrich H, Muller D, Thumfart J, Schermer B, Pazour GJ, Neumann HP, Zentgraf H, Benzing T, and Omran H (2006). Nephrocystin specifically localizes to the transition zone of renal and respiratory cilia and photoreceptor connecting cilia. *J. Am. Soc. Nephrol* 17, 2424–2433. [PubMed: 16885411]
100. Forsythe E and Beales PL (2013). Bardet-Biedl syndrome. *Eur. J. Hum. Genet* 21, 8–13. [PubMed: 22713813]
101. Friedberg F (2006). Centrin isoforms in mammals. Relation to calmodulin. *Mol. Biol. Rep* 33, 243–252. [PubMed: 17089211]
102. Fu Y and Yau KW (2007). Phototransduction in mouse rods and cones. *Pflugers Arch*
103. Garanto A, Chung DC, Duijkers L, Corral-Serrano JC, Messchaert M, Xiao R, Bennett J, Vandenberghe LH, and Collin RW (2016). In vitro and in vivo rescue of aberrant splicing in CEP290-associated LCA by antisense oligonucleotide delivery. *Hum. Mol. Genet* 25, 2552–2563. [PubMed: 27106101]
104. Garanto A, van Beersum SE, Peters TA, Roepman R, Cremers FP, and Collin RW (2013). Unexpected CEP290 mRNA splicing in a humanized knock-in mouse model for Leber congenital amaurosis. *PLoS. ONE* 8, e79369. [PubMed: 24223178]
105. Garcia G III and Reiter JF (2016). A primer on the mouse basal body. *Cilia* 5, 17. [PubMed: 27114821]
106. Gavet O, Alvarez C, Gaspar P, and Bornens M (2003). Centrin4p, a novel mammalian centrin specifically expressed in ciliated cells. *Mol. Biol. Cell* 14, 1818–1834. [PubMed: 12802058]
107. Geimer S and Melkonian M (2005). Centrin scaffold in *Chlamydomonas reinhardtii* revealed by immunoelectron microscopy. *Eukaryot. Cell* 4, 1253–1263. [PubMed: 16002651]
108. Geister KA, Brinkmeier ML, Cheung LY, Wendt J, Oatley MJ, Burgess DL, Kozloff KM, Cavalcoli JD, Oatley JM, and Camper SA (2015). LINE-1 Mediated Insertion into *Poc1a* (Protein of Centriole 1 A) Causes Growth Insufficiency and Male Infertility in Mice. *PLoS. Genet* 11, e1005569. [PubMed: 26496357]
109. Gerner M, Haribaskar R, Putz M, Czerwitzki J, Walz G, and Schafer T (2010). The retinitis pigmentosa GTPase regulator interacting protein 1 (RPGRIP1) links RPGR to the nephronophthisis protein network. *Kidney Int* 77, 891–896. [PubMed: 20200501]
110. Gerth-Kahlert C, Tiwari A, Hanson JVM, Batmanabane V, Traboulsi E, Pennesi ME, Al-Qahtani AA, Lam BL, Heckenlively J, Zweifel SA, Vincent A, Fierz F, Barthelmes D, Branham K, Khan N, Bahr A, Baehr L, Magyar I, Koller S, Azzarello-Burri S, Niedrist D, Heon E, and Berger W (2017). *C2orf71* Mutations as a Frequent Cause of Autosomal-Recessive Retinitis Pigmentosa: Clinical Analysis and Presentation of 8 Novel Mutations. *Invest Ophthalmol. Vis. Sci* 58, 3840–3850. [PubMed: 28763557]
111. Giessler A, Pulvermuller A, Trojan P, Park JH, Choe HW, Ernst OP, Hofmann KP, and Wolfrum U (2004). Differential expression and interaction with the visual G-protein transducin of centrin isoforms in mammalian photoreceptor cells. *J. Biol. Chem* 279, 51472–51481. [PubMed: 15347651]
112. Giessler A, Trojan P, Rausch S, Pulvermuller A, and Wolfrum U (2006). Centrins, gatekeepers for the light-dependent translocation of transducin through the photoreceptor cell connecting cilium. *Vision REs* 46, 4502–4509. [PubMed: 17027897]

113. Gilliam JC, Chang JT, Sandoval IM, Zhang Y, Li T, Pittler SJ, Chiu W, and Wensel TG (2012). Three-dimensional architecture of the rod sensory cilium and its disruption in retinal neurodegeneration. *Cell* 151, 1029–1041. [PubMed: 23178122]
114. Goetz SC and Anderson KV (2010). The primary cilium: a signalling centre during vertebrate development. *Nat. Rev. Genet* 11, 331–344. [PubMed: 20395968]
115. Goldberg AF, Moritz OL, and Williams DS (2016). Molecular basis for photoreceptor outer segment architecture. *Prog. Retin. Eye Res. Prog. Retin. Eye Res* 55, 52–81. [PubMed: 27260426]
116. Goldstein O, Mezey JG, Schweitzer PA, Boyko AR, Gao C, Bustamante CD, Jordan JA, Aguirre GD, and Acland GM (2013). IQCB1 and PDE6B mutations cause similar early onset retinal degenerations in two closely related terrier dog breeds. *Invest. Ophthalmol. Vis. Sci* 54, 7005–7019. [PubMed: 24045995]
117. Goncalves J and Pelletier L (2017). The Ciliary Transition Zone: Finding the Pieces and Assembling the Gate. *Mol. Cells* 40, 243–253. [PubMed: 28401750]
118. Gorden NT, Arts HH, Parisi MA, Coene KL, Letteboer SJ, van Beersum SE, Mans DA, Hikida A, Eckert M, Knutzen D, Alswaid AF, Ozyurek H, Dibooglu S, Otto EA, Liu Y, Davis EE, Hutter CM, Bammler TK, Farin FM, Dorschner M, Topcu M, Zackai EH, Rosenthal P, Owens KN, Katsanis N, Vincent JB, Hildebrandt F, Rubel EW, Raible DW, Knoers NV, Chance PF, Roepman R, Moens CB, Glass IA, and Doherty D (2008). CC2D2A Is mutated in joubert syndrome and interacts with the ciliopathy-associated basal body protein CEP290. *Am. J Hum. Genet* 83, 559–571. [PubMed: 18950740]
119. Gotthardt K, Lokaj M, Koerner C, Falk N, Giessl A, and Wittinghofer A (2015). A G-protein activation cascade from Arl13b to Arl3 and implications for ciliary targeting of lipidated proteins. *eLife* 4:e11859. [PubMed: 26551564]
120. Graser S, Stierhof YD, Lavoie SB, Gassner OS, Lamla S, Le CM, and Nigg EA (2007a). Cep164, a novel centriole appendage protein required for primary cilium formation. *J. Cell Biol* 179, 321–330. [PubMed: 17954613]
121. Graser S, Stierhof YD, and Nigg EA (2007b). Cep68 and Cep215 (Cdk5rap2) are required for centrosome cohesion. *J. Cell Sci* 120, 4321–4331. [PubMed: 18042621]
122. Grayson C, Bartolini F, Chapple JP, Willison KR, Bhamidipati A, Lewis SA, Luthert PJ, Hardcastle AJ, Cowan NJ, and Cheetham ME (2002). Localization in the human retina of the X-linked retinitis pigmentosa protein RP2, its homologue cofactor C and the RP2 interacting protein Arl3. *Hum. Mol. Genet* 11, 3065–3074. [PubMed: 12417528]
123. Gromley A, Jurczyk A, Sillibourne J, Halilovic E, Mogensen M, Groisman I, Blomberg M, and Doxsey S (2003). A novel human protein of the maternal centriole is required for the final stages of cytokinesis and entry into S phase. *J. Cell Biol* 161, 535–545. [PubMed: 12732615]
124. Guarguaglini G, Duncan PI, Stierhof YD, Holmstrom T, Duensing S, and Nigg EA (2005). The forkhead-associated domain protein Cep170 interacts with Polo-like kinase 1 and serves as a marker for mature centrioles. *Mol. Biol. Cell* 16, 1095–1107. [PubMed: 15616186]
125. Gupta GD, Coyaud E, Goncalves J, Mojarad BA, Liu Y, Wu Q, Gheiratmand L, Comartin D, Tkach JM, Cheung SW, Bashkurov M, Hasegan M, Knight JD, Lin ZY, Schueler M, Hildebrandt F, Moffat J, Gingras AC, Raught B, and Pelletier L (2015). A Dynamic Protein Interaction Landscape of the Human Centrosome-Cilium Interface. *Cell* 163, 1484–1499. [PubMed: 26638075]
126. Guyon R, Pearce-Kelling SE, Zeiss CJ, Acland GM, and Aguirre GD (2007). Analysis of six candidate genes as potential modifiers of disease expression in canine XLPRA1, a model for human X-linked retinitis pigmentosa 3. *Mol. Vis* 13, 1094–1105. [PubMed: 17653054]
127. Halbritter J, Porath JD, Diaz KA, Braun DA, Kohl S, Chaki M, Allen SJ, Soliman NA, Hildebrandt F, and Otto EA (2013). Identification of 99 novel mutations in a worldwide cohort of 1,056 patients with a nephronophthisis-related ciliopathy. *Hum. Genet* 132, 865–884. [PubMed: 23559409]
128. Hames RS, Hames R, Prosser SL, Euteneuer U, Lopes CA, Moore W, Woodland HR, and Fry AM (2008). Pix1 and Pix2 are novel WD40 microtubule-associated proteins that colocalize with mitochondria in *Xenopus* germ plasm and centrosomes in human cells. *Exp Cell Res* 314, 574–589. [PubMed: 18068700]

129. Hanke-Gogokhia C, Frederick JM, and Baehr W (2018). Rescue of cone function in ‘cone-only’ Nphp5 knockout mouse model with Leber congenital amaurosis phenotype. *Mol. Vis* in press.
130. Hanke-Gogokhia C, Wu Z, Gerstner CD, Frederick JM, Zhang H, and Baehr W (2016). Arf-like protein 3 (ARL3) regulates protein trafficking and ciliogenesis in mouse photoreceptors. *J. Biol. Chem* 291, 7142–7155. [PubMed: 26814127]
131. Hanke-Gogokhia C, Wu Z, Sharif A, Yazigi H, Frederick JM, and Baehr W (2017). The guanine nucleotide exchange factor, Arf-like protein 13b, is essential for assembly of the mouse photoreceptor transition zone and outer segment. *J. Biol. Chem* 292, 21442–21456. [PubMed: 29089384]
132. Hanzal-Bayer M, Renault L, Roversi P, Wittinghofer A, and Hillig RC (2002). The complex of Arl2-GTP and PDE delta: from structure to function. *EMBO J* 21, 2095–2106. [PubMed: 11980706]
133. Hart PE, Glantz JN, Orth JD, Poynter GM, and Salisbury JL (1999). Testis-specific murine centrin, *Cetn1*: genomic characterization and evidence for retroposition of a gene encoding a centrosome protein. *Genomics* 60, 111–120. [PubMed: 10486202]
134. Hartman H and Fedorov A (2002). The origin of the eukaryotic cell: a genomic investigation. *Proc. Natl. Acad. Sci. U. S. A* 99, 1420–1425. [PubMed: 11805300]
135. Hartong DT, Berson EL, and Dryja TP (2006). Retinitis pigmentosa. *Lancet* 368, 1795–1809. [PubMed: 17113430]
136. Helou J, Otto EA, Attanasio M, Allen SJ, Parisi MA, Glass I, Utsch B, Hashmi S, Fazzi E, Omran H, O’Toole JF, Sayer JA, and Hildebrandt F (2007). Mutation analysis of NPHP6/CEP290 in patients with Joubert syndrome and Senior-Loken syndrome. *J. Med. Genet* 44, 657–663. [PubMed: 17617513]
137. Heon E, Kim G, Qin S, Garrison JE, Tavares E, Vincent A, Nuangchamnon N, Scott CA, Slusarski DC, and Sheffield VC (2016). Mutations in C8ORF37 cause Bardet Biedl syndrome (BBS21). *Hum. Mol. Genet* 25, 2283–2294. [PubMed: 27008867]
138. Higginbotham H, Bielas S, Tanaka T, and Gleeson JG (2004). Transgenic mouse line with green-fluorescent protein-labeled Centrin 2 allows visualization of the centrosome in living cells. *Transgenic. Res* 13, 155–164. [PubMed: 15198203]
139. Higginbotham H, Guo J, Yokota Y, Umberger NL, Su CY, Li J, Verma N, Hirt J, Ghukasyan V, Caspary T, and Anton ES (2013). Arl13b-regulated cilia activities are essential for polarized radial glial scaffold formation. *Nat. Neurosci* 16, 1000–1007. [PubMed: 23817546]
140. Hildebrandt F, Otto E, Rensing C, Nothwang HG, Vollmer M, Adolphs J, Hanusch H, and Brandis M (1997). A novel gene encoding an SH3 domain protein is mutated in nephronophthisis type 1. *Nat. Genet* 17, 149–153. [PubMed: 9326933]
141. Hong DH, Pawlyk BS, Shang J, Sandberg MA, Berson EL, and Li T (2000). A retinitis pigmentosa GTPase regulator (RPGR)- deficient mouse model for X-linked retinitis pigmentosa (RP3) [In Process Citation]. *Proc. Natl. Acad. Sci. U. S. A* 97, 3649–3654. [PubMed: 10725384]
142. Hoon M, Okawa H, Della SL, and Wong RO (2014). Functional architecture of the retina: development and disease. *Prog. Retin. Eye Res* 42, 44–84. [PubMed: 24984227]
143. Hoover AN, Wynkoop A, Zeng H, Jia J, Niswander LA, and Liu A (2008). C2cd3 is required for cilia formation and Hedgehog signaling in mouse. *Development* 135, 4049–4058. [PubMed: 19004860]
144. Hori A and Toda T (2017). Regulation of centriolar satellite integrity and its physiology. *Cell Mol. Life Sci* 74, 213–229. [PubMed: 27484406]
145. Hoyer-Fender S (2010). Centriole maturation and transformation to basal body. *Semin. Cell Dev. Biol* 21, 142–147. [PubMed: 19595783]
146. Hsiao YC, Tong ZJ, Westfall JE, Ault JG, Page-McCaw PS, and Ferland RJ (2009). Ahi1, whose human ortholog is mutated in Joubert syndrome, is required for Rab8a localization, ciliogenesis and vesicle trafficking. *Hum. Mol. Genet* 18, 3926–3941. [PubMed: 19625297]
147. Hu L, Su P, Li R, Yin C, Zhang Y, Shang P, Yang T, and Qian A (2016). Isoforms, structures, and functions of versatile spectraplakins MACF1. *BMB. Rep* 49, 37–44. [PubMed: 26521939]

148. Hu L, Xiao Y, Xiong Z, Zhao F, Yin C, Zhang Y, Su P, Li D, Chen Z, Ma X, Zhang G, and Qian A (2017). MACF1, versatility in tissue-specific function and in human disease. *Semin. Cell Dev. Biol* 69, 3–8. [PubMed: 28577926]
149. Huang N, Xia Y, Zhang D, Wang S, Bao Y, He R, Teng J, and Chen J (2017). Hierarchical assembly of centriole subdistal appendages via centrosome binding proteins CCDC120 and CCDC68. *Nat. Commun* 8, 15057. [PubMed: 28422092]
150. Huang WC, Wright AF, Roman AJ, Cideciyan AV, Manson FD, Gewaily DY, Schwartz SB, Sadigh S, Limberis MP, Bell P, Wilson JM, Swaroop A, and Jacobson SG (2012). RPGR-associated retinal degeneration in human X-linked RP and a murine model. *Invest Ophthalmol. Vis. Sci* 53, 5594–5608. [PubMed: 22807293]
151. Humbert MC, Weihbrecht K, Searby CC, Li Y, Pope RM, Sheffield VC, and Seo S (2012). ARL13B, PDE6D, and CEP164 form a functional network for INPP5E ciliary targeting. *Proc. Natl. Acad. Sci. U. S. A* 109, 19691–19696. [PubMed: 23150559]
152. Hynes AM, Giles RH, Srivastava S, Eley L, Whitehead J, Danilenko M, Raman S, Slaats GG, Colville JG, Ajzenberg H, Kroes HY, Thelwall PE, Simmons NL, Miles CG, and Sayer JA (2014). Murine Joubert syndrome reveals Hedgehog signaling defects as a potential therapeutic target for nephronophthisis. *Proc. Natl. Acad. Sci. U. S. A* 111, 9893–9898. [PubMed: 24946806]
153. Insinna C, Luby-Phelps K, Link BA, and Besharse JC (2009). Analysis of IFT kinesins in developing zebrafish cone photoreceptor sensory cilia. *Methods Cell Biol* 93, 219–234. [PubMed: 20409820]
154. Insolera R, Shao W, Airik R, Hildebrandt F, and Shi SH (2014). SDCCAG8 regulates pericentriolar material recruitment and neuronal migration in the developing cortex. *Neuron* 83, 805–822. [PubMed: 25088364]
155. Ishikawa H, Kubo A, Tsukita S, and Tsukita S (2005). Odf2-deficient mother centrioles lack distal/subdistal appendages and the ability to generate primary cilia. *Nat. Cell Biol* 7, 517–524. [PubMed: 15852003]
156. Ismail SA, Chen YX, Miertzschke M, Vetter IR, Koerner C, and Wittinghofer A (2012). Structural basis for Arl3-specific release of myristoylated ciliary cargo from UNC119. *EMBO J* 31, 4085–4094. [PubMed: 22960633]
157. Ismail SA, Chen YX, Rusinova A, Chandra A, Bierbaum M, Gremer L, Triola G, Waldmann H, Bastiaens PI, and Wittinghofer A (2011). Arl2-GTP and Arl3-GTP regulate a GDI-like transport system for farnesylated cargo. *Nat. Chem. Biol* 7, 942–949. [PubMed: 22002721]
158. Ivanova AA, Caspary T, Seyfried NT, Duong DM, West AB, Liu Z, and Kahn RA (2017). Biochemical characterization of purified mammalian ARL13B protein indicates that it is an atypical GTPase and ARL3 guanine nucleotide exchange factor (GEF). *J. Biol. Chem* 292, 11091–11108. [PubMed: 28487361]
159. Jacoby M, Cox JJ, Gayral S, Hampshire DJ, Ayub M, Blockmans M, Pernot E, Kisseleva MV, Compere P, Schiffmann SN, Gergely F, Riley JH, Perez-Morga D, Woods CG, and Schurmans S (2009). INPP5E mutations cause primary cilium signaling defects, ciliary instability and ciliopathies in human and mouse. *Nat. Genet* 41, 1027–1031. [PubMed: 19668215]
160. Jakobsen L, Vanselow K, Skogs M, Toyoda Y, Lundberg E, Poser I, Falkenby LG, Bennetzen M, Westendorf J, Nigg EA, Uhlen M, Hyman AA, and Andersen JS (2011). Novel asymmetrically localizing components of human centrosomes identified by complementary proteomics methods. *EMBO J* 30, 1520–1535. [PubMed: 21399614]
161. Jiang L, Tam BM, Ying G, Wu S, Hauswirth WW, Frederick JM, Moritz OL, and Baehr W (2015a). Kinesin family 17 (osmotic avoidance abnormal-3) is dispensable for photoreceptor morphology and function. *FASEB J* 29, 4866–4880. [PubMed: 26229057]
162. Jiang L, Wei Y, Ronquillo CC, Marc RE, Yoder BK, Frederick JM, and Baehr W (2015b). Heterotrimeric kinesin-2 (KIF3) mediates transition zone and axoneme formation of mouse photoreceptors. *J. Biol. Chem* 290, 12765–12778. [PubMed: 25825494]
163. Jiang ST, Chiou YY, Wang E, Chien YL, Ho HH, Tsai FJ, Lin CY, Tsai SP, and Li H (2009). Essential role of nephrocystin in photoreceptor intraflagellar transport in mouse. *Hum. Mol. Genet* 18, 1566–1577. [PubMed: 19208653]

164. Jiang ST, Chiou YY, Wang E, Lin HK, Lee SP, Lu HY, Wang CK, Tang MJ, and Li H (2008). Targeted disruption of *Nphp1* causes male infertility due to defects in the later steps of sperm morphogenesis in mice. *Hum. Mol. Genet* 17, 3368–3379. [PubMed: 18684731]
165. Jimeno D, Lillo C, Roberts EA, Goldstein LS, and Williams DS (2006). Kinesin-2 and photoreceptor cell death: requirement of motor subunits. *Exp Eye Res* 82, 351–353. [PubMed: 16337628]
166. Joiner AM, Green WW, McIntyre JC, Allen BL, Schwob JE, and Martens JR (2015). Primary Cilia on Horizontal Basal Cells Regulate Regeneration of the Olfactory Epithelium. *J. Neurosci* 35, 13761–13772. [PubMed: 26446227]
167. Joo K, Kim CG, Lee MS, Moon HY, Lee SH, Kim MJ, Kweon HS, Park WY, Kim CH, Gleeson JG, and Kim J (2013). CCDC41 is required for ciliary vesicle docking to the mother centriole. *Proc. Natl. Acad. Sci. U. S. A* 110, 5987–5992. [PubMed: 23530209]
168. Jurczyk A, Gromley A, Redick S, San AJ, Witman G, Pazour GJ, Peters DJ, and Doxsey S (2004). Pericentrin forms a complex with intraflagellar transport proteins and polycystin-2 and is required for primary cilia assembly. *J. Cell Biol* 166, 637–643. [PubMed: 15337773]
169. Juric-Sekhar G, Adkins J, Doherty D, and Hevner RF (2012). Joubert syndrome: brain and spinal cord malformations in genotyped cases and implications for neurodevelopmental functions of primary cilia. *Acta Neuropathol* 123, 695–709. [PubMed: 22331178]
170. Karlstetter M, Soroush N, Caramoy A, Dannhausen K, Aslanidis A, Fauser S, Boesl MR, Nagel-Wolfrum K, Tamm ER, Jagle H, Stoehr H, Wolfrum U, and Langmann T (2014). Disruption of the retinitis pigmentosa 28 gene *Fam161a* in mice affects photoreceptor ciliary structure and leads to progressive retinal degeneration. *Hum. Mol. Genet* 23, 5197–5210. [PubMed: 24833722]
171. Kaupp UB (2010). Olfactory signalling in vertebrates and insects: differences and commonalities. *Nat. Rev. Neurosci* 11, 188–200. [PubMed: 20145624]
172. Keller LC, Geimer S, Romijn E, Yates J III, Zamora I, and Marshall WF (2009). Molecular architecture of the centriole proteome: the conserved WD40 domain protein POC1 is required for centriole duplication and length control. *Mol. Biol. Cell* 20, 1150–1166. [PubMed: 19109428]
173. Kenedy AA, Cohen KJ, Loveys DA, Kato GJ, and Dang CV (2003). Identification and characterization of the novel centrosome-associated protein CCCAP. *Gene* 303, 35–46. [PubMed: 12559564]
174. Kevany BM, Zhang N, Jastrzebska B, and Palczewski K (2015). Animals deficient in *C2Orf71*, an autosomal recessive retinitis pigmentosa-associated locus, develop severe early-onset retinal degeneration. *Hum. Mol. Genet* 24, 2627–2640. [PubMed: 25616964]
175. Kim J, Krishnaswami SR, and Gleeson JG (2008). CEP290 interacts with the centriolar satellite component PCM-1 and is required for Rab8 localization to the primary cilium. *Hum. Mol. Genet* 17, 3796–3805. [PubMed: 18772192]
176. Kim SY, Kim DS, Hong JE, and Park JH (2017). Crystal Structure of Wild-Type Centrin 1 from *Mus musculus* Occupied by Ca²⁺. *Biochemistry (Mosc.)* 82, 1129–1139. [PubMed: 29037133]
177. Kim YK, Kim JH, Yu YS, Ko HW, and Kim JH (2013). Localization of primary cilia in mouse retina. *Acta Histochem* 115, 789–794. [PubMed: 23608602]
178. Kobayashi A, Kubota S, Mori N, McLaren MJ, and Inana G (2003). Photoreceptor synaptic protein HRG4 (UNC119) interacts with ARL2 via a putative conserved domain. *FEBS Lett* 534, 26–32. [PubMed: 12527357]
179. Kobayashi T, Kim S, Lin YC, Inoue T, and Dynlacht BD (2014). The CP110-interacting proteins Talpid3 and Cep290 play overlapping and distinct roles in cilia assembly. *J. Cell Biol* 204, 215–229. [PubMed: 24421332]
180. Kobayashi T, Tsang WY, Li J, Lane W, and Dynlacht BD (2011). Centriolar kinesin Kif24 interacts with CP110 to remodel microtubules and regulate ciliogenesis. *Cell* 145, 914–925. [PubMed: 21620453]
181. Kodani A, Salome Sirerol-Piquer M, Seol A, Garcia-Verdugo JM, and Reiter JF (2013). Kif3a interacts with Dynactin subunit p150 Glued to organize centriole subdistal appendages. *EMBO J* 32, 597–607. [PubMed: 23386061]

182. Kondo S, Sato-Yoshitake R, Noda Y, Aizawa H, Nakata T, Matsuura Y, and Hirokawa N (1994). KIF3A is a new microtubule-based anterograde motor in the nerve axon. *J. Cell Biol* 125, 1095–1107. [PubMed: 7515068]
183. Kong AM, Speed CJ, O'Malley CJ, Layton MJ, Meehan T, Loveland KL, Cheema S, Ooms LM, and Mitchell CA (2000). Cloning and characterization of a 72-kDa inositol-polyphosphate 5-phosphatase localized to the Golgi network. *J. Biol. Chem* 275, 24052–24064. [PubMed: 10806194]
184. Kosling SK, Fansa EK, Maffini S, and Wittinghofer A (2018). Mechanism and dynamics of INPP5E transport into and inside the ciliary compartment. *Biol. Chem* 399, 277–292. [PubMed: 29140789]
185. Kozminski KG, Forscher P, and Rosenbaum JL (1998). Three flagellar motilities in *Chlamydomonas* unrelated to flagellar beating. Video supplement. *Cell Motil. Cytoskeleton* 39, 347–348. [PubMed: 9556339]
186. Kubo A, Sasaki H, Yuba-Kubo A, Tsukita S, and Shiina N (1999). Centriolar satellites: molecular characterization, ATP-dependent movement toward centrioles and possible involvement in ciliogenesis. *J. Cell Biol* 147, 969–980. [PubMed: 10579718]
187. Kubo A and Tsukita S (2003). Non-membranous granular organelle consisting of PCM-1: subcellular distribution and cell-cycle-dependent assembly/disassembly. *J. Cell Sci* 116, 919–928. [PubMed: 12571289]
188. Kumar A, Rajendran V, Sethumadhavan R, and Purohit R (2013). CEP proteins: the knights of centrosome dynasty. *Protoplasma* 250, 965–983. [PubMed: 23456457]
189. Kunimoto K, Yamazaki Y, Nishida T, Shinohara K, Ishikawa H, Hasegawa T, Okanou T, Hamada H, Noda T, Tamura A, Tsukita S, and Tsukita S (2012). Coordinated ciliary beating requires Odf2-mediated polarization of basal bodies via basal feet. *Cell* 148, 189–200. [PubMed: 22265411]
190. Langmann T, Lai CC, Weigelt K, Tam BM, Warneke-Wittstock R, Moritz OL, and Weber BH (2008). CRX controls retinal expression of the X-linked juvenile retinoschisis (RS1) gene. *Nucleic Acids Res* 36, 6523–6534. [PubMed: 18927113]
191. Laoukili J, Perret E, Middendorp S, Houcine O, Guennou C, Marano F, Bornens M, and Tournier F (2000). Differential expression and cellular distribution of centrin isoforms during human ciliated cell differentiation in vitro. *J. Cell Sci* 113 (Pt 8), 1355–1364. [PubMed: 10725219]
192. Lau L, Lee YL, Sahl SJ, Stearns T, and Moerner WE (2012). STED microscopy with optimized labeling density reveals 9-fold arrangement of a centriole protein. *Biophys. J* 102, 2926–2935. [PubMed: 22735543]
193. Lehti MS, Kotaja N, and Sironen A (2013). KIF3A is essential for sperm tail formation and manchette function. *Mol. Cell Endocrinol* 377, 44–55. [PubMed: 23831641]
194. Lessieur EM, Fogerty J, Gaivin RJ, Song P, and Perkins BD (2017). The Ciliopathy Gene *ahi1* Is Required for Zebrafish Cone Photoreceptor Outer Segment Morphogenesis and Survival. *Invest Ophthalmol. Vis. Sci* 58, 448–460. [PubMed: 28118669]
195. Lewis TR, Kundinger SR, Pavlovich AL, Bostrom JR, Link BA, and Besharse JC (2017). *Cos2/Kif7* and *Osm-3/Kif17* regulate onset of outer segment development in zebrafish photoreceptors through distinct mechanisms. *Dev. Biol* 425, 176–190. [PubMed: 28341548]
196. Li C, Jensen VL, Park K, Kennedy J, Garcia-Gonzalo FR, Romani M, De MR, Bruel AL, Gaillard D, Doray B, Lopez E, Riviere JB, Faivre L, Thauvin-Robinet C, Reiter JF, Blacque OE, Valente EM, and Leroux MR (2016a). MKS5 and CEP290 Dependent Assembly Pathway of the Ciliary Transition Zone. *PLoS. Biol* 14, e1002416. [PubMed: 26982032]
197. Li J and Zhan Q (2011). The role of centrosomal Nlp in the control of mitotic progression and tumorigenesis. *Br. J. Cancer* 104, 1523–1528. [PubMed: 21505454]
198. Li S, Fernandez JJ, Marshall WF, and Agard DA (2012). Three-dimensional structure of basal body triplet revealed by electron cryo-tomography. *EMBO J* 31, 552–562. [PubMed: 22157822]
199. Li Y, Tian X, Ma M, Jerman S, Kong S, Somlo S, and Sun Z (2016b). Deletion of ADP Ribosylation Factor-Like GTPase 13B Leads to Kidney Cysts. *J. Am. Soc. Nephrol* 27 (12), 3628–3638. [PubMed: 27153923]

200. Li Y, Wei Q, Zhang Y, Ling K, and Hu J (2010). The small GTPases ARL-13 and ARL-3 coordinate intraflagellar transport and ciliogenesis. *J. Cell Biol* 189, 1039–1051. [PubMed: 20530210]
201. Lin F, Hiesberger T, Cordes K, Sinclair AM, Goldstein LS, Somlo S, and Igarashi P (2003). Kidney-specific inactivation of the KIF3A subunit of kinesin-II inhibits renal ciliogenesis and produces polycystic kidney disease. *Proc. Natl. Acad. Sci U. S. A* 100, 5286–5291. [PubMed: 12672950]
202. Linari M, Hanzal-Bayer M, and Becker J (1999). The delta subunit of rod specific cyclic GMP phosphodiesterase, PDE delta, interacts with the Arf-like protein Arl3 in a GTP specific manner. *FEBS. Lett* 458, 55–59. [PubMed: 10518933]
203. Liu C, Cummins TR, Tyrrell L, Black JA, Waxman SG, and Dib-Hajj SD (2005). CAP-1A is a novel linker that binds clathrin and the voltage-gated sodium channel Na(v)1.8. *Mol. Cell Neurosci* 28, 636–649. [PubMed: 15797711]
204. Liu Q, Tan G, Levenkova N, Li T, Pugh EN Jr., Rux JJ, Speicher DW, and Pierce EA (2007). The proteome of the mouse photoreceptor sensory cilium complex. *Mol. Cell Proteomics* 6, 1299–1317. [PubMed: 17494944]
205. Liu Q, Zuo J, and Pierce EA (2004). The retinitis pigmentosa 1 protein is a photoreceptor microtubule-associated protein. *J Neurosci* 24, 6427–6436. [PubMed: 15269252]
206. Lizarraga SB, Margossian SP, Harris MH, Campagna DR, Han AP, Blevins S, Muddbary R, Barker JE, Walsh CA, and Fleming MD (2010). Cdk5rap2 regulates centrosome function and chromosome segregation in neuronal progenitors. *Development* 137, 1907–1917. [PubMed: 20460369]
207. Loktev AV, Zhang Q, Beck JS, Searby CC, Scheetz TE, Bazan JF, Slusarski DC, Sheffield VC, Jackson PK, and Nachury MV (2008). A BBSome subunit links ciliogenesis, microtubule stability, and acetylation. *Dev. Cell* 15, 854–865. [PubMed: 19081074]
208. Louie CM, Caridi G, Lopes VS, Brancati F, Kispert A, Lancaster MA, Schlossman AM, Otto EA, Leitges M, Grone HJ, Lopez I, Gudiseva HV, O'Toole JF, Vallespin E, Ayyagari R, Ayuso C, Cremers FP, den Hollander AI, Koenekoop RK, Dallapiccola B, Ghiggeri GM, Hildebrandt F, Valente EM, Williams DS, and Gleeson JG (2010). AHI1 is required for photoreceptor outer segment development and is a modifier for retinal degeneration in nephronophthisis. *Nat. Genet* 42, 175–180. [PubMed: 20081859]
209. Luby-Phelps K, Fogerty J, Baker SA, Pazour GJ, and Besharse JC (2008). Spatial distribution of intraflagellar transport proteins in vertebrate photoreceptors. *Vision REs* 48, 413–423. [PubMed: 17931679]
210. Luders J (2012). The amorphous pericentriolar cloud takes shape. *Nat. Cell Biol* 14, 1126–1128. [PubMed: 23131920]
211. Malicki J and Avidor-Reiss T (2014). From the cytoplasm into the cilium: bon voyage. *Organogenesis* 10, 138–157. [PubMed: 24786986]
212. Malicki J and Besharse JC (2012). Kinesin-2 family motors in the unusual photoreceptor cilium. *Vision REs* 75, 33–36. [PubMed: 23123805]
213. Marszalek JR, Liu X, Roberts EA, Chui D, Marth JD, Williams DS, and Goldstein LS (2000). Genetic evidence for selective transport of opsin and arrestin by kinesin-II in mammalian photoreceptors. *Cell* 102, 175–187. [PubMed: 10943838]
214. Marszalek JR, Ruiz-Lozano P, Roberts E, Chien KR, and Goldstein LS (1999). Situs inversus and embryonic ciliary morphogenesis defects in mouse mutants lacking the KIF3A subunit of kinesin-II. *Proc. Natl. Acad. Sci U. S. A* 96, 5043–5048. [PubMed: 10220415]
215. Martinez-Sanz J, Yang A, Blouquit Y, Duchambon P, Assairi L, and Craescu CT (2006). Binding of human centrin 2 to the centrosomal protein hSfi1. *FEBS J* 273, 4504–4515. [PubMed: 16956364]
216. May-Simera H, Nagel-Wolfrum K, and Wolfrum U (2017). Cilia - The sensory antennae in the eye. *Prog. Retin. Eye Res* 60, 144–180. [PubMed: 28504201]
217. May-Simera HL, Gumerson JD, Gao C, Campos M, Cologna SM, Beyer T, Boldt K, Kaya KD, Patel N, Kretschmer F, Kelley MW, Petralia RS, Davey MG, and Li T (2016). Loss of MACF1

- Abolishes Ciliogenesis and Disrupts Apicobasal Polarity Establishment in the Retina. *Cell Rep* 17, 1399–1413. [PubMed: 27783952]
218. McEwen DP, Koenekoop RK, Khanna H, Jenkins PM, Lopez I, Swaroop A, and Martens JR (2007). Hypomorphic CEP290/NPHP6 mutations result in anosmia caused by the selective loss of G proteins in cilia of olfactory sensory neurons. *Proc. Natl. Acad. Sci U. S. A* 104, 15917–15922. [PubMed: 17898177]
219. Mears AJ, Kondo M, Swain PK, Takada Y, Bush RA, Saunders TL, Sieving PA, and Swaroop A (2001). Nrl is required for rod photoreceptor development. *Nat. Genet* 29, 447–452. [PubMed: 11694879]
220. Megaw RD, Soares DC, and Wright AF (2015). RPGR: Its role in photoreceptor physiology, human disease, and future therapies. *Exp Eye Res* 138, 32–41. [PubMed: 26093275]
221. Mellersh CS, Boursnell ME, Pettitt L, Ryder EJ, Holmes NG, Grafham D, Forman OP, Sampson J, Barnett KC, Blanton S, Binns MM, and Vaudin M (2006). Canine RPGRIP1 mutation establishes cone-rod dystrophy in miniature longhaired dachshunds as a homologue of human Leber congenital amaurosis. *Genomics* 88, 293–301. [PubMed: 16806805]
222. Mennella V, Agard DA, Huang B, and Pelletier L (2014). Amorphous no more: subdiffraction view of the pericentriolar material architecture. *Trends Cell Biol* 24, 188–197. [PubMed: 24268653]
223. Miao Z, Ali A, Hu L, Zhao F, Yin C, Chen C, Yang T, and Qian A (2017). Microtubule actin cross-linking factor 1, a novel potential target in cancer. *Cancer Sci* 108, 1953–1958. [PubMed: 28782898]
224. Middendorp S, Kuntziger T, Abraham Y, Holmes S, Bordes N, Paintrand M, Paoletti A, and Bornens M (2000). A role for centrin 3 in centrosome reproduction. *J. Cell Biol* 148, 405–416. [PubMed: 10662768]
225. Miura H, Quadros RM, Gurumurthy CB, and Ohtsuka M (2018). Easi-CRISPR for creating knock-in and conditional knockout mouse models using long ssDNA donors. *Nat. Protoc* 13, 195–215. [PubMed: 29266098]
226. Miyoshi K, Kasahara K, Miyazaki I, Shimizu S, Taniguchi M, Matsuzaki S, Tohyama M, and Asanuma M (2009). Pericentrin, a centrosomal protein related to microcephalic primordial dwarfism, is required for olfactory cilia assembly in mice. *FASEB J* 23, 3289–3297. [PubMed: 19470799]
227. Mockel A, Perdomo Y, Stutzmann F, Letsch J, Marion V, and Dollfus H (2011). Retinal dystrophy in Bardet-Biedl syndrome and related syndromic ciliopathies. *Prog. Retin. Eye Res* 30, 258–274. [PubMed: 21477661]
228. Molday RS and Moritz OL (2015). Photoreceptors at a glance. *J. Cell Sci* 128, 4039–4045. [PubMed: 26574505]
229. Monnich M, Borgeskov L, Breslin L, Jakobsen L, Rogowski M, Doganli C, Schroder JM, Mogensen JB, Blinkenkjaer L, Harder LM, Lundberg E, Geimer S, Christensen ST, Andersen JS, Larsen LA, and Pedersen LB (2018). CEP128 Localizes to the Subdistal Appendages of the Mother Centriole and Regulates TGF-beta/BMP Signaling at the Primary Cilium. *Cell Rep* 22, 2584–2592. [PubMed: 29514088]
230. Moradi P, Davies WL, Mackay DS, Cheetham ME, and Moore AT (2011). Focus on molecules: centrosomal protein 290 (CEP290). *Exp. Eye Res* 92, 316–317. [PubMed: 20493186]
231. Morris RL and Scholey JM (1997). Heterotrimeric kinesin-II is required for the assembly of motile 9+2 ciliary axonemes on sea urchin embryos. *J Cell Biol* 138, 1009–1022. [PubMed: 9281580]
232. Morrow EM, Furukawa T, and Cepko CL (1998). Vertebrate photoreceptor cell development and disease. *Trends Cell Biol* 8, 353–358. [PubMed: 9728396]
233. Mougou-Zerelli S, Thomas S, Szenker E, Audollent S, Elkhartoufi N, Babarit C, Romano S, Salomon R, Amiel J, Esculpavit C, Gonzales M, Escudier E, Leheup B, Loget P, Odent S, Roume J, Gerard M, Delezoide AL, Khung S, Patrier S, Cordier MP, Bouvier R, Martinovic J, Gubler MC, Boddaert N, Munnich A, Encha-Razavi F, Valente EM, Saad A, Saunier S, Vekemans M, and Attie-Bitach T (2009). CC2D2A mutations in Meckel and Joubert syndromes indicate a genotype-phenotype correlation. *Hum. Mutat* 30, 1574–1582. [PubMed: 19777577]

234. Muhlhans J, Brandstatter JH, and Giessl A (2011). The centrosomal protein pericentrin identified at the basal body complex of the connecting cilium in mouse photoreceptors. *PLoS ONE* 6, e26496. [PubMed: 22031837]
235. Muhlhans J and Giessl A (2012). Pericentrin in health and disease: Exploring the patchwork of Pericentrin splice variants. *Commun. Integr. Biol* 5, 304–307. [PubMed: 23060948]
236. Murga-Zamalloa CA, Desai NJ, Hildebrandt F, and Khanna H (2010). Interaction of ciliary disease protein retinitis pigmentosa GTPase regulator with nephronophthisis-associated proteins in mammalian retinas. *Mol. Vis* 16, 1373–1381. [PubMed: 20664800]
237. Murga-Zamalloa CA, Swaroop A, and Khanna H (2009). RPGR-containing protein complexes in syndromic and non-syndromic retinal degeneration due to ciliary dysfunction. *J. Genet* 88, 399–407. [PubMed: 20090203]
238. Nachury MV, Loktev AV, Zhang Q, Westlake CJ, Peranen J, Merdes A, Slusarski DC, Scheller RH, Bazan JF, Sheffield VC, and Jackson PK (2007). A core complex of BBS proteins cooperates with the GTPase Rab8 to promote ciliary membrane biogenesis. *Cell* 129, 1201–1213. [PubMed: 17574030]
239. Nachury MV, Seeley ES, and Jin H (2010). Trafficking to the ciliary membrane: how to get across the periciliary diffusion barrier? *Annu. Rev. Cell Dev. Biol* 26, 59–87. [PubMed: 19575670]
240. Nguyen TT, Hull S, Roepman R, Van den Born LI, Oud MM, de VE, Heterschijt L, Letteboer SJF, van Beersum SEC, Blokland EA, Yntema HG, Cremers FPM, van der Zwaag PA, Arno G, van WE, Webster AR, and Haer-Wigman L (2017). Missense mutations in the WD40 domain of AHI1 cause non-syndromic retinitis pigmentosa. *J. Med Genet* 54, 624–632. [PubMed: 28442542]
241. Nickell S, Park PS, Baumeister W, and Palczewski K (2007). Three-dimensional architecture of murine rod outer segments determined by cryoelectron tomography. *J Cell Biol* 177, 917–925. [PubMed: 17535966]
242. Nigg EA and Holland AJ (2018). Once and only once: mechanisms of centriole duplication and their deregulation in disease. *Nat. Rev. Mol. Cell Biol* 19 (5), 297–312. [PubMed: 29363672]
243. Nishimura DY, Baye LM, Perveen R, Searby CC, Avila-Fernandez A, Pereiro I, Ayuso C, Valverde D, Bishop PN, Manson FD, Urquhart J, Stone EM, Slusarski DC, Black GC, and Sheffield VC (2010). Discovery and functional analysis of a retinitis pigmentosa gene, C2ORF71. *Am. J. Hum. Genet* 86, 686–695. [PubMed: 20398886]
244. Noor A, Windpassinger C, Patel M, Stachowiak B, Mikhailov A, Azam M, Irfan M, Siddiqui ZK, Naeem F, Paterson AD, Lutfullah M, Vincent JB, and Ayub M (2008). CC2D2A, encoding a coiled-coil and C2 domain protein, causes autosomal-recessive mental retardation with retinitis pigmentosa. *Am. J. Hum. Genet* 82, 1011–1018. [PubMed: 18387594]
245. Norris DP and Grimes DT (2012). Mouse models of ciliopathies: the state of the art. *Dis. Model. Mech* 5, 299–312. [PubMed: 22566558]
246. Nozaki S, Katoh Y, Terada M, Michisaka S, Funabashi T, Takahashi S, Kontani K, and Nakayama K (2017). Regulation of ciliary retrograde protein trafficking by the Joubert syndrome proteins ARL13B and INPP5E. *J. Cell Sci* 130, 563–576. [PubMed: 27927754]
247. Ojeda Naharros I, Gesemann M, Mateos JM, Barmettler G, Forbes A, Ziegler U, Neuhaus SCF, and Bachmann-Gagescu R (2017). Loss-of-function of the ciliopathy protein Cc2d2a disorganizes the vesicle fusion machinery at the periciliary membrane and indirectly affects Rab8-trafficking in zebrafish photoreceptors. *PLoS. Genet* 13, e1007150. [PubMed: 29281629]
248. Otto EA, Hurd TW, Airik R, Chaki M, Zhou W, Stoetzel C, Patil SB, Levy S, Ghosh AK, Murga-Zamalloa CA, van RJ, Letteboer SJ, Sang L, Giles RH, Liu Q, Coene KL, Estrada-Cuzcano A, Collin RW, McLaughlin HM, Held S, Kasanuki JM, Ramaswami G, Conte J, Lopez I, Washburn J, Macdonald J, Hu J, Yamashita Y, Maher ER, Guay-Woodford LM, Neumann HP, Obermuller N, Koenekeop RK, Bergmann C, Bei X, Lewis RA, Katsanis N, Lopes V, Williams DS, Lyons RH, Dang CV, Brito DA, Dias MB, Zhang X, Cavalcoli JD, Nurnberg G, Nurnberg P, Pierce EA, Jackson PK, Antignac C, Saunier S, Roepman R, Dollfus H, Khanna H, and Hildebrandt F (2010). Candidate exome capture identifies mutation of SDCCAG8 as the cause of a retinal-renal ciliopathy. *Nat. Genet* 42, 840–850. [PubMed: 20835237]
249. Otto EA, Loeyes B, Khanna H, Hellemans J, Sudbrak R, Fan S, Muerb U, O’Toole JF, Helou J, Attanasio M, Utsch B, Sayer JA, Lillo C, Jimeno D, Coucke P, De PA, Reinhardt R, Klages S,

- Tsuda M, Kawakami I, Kusakabe T, Omran H, Imm A, Tippens M, Raymond PA, Hill J, Beales P, He S, Kispert A, Margolis B, Williams DS, Swaroop A, and Hildebrandt F (2005). Nephrocystin-5, a ciliary IQ domain protein, is mutated in Senior-Loken syndrome and interacts with RPGR and calmodulin. *Nat. Genet* 37, 282–288. [PubMed: 15723066]
250. Pagan JK, Marzio A, Jones MJ, Saraf A, Jallepalli PV, Florens L, Washburn MP, and Pagano M (2015). Degradation of Cep68 and PCNT cleavage mediate Cep215 removal from the PCM to allow centriole separation, disengagement and licensing. *Nat. Cell Biol* 17, 31–43. [PubMed: 25503564]
251. Pan X, Ou G, Civelekoglu-Scholey G, Blacque OE, Endres NF, Tao L, Mogilner A, Leroux MR, Vale RD, and Scholey JM (2006). Mechanism of transport of IFT particles in *C. elegans* cilia by the concerted action of kinesin-II and OSM-3 motors. *J Cell Biol* 174, 1035–1045. [PubMed: 17000880]
252. Parfitt DA, Lane A, Ramsden C, Jovanovic K, Coffey PJ, Hardcastle AJ, and Cheetham ME (2016). Using induced pluripotent stem cells to understand retinal ciliopathy disease mechanisms and develop therapies. *Biochem. Soc. Trans* 44, 1245–1251. [PubMed: 27911706]
253. Paridaen JT, Wilsch-Brauninger M, and Huttner WB (2013). Asymmetric inheritance of centrosome-associated primary cilium membrane directs ciliogenesis after cell division. *Cell* 155, 333–344. [PubMed: 24120134]
254. Patil H, Tserentsoodol N, Saha A, Hao Y, Webb M, and Ferreira PA (2012). Selective loss of RPGRIP1-dependent ciliary targeting of NPHP4, RPGR and SDCCAG8 underlies the degeneration of photoreceptor neurons. *Cell Death. Dis* 3, e355. [PubMed: 22825473]
255. Pawlyk BS, Bulgakov OV, Liu X, Xu X, Adamian M, Sun X, Khani SC, Berson EL, Sandberg MA, and Li T (2010). Replacement gene therapy with a human RPGRIP1 sequence slows photoreceptor degeneration in a murine model of Leber congenital amaurosis. *Hum. Gene Ther* 21, 993–1004. [PubMed: 20384479]
256. Pawlyk BS, Smith AJ, Buch PK, Adamian M, Hong DH, Sandberg MA, Ali RR, and Li T (2005). Gene replacement therapy rescues photoreceptor degeneration in a murine model of Leber congenital amaurosis lacking RPGRIP. *Invest Ophthalmol. Vis. Sci* 46, 3039–3045. [PubMed: 16123399]
257. Pazour GJ, Baker SA, Deane JA, Cole DG, Dickert BL, Rosenbaum JL, Witman GB, and Besharse JC (2002). The intraflagellar transport protein, IFT88, is essential for vertebrate photoreceptor assembly and maintenance. *J Cell Biol* 157, 103–113. [PubMed: 11916979]
258. Pearring JN, Salinas RY, Baker SA, and Arshavsky VY (2013). Protein sorting, targeting and trafficking in photoreceptor cells. *Prog. Retin. Eye. Res* 36, 24–51. [PubMed: 23562855]
259. Pearson CG and Winey M (2009). Basal body assembly in ciliates: the power of numbers. *Traffic* 10, 461–471. [PubMed: 19192246]
260. Peet JA, Bragin A, Calvert PD, Nikonov SS, Mani S, Zhao X, Besharse JC, Pierce EA, Knox BE, and Pugh EN Jr. (2004). Quantification of the cytoplasmic spaces of living cells with EGFP reveals arrestin-EGFP to be in disequilibrium in dark adapted rod photoreceptors. *J. Cell Sci* 117, 3049–3059. [PubMed: 15197244]
261. Perrault I, Hanein S, Gerard X, Delphin N, Fares-Taie L, Gerber S, Pelletier V, Merce E, Dollfus H, Puech B, Defoort-Dhellemmes S, Petersen MD, Zafeiriou D, Munnich A, Kaplan J, Roche O, and Rozet JM (2010). Spectrum of SPATA7 mutations in Leber congenital amaurosis and delineation of the associated phenotype. *Hum. Mutat* 31, E1241–E1250. [PubMed: 20104588]
262. Phua SC, Chiba S, Suzuki M, Su E, Roberson EC, Pusapati GV, Setou M, Rohatgi R, Reiter JF, Ikegami K, and Inoue T (2017). Dynamic Remodeling of Membrane Composition Drives Cell Cycle through Primary Cilia Excision. *Cell* 168, 264–279. [PubMed: 28086093]
263. Pinheiro PS, Houy S, and Sorensen JB (2016). C2-domain containing calcium sensors in neuroendocrine secretion. *J. Neurochem* 139, 943–958. [PubMed: 27731902]
264. Poirier K, Lebrun N, Broix L, Tian G, Saillour Y, Boscheron C, Parrini E, Valence S, Pierre BS, Oger M, Lacombe D, Genevieve D, Fontana E, Darra F, Cancas C, Barth M, Bonneau D, Bernadina BD, N'guyen S, Gitiaux C, Parent P, des P, V, Pedespan JM, Legrez V, Castelnaud-Ptakine L, Nitschke P, Hieu T, Masson C, Zelenika D, Andrieux A, Francis F, Guerrini R, Cowan NJ, Bahi-Buisson N, and Chelly J (2013). Mutations in TUBG1, DYNC1H1, KIF5C and KIF2A

- cause malformations of cortical development and microcephaly. *Nat. Genet* 45, 639–647. [PubMed: 23603762]
265. Pooranachandran N and Malicki JJ (2016). Unexpected Roles for Ciliary Kinesins and Intraflagellar Transport Proteins. *Genetics* 203, 771–785. [PubMed: 27038111]
266. Portran D, Schaedel L, Xu Z, Thery M, and Nachury MV (2017). Tubulin acetylation protects long-lived microtubules against mechanical ageing. *Nat. Cell Biol* 19, 391–398. [PubMed: 28250419]
267. Praetorius HA and Spring KR (2003). The renal cell primary cilium functions as a flow sensor. *Curr. Opin. Nephrol. Hypertens* 12, 517–520. [PubMed: 12920399]
268. Prosser SL and Morrison CG (2015). Centrin2 regulates CP110 removal in primary cilium formation. *J. Cell Biol* 208, 693–701. [PubMed: 25753040]
269. Qiu N, Xiao Z, Cao L, Buechel MM, David V, Roan E, and Quarles LD (2012). Disruption of Kif3a in osteoblasts results in defective bone formation and osteopenia. *J. Cell Sci* 125, 1945–1957. [PubMed: 22357948]
270. Quadros RM, Miura H, Harms DW, Akatsuka H, Sato T, Aida T, Redder R, Richardson GP, Inagaki Y, Sakai D, Buckley SM, Seshacharyulu P, Batra SK, Behlke MA, Zeiner SA, Jacobi AM, Izu Y, Thoreson WB, Urness LD, Mansour SL, Ohtsuka M, and Gurusurthy CB (2017). Easi-CRISPR: a robust method for one-step generation of mice carrying conditional and insertion alleles using long ssDNA donors and CRISPR ribonucleoproteins. *Genome Biol* 18, 92. [PubMed: 28511701]
271. Rachel RA, Li T, and Swaroop A (2012). Photoreceptor sensory cilia and ciliopathies: focus on CEP290, RPGR and their interacting proteins. *Cilia* 1, 22. [PubMed: 23351659]
272. Rachel RA, Yamamoto EA, Dewanjee MK, May-Simera HL, Sergeev YV, Hackett AN, Pohida K, Munasinghe J, Gotoh N, Wickstead B, Fariss RN, Dong L, Li T, and Swaroop A (2015). CEP290 alleles in mice disrupt tissue-specific cilia biogenesis and recapitulate features of syndromic ciliopathies. *Hum. Mol. Genet* 24, 3775–3791. [PubMed: 25859007]
273. Raghupathy RK, Zhang X, Liu F, Alhasani RH, Biswas L, Akhtar S, Pan L, Moens CB, Li W, Liu M, Kennedy BN, and Shu X (2017). Rpgrip1 is required for rod outer segment development and ciliary protein trafficking in zebrafish. *Sci. Rep* 7, 16881. [PubMed: 29203866]
274. Rao KN, Li L, Anand M, and Khanna H (2015). Ablation of retinal ciliopathy protein RPGR results in altered photoreceptor ciliary composition. *Sci. Rep* 5, 11137. [PubMed: 26068394]
275. Rauch A, Thiel CT, Schindler D, Wick U, Crow YJ, Ekici AB, van Essen AJ, Goecke TO, Al-Gazali L, Chrzanowska KH, Zweier C, Brunner HG, Becker K, Curry CJ, Dallapiccola B, Devriendt K, Dorfler A, Kinning E, Megarbane A, Meinecke P, Semple RK, Spranger S, Toutain A, Trembath RC, Voss E, Wilson L, Hennekam R, de ZF, Dorr HG, and Reis A (2008). Mutations in the pericentrin (PCNT) gene cause primordial dwarfism. *Science* 319, 816–819. [PubMed: 18174396]
276. Remans K, Burger M, Vetter IR, and Wittinghofer A (2014). C2 domains as protein-protein interaction modules in the ciliary transition zone. *Cell Rep* 8, 1–9. [PubMed: 24981858]
277. Renault L, Hanzal-Bayer M, and Hillig RC (2001). Coexpression, copurification, crystallization and preliminary X-ray analysis of a complex of ARL2-GTP and PDE delta. *Acta Crystallogr. D. Biol. Crystallogr* 57, 1167–1170. [PubMed: 11468408]
278. Roehlich P (1975). The sensory cilium of retinal rods is analogous to the transitional zone of motile cilia. *Cell Tissue. Res* 161, 421–430. [PubMed: 1175211]
279. Roepman R, Bernoud-Hubac N, Schick DE, Maugeri A, Berger W, Ropers HH, Cremers FP, and Ferreira PA (2000). The retinitis pigmentosa GTPase regulator (RPGR) interacts with novel transport-like proteins in the outer segments of rod photoreceptors. *Hum. Mol. Genet* 9, 2095–2105. [PubMed: 10958648]
280. Roepman R, Letteboer SJ, Arts HH, van Beersum SE, Lu X, Krieger E, Ferreira PA, and Cremers FP (2005). Interaction of nephrocystin-4 and RPGRIP1 is disrupted by nephronophthisis or Leber congenital amaurosis-associated mutations. *Proc. Natl. Acad. Sci. U. S. A* 102, 18520–18525. [PubMed: 16339905]
281. Ronquillo CC, Bernstein PS, and Baehr W (2012). Senior-Loken syndrome: A syndromic form of retinal dystrophy associated with nephronophthisis. *Vision Res* 75, 88–97. [PubMed: 22819833]

282. Ronquillo CC, Hanke-Gogokhia C, Revelo MP, Frederick JM, Jiang L, and Baehr W (2016). Ciliopathy-associated IQCB1/NPHP5 protein is required for mouse photoreceptor outer segment formation. *FASEB J* 30, 3400–3412. [PubMed: 27328943]
283. Roosing S, Lamers IJ, de VE, Van den Born LI, Lambertus S, Arts HH, Peters TA, Hoyng CB, Kremer H, Hetterschijt L, Letteboer SJ, van WE, Roepman R, den Hollander AI, and Cremers FP (2014). Disruption of the basal body protein POC1B results in autosomal-recessive cone-rod dystrophy. *Am. J. Hum. Genet* 95, 131–142. [PubMed: 25018096]
284. Rosenbaum JL and Witman GB (2002). Intraflagellar transport. *Nat. Rev. Mol. Cell Biol* 3, 813–825. [PubMed: 12415299]
285. Roy K, Jerman S, Jozsef L, McNamara T, Onyekaba G, Sun Z, and Marin EP (2017). Palmitoylation of the ciliary GTPase Arl13b is necessary for its stability and its role in cilia formation. *J. Biol. Chem* 292 (43), 17703–17717. [PubMed: 28848045]
286. Salisbury JL (1995). Centrin, centrosomes, and mitotic spindle poles. *Curr. Opin. Cell Biol* 7, 39–45. [PubMed: 7755988]
287. Salisbury JL, Suino KM, Busby R, and Springett M (2002). Centrin-2 is required for centriole duplication in mammalian cells. *Curr. Biol* 12, 1287–1292. [PubMed: 12176356]
- Salmon NA, Reijo Pera RA, Xu EY, 2006 A gene trap knockout of the abundant sperm tail protein, outer dense fiber 2, results in preimplantation lethality. *Genesis* 44 (11), 515–522. [PubMed: 17078042]
288. Sang L, Miller JJ, Corbit KC, Giles RH, Brauer MJ, Otto EA, Baye LM, Wen X, Scales SJ, Kwong M, Huntzicker EG, Sfakianos MK, Sandoval W, Bazan JF, Kulkarni P, Garcia-Gonzalo FR, Seol AD, O'Toole JF, Held S, Reutter HM, Lane WS, Rafiq MA, Noor A, Ansar M, Devi AR, Sheffield VC, Slusarski DC, Vincent JB, Doherty DA, Hildebrandt F, Reiter JF, and Jackson PK (2011). Mapping the NPHP-JBTS-MKS protein network reveals ciliopathy disease genes and pathways. *Cell* 145, 513–528. [PubMed: 21565611]
289. Sarig O, Nahum S, Rapaport D, Ishida-Yamamoto A, Fuchs-Telem D, Qiaoli L, Cohen-Katsenelson K, Spiegel R, Nousbeck J, Israeli S, Borochowitz ZU, Padalon-Brauch G, Uitto J, Horowitz M, Shalev S, and Sprecher E (2012). Short stature, onychodysplasia, facial dysmorphism, and hypotrichosis syndrome is caused by a POC1A mutation. *Am. J. Hum. Genet* 91, 337–342. [PubMed: 22840363]
290. Satir P and Christensen ST (2007). Overview of structure and function of mammalian cilia. *Annu. Rev. Physiol* 69, 377–400. [PubMed: 17009929]
291. Satir P, Mitchell DR, and Jekely G (2008). How did the cilium evolve? *Curr. Top. Dev. Biol* 85, 63–82. [PubMed: 19147002]
292. Satir P, Pedersen LB, and Christensen ST (2010). The primary cilium at a glance. *J. Cell Sci* 123, 499–503. [PubMed: 20144997]
293. Sawant DB, Majumder S, Perkins JL, Yang CH, Eyers PA, and Fisk HA (2015). Centrin 3 is an inhibitor of centrosomal Mps1 and antagonizes centrin 2 function. *Mol. Biol. Cell* 26, 3741–3753. [PubMed: 26354417]
294. Sayer JA, Otto EA, O'Toole JF, Nurnberg G, Kennedy MA, Becker C, Hennies HC, Helou J, Attanasio M, Fausett BV, Utsch B, Khanna H, Liu Y, Drummond I, Kawakami I, Kusakabe T, Tsuda M, Ma L, Lee H, Larson RG, Allen SJ, Wilkinson CJ, Nigg EA, Shou C, Lillo C, Williams DS, Hoppe B, Kemper MJ, Neuhaus T, Parisi MA, Glass IA, Petry M, Kispert A, Gloy J, Ganner A, Walz G, Zhu X, Goldman D, Nurnberg P, Swaroop A, Leroux MR, and Hildebrandt F (2006). The centrosomal protein nephrocystin-6 is mutated in Joubert syndrome and activates transcription factor ATF4. *Nat. Genet* 38, 674–681. [PubMed: 16682973]
295. Schaefer E, Zaloszc A, Lauer J, Durand M, Stutzmann F, Perdomo-Trujillo Y, Redin C, Bennouna G, V, Toutain A, Perrin L, Gerard M, Caillard S, Bei X, Lewis RA, Christmann D, Letsch J, Kribs M, Mutter C, Muller J, Stoetzel C, Fischbach M, Marion V, Katsanis N, and Dollfus H (2011). Mutations in SDCCAG8/NPHP10 Cause Bardet-Biedl Syndrome and Are Associated with Penetrant Renal Disease and Absent Polydactyly. *Mol. Syndromol* 1, 273–281. [PubMed: 22190896]
296. Schafer T, Putz M, Lienkamp S, Ganner A, Bergbreiter A, Ramachandran H, Gieloff V, Gerner M, Mattonet C, Czarnecki PG, Sayer JA, Otto EA, Hildebrandt F, Kramer-Zucker A, and Walz G

- (2008). Genetic and physical interaction between the NPHP5 and NPHP6 gene products. *Hum. Mol. Genet* 17, 3655–3662. [PubMed: 18723859]
297. Schmidt KN, Kuhns S, Neuner A, Hub B, Zentgraf H, and Pereira G (2012). Cep164 mediates vesicular docking to the mother centriole during early steps of ciliogenesis. *J. Cell Biol* 199, 1083–1101. [PubMed: 23253480]
298. Schmidt T, Karsunky H, Frass B, Baum W, Denzel A, and Moroy T (2000). A novel protein (Fbf-1) that binds to CD95/APO-1/FAS and shows sequence similarity to trichohyalin and plectin. *Biochim. Biophys. Acta* 1493, 249–254. [PubMed: 10978533]
299. Scholey JM (2008). Intraflagellar transport motors in cilia: moving along the cell's antenna. *J Cell Biol* 180, 23–29. [PubMed: 18180368]
300. Scholey JM (2013). Cilium assembly: delivery of tubulin by kinesin-2-powered trains. *Curr. Biol* 23, R956–R959. [PubMed: 24200322]
301. Schrick JJ, Vogel P, Abuin A, Hampton B, and Rice DS (2006). ADP-ribosylation factor-like 3 is involved in kidney and photoreceptor development. *Am. J. Pathol* 168, 1288–1298. [PubMed: 16565502]
302. Schwarz N, Hardcastle AJ, and Cheetham ME (2012). Arl3 and RP2 mediated assembly and traffic of membrane associated cilia proteins. *Vision Res* 75, 2–4. [PubMed: 22884633]
303. Schweizer S and Hoyer-Fender S (2009). Mouse Odf2 localizes to centrosomes and basal bodies in adult tissues and to the photoreceptor primary cilium. *Cell Tissue Res* 338, 295–301. [PubMed: 19756757]
304. Sedmak T and Wolfrum U (2011). Intraflagellar transport proteins in ciliogenesis of photoreceptor cells. *Biol. Cell* 103, 449–466. [PubMed: 21732910]
305. Seixas C, Choi SY, Polgar N, Umberger NL, East MP, Zuo X, Moreiras H, Ghossoub R, Benmerah A, Kahn RA, Fogelgren B, Caspary T, Lipschutz JH, and Barral DC (2016). Arl13b and the exocyst interact synergistically in ciliogenesis. *Mol. Biol. Cell* 27, 308–320. [PubMed: 26582389]
306. Shaheen R, Faqeih E, Shamseldin HE, Noche RR, Sunker A, Alshammari MJ, Al-Sheddi T, Adly N, Al-Dosari MS, Megason SG, Al-Husain M, Al-Mohanna F, and Alkuraya FS (2012). POC1A truncation mutation causes a ciliopathy in humans characterized by primordial dwarfism. *Am. J. Hum. Genet* 91, 330–336. [PubMed: 22840364]
307. Sharif AS, Yu D, Loertscher S, Austin R, Nguyen K, Mathur PD, Clark AM, Zou J, Lobanova ES, Arshavsky VY, and Yang J (2018). C8ORF37 Is Required for Photoreceptor Outer Segment Disc Morphogenesis by Maintaining Outer Segment Membrane Protein Homeostasis. *J. Neurosci* 38, 3160–3176. [PubMed: 29440555]
308. Shi X, Garcia G III, Van De Weghe JC, McGorty R, Pazour GJ, Doherty D, Huang B, and Reiter JF (2017). Super-resolution microscopy reveals that disruption of ciliary transition-zone architecture causes Joubert syndrome. *Nat. Cell Biol* 19, 1178–1188. [PubMed: 28846093]
309. Shu X, Black GC, Rice JM, Hart-Holden N, Jones A, O'Grady A, Ramsden S, and Wright AF (2007). RPGR mutation analysis and disease: an update. *Hum. Mutat* 28, 322–328. [PubMed: 17195164]
310. Signor D, Wedaman KP, Rose LS, and Scholey JM (1999). Two heteromeric kinesin complexes in chemosensory neurons and sensory cilia of *Caenorhabditis elegans*. *Mol. Biol. Cell* 10, 345–360. [PubMed: 9950681]
311. Siller SS, Sharma H, Li S, Yang J, Zhang Y, Holtzman MJ, Winuthayanon W, Colognato H, Holdener BC, Li FQ, and Takemaru KI (2017). Conditional knockout mice for the distal appendage protein CEP164 reveal its essential roles in airway multiciliated cell differentiation. *PLoS. Genet* 13, e1007128. [PubMed: 29244804]
312. Sillibourne JE, Hurbain I, Grand-Perret T, Goud B, Tran P, and Bornens M (2013). Primary ciliogenesis requires the distal appendage component Cep123. *Biol. Open* 2, 535–545. [PubMed: 23789104]
313. Singla V and Reiter JF (2006). The primary cilium as the cell's antenna: signaling at a sensory organelle. *Science* 313, 629–633. [PubMed: 16888132]
314. Slaats GG, Ghosh AK, Falke LL, Le CS, Shaltiel IA, van de Hoek G, Klasson TD, Stokman MF, Logister I, Verhaar MC, Goldschmeding R, Nguyen TQ, Drummond IA, Hildebrandt F, and Giles

- RH (2014). Nephronophthisis-associated CEP164 regulates cell cycle progression, apoptosis and epithelial-to-mesenchymal transition. *PLoS. Genet* 10, e1004594. [PubMed: 25340510]
315. Slepak VZ and Hurley JB (2008). Mechanism of light-induced translocation of arrestin and transducin in photoreceptors: interaction-restricted diffusion. *IUBMB. Life* 60, 2–9. [PubMed: 18379987]
316. Smrzka OW, Delgehr N, and Bornens M (2000). Tissue-specific expression and subcellular localisation of mammalian delta-tubulin. *Curr. Biol* 10, 413–416. [PubMed: 10753753]
317. Song P, Dudinsky L, Fogerty J, Gaivin R, and Perkins BD (2016). Arl13b Interacts With Vangl2 to Regulate Cilia and Photoreceptor Outer Segment Length in Zebrafish. *Invest Ophthalmol. Vis. Sci* 57, 4517–4526. [PubMed: 27571019]
318. Sonnen KF, Schermelleh L, Leonhardt H, and Nigg EA (2012). 3D-structured illumination microscopy provides novel insight into architecture of human centrosomes. *Biol. Open* 1, 965–976. [PubMed: 23213374]
319. Sorokin S (1962). Centrioles and the formation of rudimentary cilia by fibroblasts and smooth muscle cells. *J. Cell Biol* 15, 363–377. [PubMed: 13978319]
320. Sorokin SP (1968). Reconstructions of centriole formation and ciliogenesis in mammalian lungs. *J. Cell Sci* 3, 207–230. [PubMed: 5661997]
321. Spektor A, Tsang WY, Khoo D, and Dynlacht BD (2007). Cep97 and CP110 suppress a cilia assembly program. *Cell* 130, 678–690. [PubMed: 17719545]
322. Stone EM, Cideciyan AV, Aleman TS, Scheetz TE, Sumaroka A, Ehlinger MA, Schwartz SB, Fishman GA, Traboulsi EI, Lam BL, Fulton AB, Mullins RF, Sheffield VC, and Jacobson SG (2011). Variations in NPHP5 in patients with nonsyndromic leber congenital amaurosis and Senior-Loken syndrome. *Arch. Ophthalmol* 129, 81–87. [PubMed: 21220633]
323. Sudhof TC and Rizo J (1996). Synaptotagmins: C2-domain proteins that regulate membrane traffic. *Neuron* 17, 379–388. [PubMed: 8816702]
324. Sukumaran SK, Lewandowski BC, Qin Y, Kotha R, Bachmanov AA, and Margolskee RF (2017). Whole transcriptome profiling of taste bud cells. *Sci. Rep* 7, 7595. [PubMed: 28790351]
325. Sun TY, Wang HY, Kwon JW, Yuan B, Lee IW, Cui XS, and Kim NH (2017). Centriolin, a centriole-appendage protein, regulates peripheral spindle migration and asymmetric division in mouse meiotic oocytes. *Cell Cycle* 16, 1774–1780. [PubMed: 28075662]
326. Sun Z, Amsterdam A, Pazour GJ, Cole DG, Miller MS, and Hopkins N (2004). A genetic screen in zebrafish identifies cilia genes as a principal cause of cystic kidney. *Development* 131, 4085–4093. [PubMed: 15269167]
327. Sung CH and Chuang JZ (2010). The cell biology of vision. *J Cell Biol* 190, 953–963. [PubMed: 20855501]
328. Swaroop A, Kim D, and Forrest D (2010). Transcriptional regulation of photoreceptor development and homeostasis in the mammalian retina. *Nat. Rev. Neurosci* 11, 563–576. [PubMed: 20648062]
329. Tabish M, Siddiqui ZK, Nishikawa K, and Siddiqui SS (1995). Exclusive expression of *C. elegans* *osm-3* kinesin gene in chemosensory neurons open to the external environment. *J Mol. Biol* 247, 377–389. [PubMed: 7714894]
330. Takeda S, Yonekawa Y, Tanaka Y, Okada Y, Nonaka S, and Hirokawa N (1999). Left-right asymmetry and kinesin superfamily protein KIF3A: new insights in determination of laterality and mesoderm induction by *kif3A*^{-/-} mice analysis. *J. Cell Biol* 145, 825–836. [PubMed: 10330409]
331. Tallila J, Jakkula E, Peltonen L, Salonen R, and Kestila M (2008). Identification of CC2D2A as a Meckel syndrome gene adds an important piece to the ciliopathy puzzle. *Am. J. Hum. Genet* 82, 1361–1367. [PubMed: 18513680]
332. Tanos BE, Yang HJ, Soni R, Wang WJ, Macaluso FP, Asara JM, and Tsou MF (2013). Centriole distal appendages promote membrane docking, leading to cilia initiation. *Genes Dev* 27, 163–168. [PubMed: 23348840]
333. Temiyasathit S, Tang WJ, Leucht P, Anderson CT, Monica SD, Castillo AB, Helms JA, Stearns T, and Jacobs CR (2012). Mechanosensing by the primary cilium: deletion of *Kif3A* reduces bone formation due to loading. *PLoS. One* 7, e33368. [PubMed: 22428034]

334. Thauvin-Robinet C, Lee JS, Lopez E, Herranz-Perez V, Shida T, Franco B, Jego L, Ye F, Pasquier L, Loget P, Gigot N, Aral B, Lopes CA, St-Onge J, Bruel AL, Thevenon J, Gonzalez-Granero S, Alby C, Munnich A, Vekemans M, Huet F, Fry AM, Saunier S, Riviere JB, Attie-Bitach T, Garcia-Verdugo JM, Faivre L, Megarbane A, and Nachury MV (2014). The oral-facial-digital syndrome gene C2CD3 encodes a positive regulator of centriole elongation. *Nat. Genet* 46, 905–911. [PubMed: 24997988]
335. Thomas S, Cantagrel V, Mariani L, Serre V, Lee JE, Elkhartoufi N, de LP, Desguerre I, Munnich A, Boddaert N, Lyonnet S, Vekemans M, Lisgo SN, Caspary T, Gleeson J, and Attie-Bitach T (2015). Identification of a novel ARL13B variant in a Joubert syndrome-affected patient with retinal impairment and obesity. *Eur. J. Hum. Genet* 23, 621–627. [PubMed: 25138100]
336. Thomas S, Wright KJ, Le CS, Micalizzi A, Romani M, Abhyankar A, Saada J, Perrault I, Amiel J, Litzler J, Filhol E, Elkhartoufi N, Kwong M, Casanova JL, Boddaert N, Baehr W, Lyonnet S, Munnich A, Burglen L, Chassaing N, Encha-Ravazi F, Vekemans M, Gleeson JG, Valente EM, Jackson PK, Drummond IA, Saunier S, and Attie-Bitach T (2014). A homozygous PDE6D mutation in Joubert syndrome impairs targeting of farnesylated INPP5E protein to the primary cilium. *Hum. Mutat* 35, 137–146. [PubMed: 24166846]
337. Thompson DA, Khan NW, Othman MI, Chang B, Jia L, Grahek G, Wu Z, Hirianna S, Nellissery J, Li T, Khanna H, Colosi P, Swaroop A, and Heckenlively JR (2012). Rd9 is a naturally occurring mouse model of a common form of retinitis pigmentosa caused by mutations in RPGR-ORF15. *PLoS. ONE* 7, e35865. [PubMed: 22563472]
338. Tian G, Ropelewski P, Nemet I, Lee R, Lodowski KH, and Imanishi Y (2014). An unconventional secretory pathway mediates the cilia targeting of peripherin/rds. *J. Neurosci* 34, 992–1006. [PubMed: 24431457]
339. Tollenaere MA, Mailand N, and Bekker-Jensen S (2015). Centriolar satellites: key mediators of centrosome functions. *Cell Mol. Life Sci* 72, 11–23. [PubMed: 25173771]
340. Travaglini L, Brancati F, Silhavy J, Iannicelli M, Nickerson E, Elkhartoufi N, Scott E, Spencer E, Gabriel S, Thomas S, Ben-Zeev B, Bertini E, Boltshauser E, Chaouch M, Cilio MR, de Jong MM, Kayserili H, Ogur G, Poretti A, Signorini S, Uziel G, Zaki MS, Johnson C, Attie-Bitach T, Gleeson JG, and Valente EM (2013). Phenotypic spectrum and prevalence of INPP5E mutations in Joubert syndrome and related disorders. *Eur. J. Hum. Genet* 21, 1074–1078. [PubMed: 23386033]
341. Trojan P, Krauss N, Choe HW, Giessl A, Pulvermuller A, and Wolfrum U (2008). Centrioles in retinal photoreceptor cells: regulators in the connecting cilium. *Prog. Retin. Eye Res* 27, 237–259. [PubMed: 18329314]
342. Troutt LL, Wang E, Pagh-Roehl K, and Burnside B (1990). Microtubule nucleation and organization in teleost photoreceptors: microtubule recovery after elimination by cold. *J. Neurocytol* 19, 213–223. [PubMed: 2358830]
343. Tsang WY, Bossard C, Khanna H, Peranen J, Swaroop A, Malhotra V, and Dynlacht BD (2008). CP110 suppresses primary cilia formation through its interaction with CEP290, a protein deficient in human ciliary disease. *Dev. Cell* 15, 187–197. [PubMed: 18694559]
344. Tsang WY and Dynlacht BD (2013). CP110 and its network of partners coordinately regulate cilia assembly. *Cilia* 2, 9. [PubMed: 24053599]
345. Tsang WY, Spektor A, Luciano DJ, Indjeian VB, Chen Z, Salisbury JL, Sanchez I, and Dynlacht BD (2006). CP110 cooperates with two calcium-binding proteins to regulate cytokinesis and genome stability. *Mol. Biol. Cell* 17, 3423–3434. [PubMed: 16760425]
346. Tuz K, Hsiao YC, Juarez O, Shi B, Harmon EY, Phelps IG, Lennartz MR, Glass IA, Doherty D, and Ferland RJ (2013). The Joubert syndrome-associated missense mutation (V443D) in the Abelson-helper integration site 1 (AHI1) protein alters its localization and protein-protein interactions. *J. Biol. Chem* 288, 13676–13694. [PubMed: 23532844]
347. Uzbekov R and Alieva I (2018). Who are you, subdistal appendages of centriole? *Open. Biol* 8.
348. Valente EM, Silhavy JL, Brancati F, Barrano G, Krishnaswami SR, Castori M, Lancaster MA, Boltshauser E, Boccone L, Al-Gazali L, Fazzi E, Signorini S, Louie CM, Bellacchio E, Bertini E, Dallapiccola B, and Gleeson JG (2006). Mutations in CEP290, which encodes a centrosomal protein, cause pleiotropic forms of Joubert syndrome. *Nat. Genet* 38, 623–625. [PubMed: 16682970]

349. van Huet RA, Estrada-Cuzcano A, Banin E, Rotenstreich Y, Hipp S, Kohl S, Hoyng CB, den Hollander AI, Collin RW, and Klevering BJ (2013). Clinical characteristics of rod and cone photoreceptor dystrophies in patients with mutations in the C8orf37 gene. *Invest Ophthalmol. Vis. Sci* 54, 4683–4690. [PubMed: 23788369]
350. van Wijk E, Kersten FF, Kartono A, Mans DA, Brandwijk K, Letteboer SJ, Peters TA, Marker T, Yan X, Cremers CW, Cremers FP, Wolfrum U, Roepman R, and Kremer H (2009). Usher syndrome and Leber congenital amaurosis are molecularly linked via a novel isoform of the centrosomal ninein-like protein. *Hum. Mol. Genet* 18, 51–64. [PubMed: 18826961]
351. Veleri S, Manjunath SH, Fariss RN, May-Simera H, Brooks M, Foskett TA, Gao C, Longo TA, Liu P, Nagashima K, Rachel RA, Li T, Dong L, and Swaroop A (2014). Ciliopathy-associated gene Cc2d2a promotes assembly of subdistal appendages on the mother centriole during cilia biogenesis. *Nat. Commun* 5, 4207. [PubMed: 24947469]
352. Veltel S, Gasper R, Eisenacher E, and Wittinghofer A (2008). The retinitis pigmentosa 2 gene product is a GTPase-activating protein for Arf-like 3. *Nat. Struct. Mol. Biol* 15, 373–380. [PubMed: 18376416]
353. Vlijm R, Li X, Panic M, Ruthnick D, Hata S, Herrmannsdorfer F, Kuner T, Heilemann M, Engelhardt J, Hell SW, and Schiebel E (2018). STED nanoscopy of the centrosome linker reveals a CEP68-organized, periodic rootletin network anchored to a C-Nap1 ring at centrioles. *Proc. Natl. Acad. Sci. U. S. A* 115, E2246–E2253. [PubMed: 29463719]
354. Wang H, den Hollander AI, Moayed Y, Abulimiti A, Li Y, Collin RW, Hoyng CB, Lopez I, Abboud EB, Al-Rajhi AA, Bray M, Lewis RA, Lupski JR, Mardon G, Koenekoop RK, and Chen R (2009a). Mutations in SPATA7 cause Leber congenital amaurosis and juvenile retinitis pigmentosa. *Am. J. Hum. Genet* 84, 380–387. [PubMed: 19268277]
355. Wang X, Li N, Xiong N, You Q, Li J, Yu J, Qing H, Wang T, Cordell HJ, Isacson O, Vance JM, Martin ER, Zhao Y, Cohen BM, Buttner EA, and Lin Z (2016). Genetic Variants of Microtubule Actin Cross-linking Factor 1 (MACF1) Confer Risk for Parkinson's Disease. *Mol. Neurobiol* 54 (4), 2878–2888. [PubMed: 27021023]
356. Wang X, Tsai JW, Imai JH, Lian WN, Vallee RB, and Shi SH (2009b). Asymmetric centrosome inheritance maintains neural progenitors in the neocortex. *Nature* 461, 947–955. [PubMed: 19829375]
357. Watzlich D, Vetter I, Gotthardt K, Miertschke M, Chen YX, Wittinghofer A, and Ismail S (2013). The interplay between RPGR, PDEdelta and Arl2/3 regulate the ciliary targeting of farnesylated cargo. *EMBO Rep* 14, 465–472. [PubMed: 23559067]
358. Wei Q, Xu Q, Zhang Y, Li Y, Zhang Q, Hu Z, Harris PC, Torres VE, Ling K, and Hu J (2013). Transition fibre protein FBF1 is required for the ciliary entry of assembled intraflagellar transport complexes. *Nat. Commun* 4, 2750. [PubMed: 24231678]
359. Weihbrecht K, Goar WA, Carter CS, Sheffield VC, and Seo S (2018). Genotypic and phenotypic characterization of the Sdccag8Tn(sb-Tyr)2161B.CA1C2Ove mouse model. *PLoS. ONE* 13, e0192755. [PubMed: 29444170]
360. Wensel TG, Zhang Z, Anastassov IA, Gilliam JC, He F, Schmid MF, and Robichaux MA (2016). Structural and molecular bases of rod photoreceptor morphogenesis and disease. *Prog. Retin. Eye Res* 55, 32–51. [PubMed: 27352937]
361. Werner S, Pimenta-Marques A, and Bettencourt-Dias M (2017). Maintaining centrosomes and cilia. *J. Cell Sci* 130, 3789–3800. [PubMed: 29142065]
362. Westfall JE, Hoyt C, Liu Q, Hsiao YC, Pierce EA, Page-McCaw PS, and Ferland RJ (2010). Retinal degeneration and failure of photoreceptor outer segment formation in mice with targeted deletion of the Joubert syndrome gene, Ahi1. *J. Neurosci* 30, 8759–8768. [PubMed: 20592197]
363. Wheway G, Schmidts M, Mans DA, Szymanska K, Nguyen TT, Racher H, Phelps IG, Toedt G, Kennedy J, Wunderlich KA, Sorusch N, Abdelhamed ZA, Natarajan S, Herridge W, van RJ, Horn N, Boldt K, Parry DA, Letteboer SJF, Roosing S, Adams M, Bell SM, Bond J, Higgins J, Morrison EE, Tomlinson DC, Slaats GG, van Dam TJP, Huang L, Kessler K, Giessler A, Logan CV, Boyle EA, Shendure J, Anazi S, Aldahmesh M, Al HS, Hegele RA, Ober C, Frosk P, Mhanni AA, Chodirker BN, Chudley AE, Lamont R, Bernier FP, Beaulieu CL, Gordon P, Pon RT, Donahue C, Barkovich AJ, Wolf L, Toomes C, Thiel CT, Boycott KM, McKibbin M, Inglehearn CF, Stewart F, Omran H, Huynen MA, Sergouniotis PI, Alkuraya FS, Parboosingh JS, Innes AM,

- Willoughby CE, Giles RH, Webster AR, Ueffing M, Blacque O, Gleeson JG, Wolfrum U, Beales PL, Gibson T, Doherty D, Mitchison HM, Roepman R, and Johnson CA (2015). An siRNA-based functional genomics screen for the identification of regulators of ciliogenesis and ciliopathy genes. *Nat. Cell Biol* 17, 1074–1087. [PubMed: 26167768]
364. Whitehead JL, Wang SY, Bost-Usinger L, Hoang E, Frazer KA, and Burnside B (1999). Photoreceptor localization of the KIF3A and KIF3B subunits of the heterotrimeric microtubule motor kinesin II in vertebrate retina. *Exp. Eye Res* 69, 491–503. [PubMed: 10548469]
365. Williams CL, Li C, Kida K, Inglis PN, Mohan S, Semenec L, Bialas NJ, Stupay RM, Chen N, Blacque OE, Yoder BK, and Leroux MR (2011). MKS and NPHP modules cooperate to establish basal body/transition zone membrane associations and ciliary gate function during ciliogenesis. *J. Cell Biol* 192, 1023–1041. [PubMed: 21422230]
366. Wolf MT and Hildebrandt F (2011). Nephronophthisis. *Pediatr. Nephrol* 26, 181–194. [PubMed: 20652329]
367. Wolfrum U, Giessel A, and Pulvermuller A (2002). Centrins, a novel group of Ca²⁺-binding proteins in vertebrate photoreceptor cells. *Adv. Exp. Med. Biol* 514, 155–178. [PubMed: 12596921]
368. Wolfrum U and Salisbury JL (1998). Expression of centrin isoforms in the mammalian retina. *Exp. Cell Res* 242, 10–17. [PubMed: 9665797]
369. Won J, Gifford E, Smith RS, Yi H, Ferreira PA, Hicks WL, Li T, Naggert JK, and Nishina PM (2009). RPGRIP1 is essential for normal rod photoreceptor outer segment elaboration and morphogenesis. *Hum. Mol. Genet* 18, 4329–4339. [PubMed: 19679561]
370. Won J, Marin de EC, Smith RS, Hicks WL, Edwards MM, Longo-Guess C, Li T, Naggert JK, and Nishina PM (2011). NPHP4 is necessary for normal photoreceptor ribbon synapse maintenance and outer segment formation, and for sperm development. *Hum. Mol. Genet* 20, 482–496. [PubMed: 21078623]
371. Wong-Riley MT and Besharse JC (2012). The kinesin superfamily protein KIF17: one protein with many functions. *Biomol. Concepts* 3, 267–282. [PubMed: 23762210]
372. Wright KJ, Baye LM, Olivier-Mason A, Mukhopadhyay S, Sang L, Kwong M, Wang W, Pretorius PR, Sheffield VC, Sengupta P, Slusarski DC, and Jackson PK (2011). An ARL3-UNC119-RP2 GTPase cycle targets myristoylated NPHP3 to the primary cilium. *Genes Dev* 25, 2347–2360. [PubMed: 22085962]
373. Wright ZC, Singh RK, Alpino R, Goldberg AF, Sokolov M, and Ramamurthy V (2016). ARL3 regulates trafficking of prenylated phototransduction proteins to the rod outer segment. *Hum. Mol. Genet* 25, 2031–2044. [PubMed: 26936825]
374. Xu Z, Schaedel L, Portran D, Aguilar A, Gaillard J, Marinkovich MP, Thery M, and Nachury MV (2017). Microtubules acquire resistance from mechanical breakage through intraluminal acetylation. *Science* 356, 328–332. [PubMed: 28428427]
375. Yadav SP, Sharma NK, Liu C, Dong L, Li T, and Swaroop A (2016). Centrosomal protein CP110 controls maturation of the mother centriole during cilia biogenesis. *Development* 143, 1491–1501. [PubMed: 26965371]
376. Yang J, Adamian M, and Li T (2006). Rootletin interacts with C-Nap1 and may function as a physical linker between the pair of centrioles/basal bodies in cells. *Mol. Biol. Cell* 17, 1033–1040. [PubMed: 16339073]
377. Yang J, Gao J, Adamian M, Wen XH, Pawlyk B, Zhang L, Sanderson MJ, Zuo J, Makino CL, and Li T (2005). The ciliary rootlet maintains long-term stability of sensory cilia. *Mol. Cell Biol* 25, 4129–4137. [PubMed: 15870283]
378. Yang J and Li T (2006). Focus on molecules: rootletin. *Exp Eye Res* 83, 1–2. [PubMed: 16318850]
379. Yang J, Liu X, Yue G, Adamian M, Bulgakov O, and Li T (2002). Rootletin, a novel coiled-coil protein, is a structural component of the ciliary rootlet. *J Cell Biol* 159, 431–440. [PubMed: 12427867]
380. Yang TT, Chong WM, Wang WJ, Mazo G, Tanos B, Chen Z, Tran TMN, Chen YD, Weng RR, Huang CE, Jane WN, Tsou MB, and Liao JC (2018). Super-resolution architecture of

- mammalian centriole distal appendages reveals distinct blade and matrix functional components. *Nat. Commun* 9, 2023. [PubMed: 29789620]
381. Ye X, Zeng H, Ning G, Reiter JF, and Liu A (2014). C2cd3 is critical for centriolar distal appendage assembly and ciliary vesicle docking in mammals. *Proc. Natl. Acad. Sci. U. S. A* 111, 2164–2169. [PubMed: 24469809]
382. Yin X, Takei Y, Kido MA, and Hirokawa N (2011). Molecular motor KIF17 is fundamental for memory and learning via differential support of synaptic NR2A/2B levels. *Neuron* 70, 310–325. [PubMed: 21521616]
383. Ying G, Avasthi P, Irwin M, Gerstner CD, Frederick JM, Lucero MT, and Baehr W (2014). Centrin 2 is required for mouse olfactory ciliary trafficking and development of ependymal cilia planar polarity. *J. Neurosci* 34, 6377–6388. [PubMed: 24790208]
384. Yuba-Kubo A, Kubo A, Hata M, and Tsukita S (2005). Gene knockout analysis of two gamma-tubulin isoforms in mice. *Dev. Biol* 282, 361–373. [PubMed: 15893303]
385. Zach F, Grassmann F, Langmann T, Sorusch N, Wolfrum U, and Stohr H (2012). The retinitis pigmentosa 28 protein FAM161A is a novel ciliary protein involved in intermolecular protein interaction and microtubule association. *Hum. Mol. Genet* 21, 4573–4586. [PubMed: 22791751]
386. Zhang C, Zhang Q, Wang F, and Liu Q (2015). Knockdown of poc1b causes abnormal photoreceptor sensory cilium and vision impairment in zebrafish. *Biochem. Biophys. Res Commun* 465, 651–657. [PubMed: 26188096]
387. Zhang Q, Acland GM, Wu WX, Johnson JL, Pearce-Kelling S, Tulloch B, Vervoort R, Wright AF, and Aguirre GD (2002). Different RPGR exon ORF15 mutations in Canids provide insights into photoreceptor cell degeneration. *Hum. Mol. Genet* 11, 993–1003. [PubMed: 11978759]
388. Zhang Q, Hu J, and Ling K (2013). Molecular views of Arf-like small GTPases in cilia and ciliopathies. *Exp. Cell Res* 319, 2316–2322. [PubMed: 23548655]
389. Zhang W, Li L, Su Q, Gao G, and Khanna H (2017). Gene Therapy Using a miniCEP290 Fragment Delays Photoreceptor Degeneration in a Mouse Model of Leber Congenital Amaurosis. *Hum. Gene Ther* 29(1), 42–50. [PubMed: 28679290]
390. Zhang X, Liu H, Zhang Y, Qiao Y, Miao S, Wang L, Zhang J, Zong S, and Koide SS (2003). A novel gene, RSD-3/HSD-3.1, encodes a meiotic-related protein expressed in rat and human testis. *J. Mol. Med. (Berl)* 81, 380–387. [PubMed: 12736779]
391. Zhang Y and He CY (2011). Centrioles in unicellular organisms: functional diversity and specialization. *Protoplasma*
392. Zhang ZD, Frankish A, Hunt T, Harrow J, and Gerstein M (2010). Identification and analysis of unitary pseudogenes: historic and contemporary gene losses in humans and other primates. *Genome Biol* 11, R26. [PubMed: 20210993]
393. Zhao C and Malicki J (2011). Nephrocystins and MKS proteins interact with IFT particle and facilitate transport of selected ciliary cargos. *EMBO J* 30, 2532–2544. [PubMed: 21602787]
394. Zhao C, Omori Y, Brodowska K, Kovach P, and Malicki J (2012). Kinesin-2 family in vertebrate ciliogenesis. *Proc. Natl. Acad. Sci. U. S. A* 109, 2388–2393. [PubMed: 22308397]
395. Zhao Y, Hong DH, Pawlyk B, Yue G, Adamian M, Grynberg M, Godzik A, and Li T (2003). The retinitis pigmentosa GTPase regulator (RPGR)- interacting protein: Sub-serving RPGR function and participating in disk morphogenesis. *Proc. Natl. Acad. Sci. U. S. A* 100, 3965–3970. [PubMed: 12651948]
396. Zhong H, Eblimit A, Moayedi Y, Boye SL, Chiodo VA, Chen Y, Li Y, Nichols RM, Hauswirth WW, Chen R, and Mardon G (2015). AAV8(Y733F)-mediated gene therapy in a Spata7 knockout mouse model of Leber congenital amaurosis and retinitis pigmentosa. *Gene Ther* 22, 619–627. [PubMed: 25965394]
397. Zoubovsky S, Oh EC, Cash-Padgett T, Johnson AW, Hou Z, Mori S, Gallagher M, Katsanis N, Sawa A, and Jaaro-Peled H (2015). Neuroanatomical and behavioral deficits in mice haploinsufficient for Pericentriolar material 1 (Pcm1). *Neurosci. Res* 98, 45–49. [PubMed: 25697395]

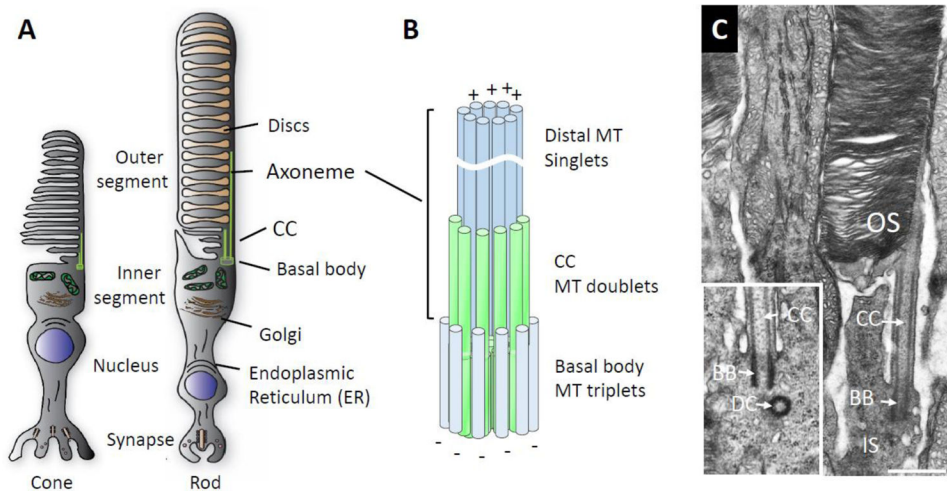


Figure 1. Basal body/axoneme cytoskeleton. A, Schematic of cone and rod photoreceptors depicting the outer segment where phototransduction occurs, the inner segment containing the endoplasmic reticulum and Golgi apparatus, the nuclear region and the synaptic terminal. B, enlarged detail of the axoneme cytoskeleton consisting of basal body (= mother centriole) proximally, transition zone and axoneme distally. C, electron micrograph of mouse rod, partial view, revealing the basal body, microtubule-stabilized CC and outer segment (OS) stacked with membrane discs. Note, the daughter centriole is out-of-plane and not visible; inset shows a different BB/DC pair. Scale, 0.5 μm .

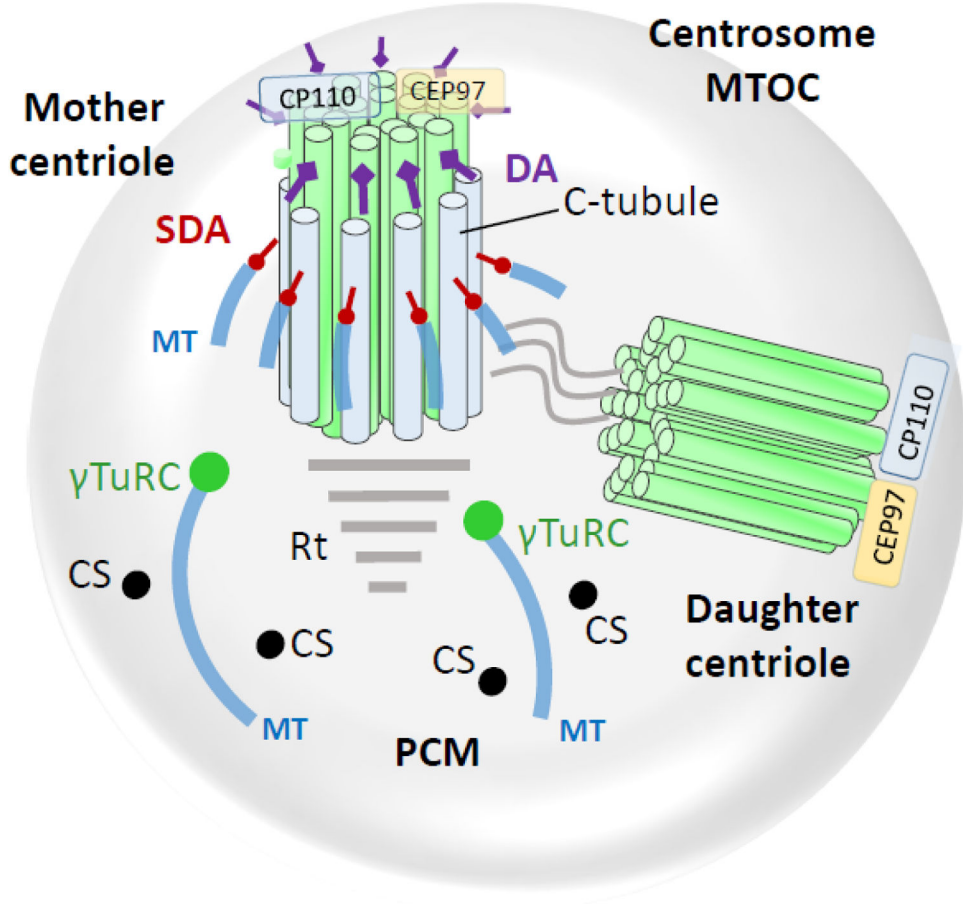


Figure 2. The centrosome (microtubule organization center, MTOC) consisting of mother centriole, daughter centriole and pericentriolar matrix (PCM). Mother and daughter centriolar microtubules consist of nine triplet barrels organized in a cartwheel array. Each triplet has A-, B- and C-tubules; C-tubules are specific for mother and daughter centrioles. Cytoplasmic microtubules connect to subdistal appendages and to PCM points (green circles) anchored by the γ -tubulin ring complex. Centriolar satellites (CS) are distributed throughout the PCM. Distal ends of both mother and daughter centrioles are protected by centriolar coiled-coil protein CP110, and centrosomal protein CEP97. DA, distal appendages; SDA, subdistal appendages; MT, microtubules; γ T, γ -tubulin ring complex; Rt, striated rootlet; CS, centriolar satellites.

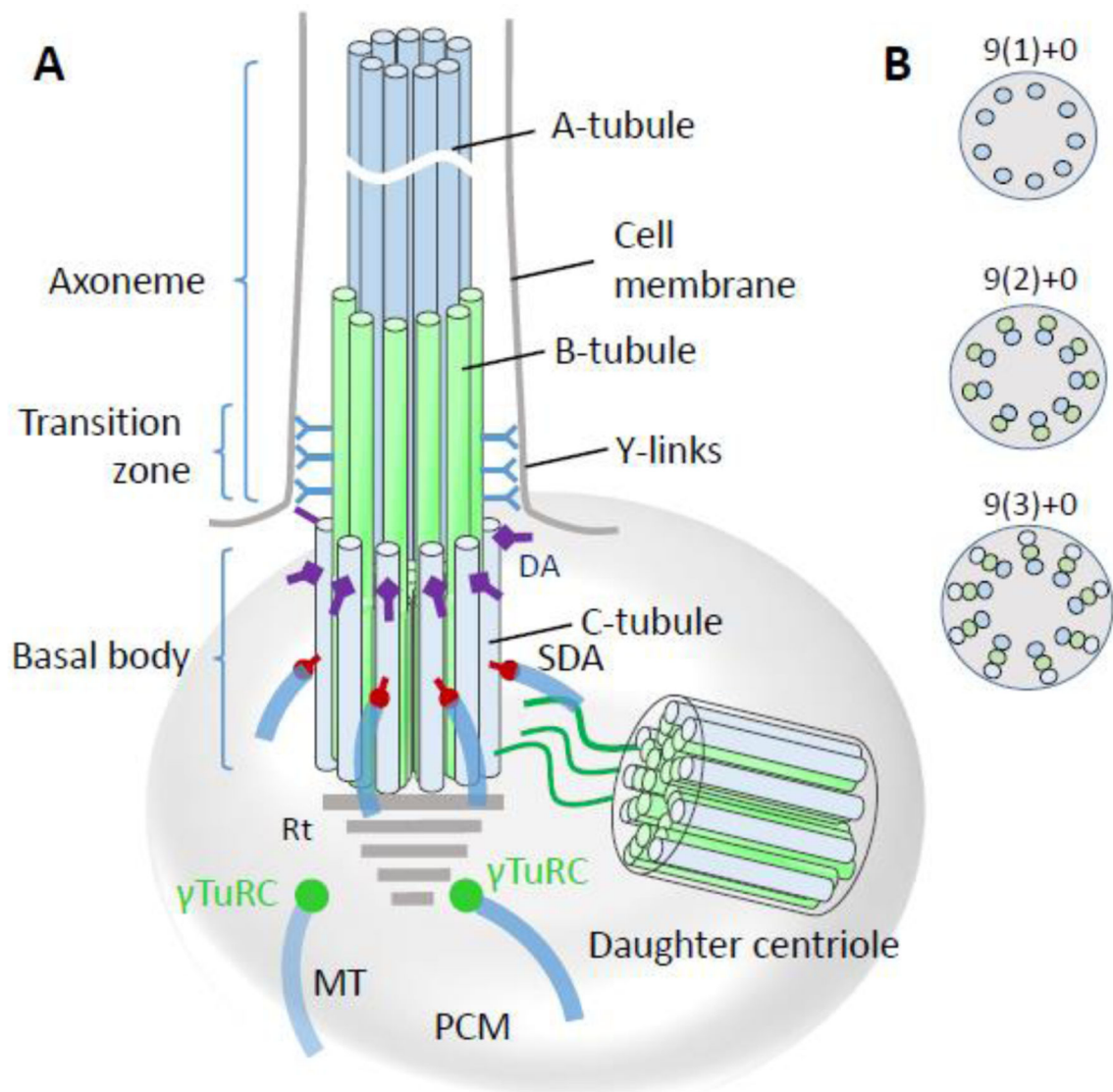


Figure 3.

Basal body/axoneme backbone. A, basal body schematic representation with transition zone and axoneme. A-tubules (blue) and B-tubules (green) emanate from the basal body to form the transition zone which is characterized by y-links connecting the tubules to the ciliary membrane. While the proximal axoneme consists of microtubule doublets, the distal axoneme has singlets. DA, distal appendages; SDA, subdistal appendages; MT, microtubules; PCM, pericentriolar matrix; γ T, γ -tubulin ring complex. B, Crosssections of the axoneme, transition zone and basal body, distal-to-proximal respectively, indicating the arrangement of microtubule arrays. “+0” indicates absence of a central MT.

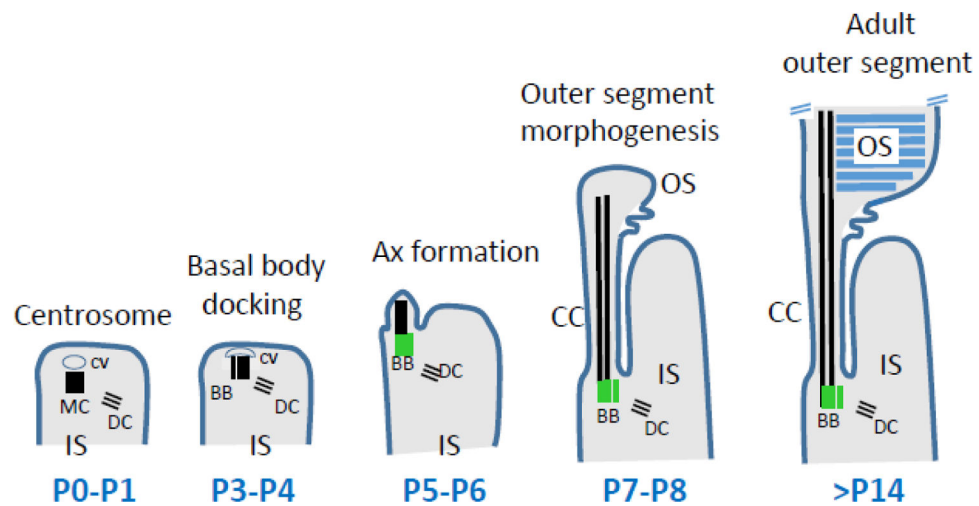


Figure 4. Stages of rod photoreceptor ciliogenesis. At P0-P1, the centrosome consisting of mother and daughter centrioles (MC, DC) acquires a ciliary vesicle (CV) at its distal end. Soon, from P3-P4, the mother centriole docks to the cortex of the inner segment. At P5-P6, the axoneme (Ax) emanates from the MC and MC becomes a basal body (green). A- and B-tubules (black) extend at P7-P8, and the transition zone TZ is established. The cell membrane evaginates and discs are formed. The outer segment is considered mature at three weeks of age (P21). Adapted from May-Simera et al., 2018.

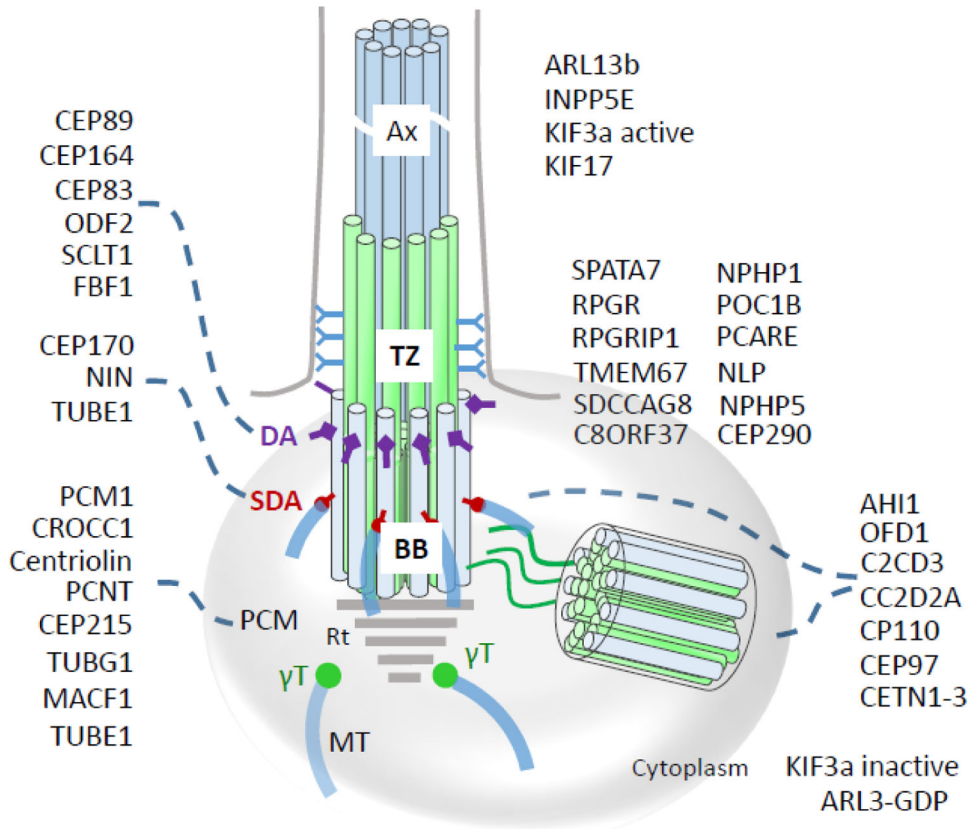


Figure 5. Localizations of centrosomal and centriolar proteins to the basal body, transition zone, and axoneme. CEP89, CEP164, CEP83, ODF2, SCLT1 and FBF1 are distal appendage (DA) proteins, while CEP170, NIN, and TUBE1 are subdistal appendage (SDA) proteins. PCM1, CROCC1 (rootletin), centriolin, PCNT (pericentrin), CEP215, TUBG1, TUBE1 and MACF1 are associated with the pericentriolar matrix (PCM) or ‘cloud.’ ARL13b and INPP5E are ciliary proteins. SPATA7, RPGR, RPGRIP1, NLP, centrin, CEP290, IQCB1/NPHP5, NPHP4, POC1B, TMEM67, SDCCAG8 (NPHP10) and C8ORF37 are located at the transition zone (TZ) distinguished by the presence of Y-linkers. AHI1, OFD1, C2CD3, CC2D2A, CP110, CEP97 localize to BB and DC. Inactive ARL3-GDP and KIF3a are cytoplasmic. Note that some proteins distribute to multiple subdomains (e.g., CETN2 associates with MC, DC and TZ) or occur in active and inactive forms altering their subdomain affiliation (ARL3-GTP and ARL3-GDP, or active/inactive KIF3a). Rt, rootlet; BB, basal body; Ax, axoneme.

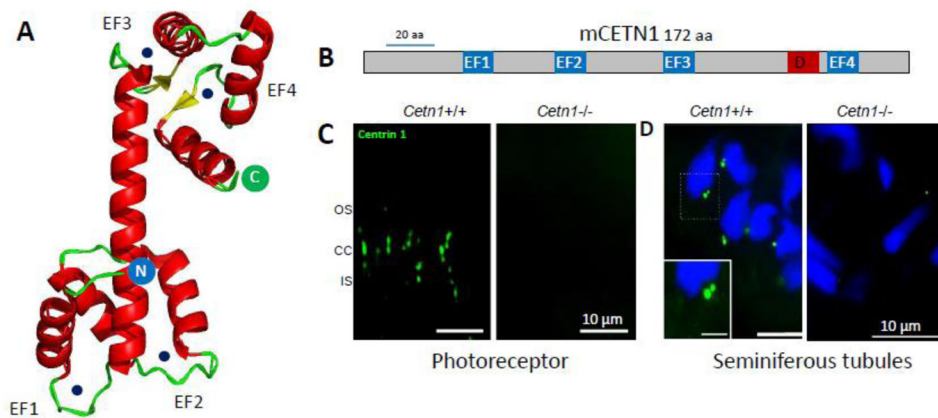


Figure 6. Centrin 1 crystal structure and localization. A, *Cctn1* (PDB 5D43) structure showing α -helical ribbons (red) and β -strand loops (green), forming the four EF-hands. Circular N (blue) and C (green) denote N- and C-terminals, respectively. Ca^{2+} ion positions (black dots) are indicated. B, CETN1 domain structure showing four high-affinity Ca^{2+} binding sites (EF-hands, blue) and *DEAD-box* subfamily ATP-dependent helicase signature (D, red). C, immunohistochemistry with anti-CETN1 (green) antibody to show labeling of centrioles and connecting cilia of wild-type photoreceptors (left), and absence in photoreceptors of germline knockout retina (right). Germline deletion of CETN1 does not affect photoreceptor function. D, immunohistochemistry with anti-CETN1 antibody in wild-type (left) and germline knockout (right) seminiferous tubules; *Cctn1*^{-/-} mice are infertile. Scale bars: 10 μm ; inset, 5 μm .

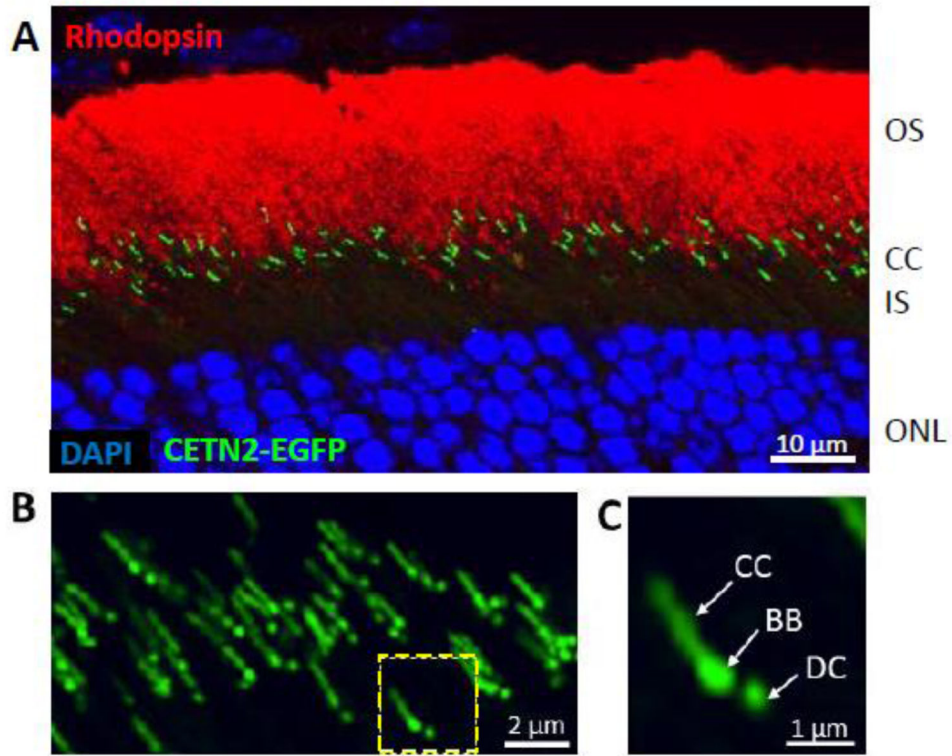


Figure 7. Transgenic expression of EGFP-CETN2 identifies photoreceptor centrioles and connecting cilia. A, rod outer segments labeled with anti-rhodopsin (red), centrioles expressing EGFP-CETN2 (green) and nuclei binding DAPI (blue). B, confocal microscopy of several connecting cilia. C, a single photoreceptor connecting cilium streak resembles the tail of a shooting star. BB, basal body; DC, daughter centriole.

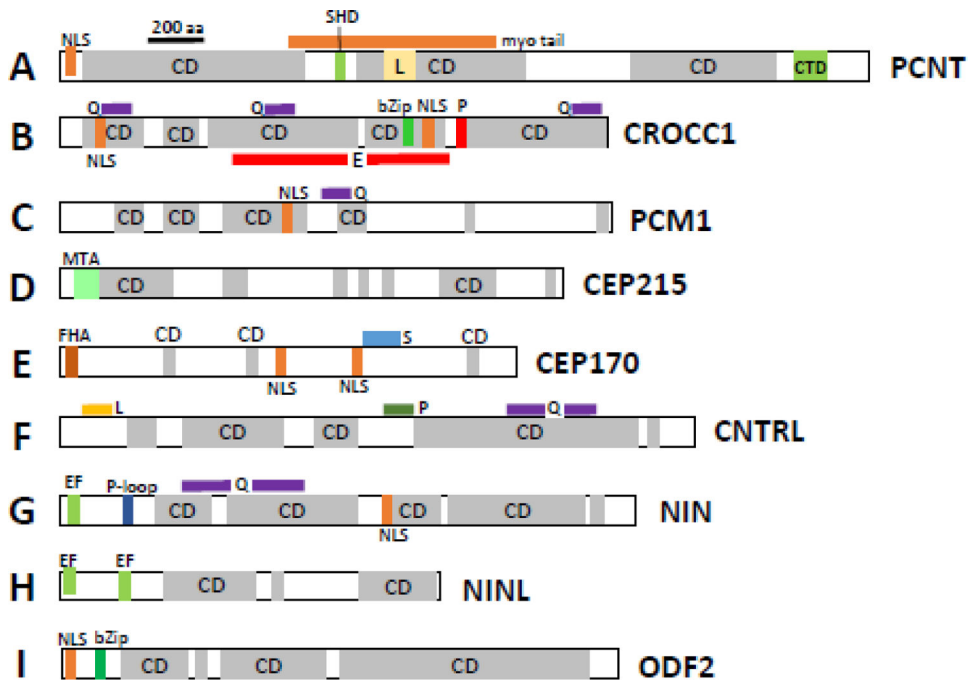


Figure 8.

Domain structures of mouse pericentriolar and subdistal appendage proteins. A, PCNT (pericentrin), B, CROCC1 (rootletin), C, PCM1 (pericentriolar material), D, CEP215 (CDK5RAP2), E, CEP170; F, CNTRL (centriolin), G, NIN (Ninein), H, Ninein-like (NINL) protein and I, ODF2. CD, coiled-coil domains. Myo-tail, myo tail region; CTD, centrosomal targeting domain; SHD, spectrin homology domain; NLS, nuclear localization signal; bZIP, basic leucine zipper domain; MTA, microtubule-associated region; FHA, forkhead-associated domain; Q, glutamine-rich region; E, glutamic acid-rich region; L, leucine-rich region; P, proline-rich region; EF, high-affinity Ca^{2+} binding site (EF-hand); P-loop, ATP/GTP-binding motif. The motifs were identified by scan “my Hits” at <http://myhits.isb-sib.ch/cgi-bin/PFSCAN>. Coiled-coil domains (CD) were retrieved using https://embnet.vital-it.ch/software/COILS_form.html.

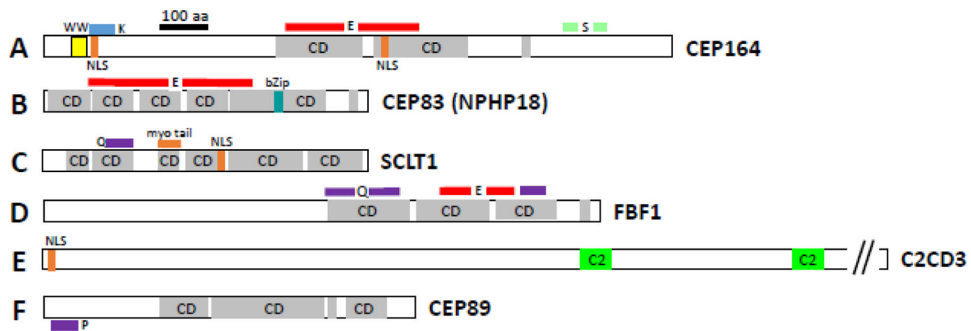


Figure 9.

Domain structures of mouse distal appendage (DA) proteins. A, CEP164, B, CEP83, C, SCLT1, D, FBF1, E, ODF2, F, C2CD3 and G, CEP89. WW, protein interaction domain flanked by tryptophan (W); CD, coiled-coil domains; NLS, nuclear localization signal; regions that are Q, glutamine-rich; E, glutamic acid-rich; K, lysine-rich; P, proline-rich; S, serine-rich are marked with colored lines; bZip, basic leucine zipper domain; myo-tail, myosin tail region;. Motifs were identified by motif scan “my Hits” at <http://myhits.isb-sib.ch/cgi-bin/PFSCAN>. Coiled-coil domains were retrieved using https://embnet.vital-it.ch/software/COILS_form.html.

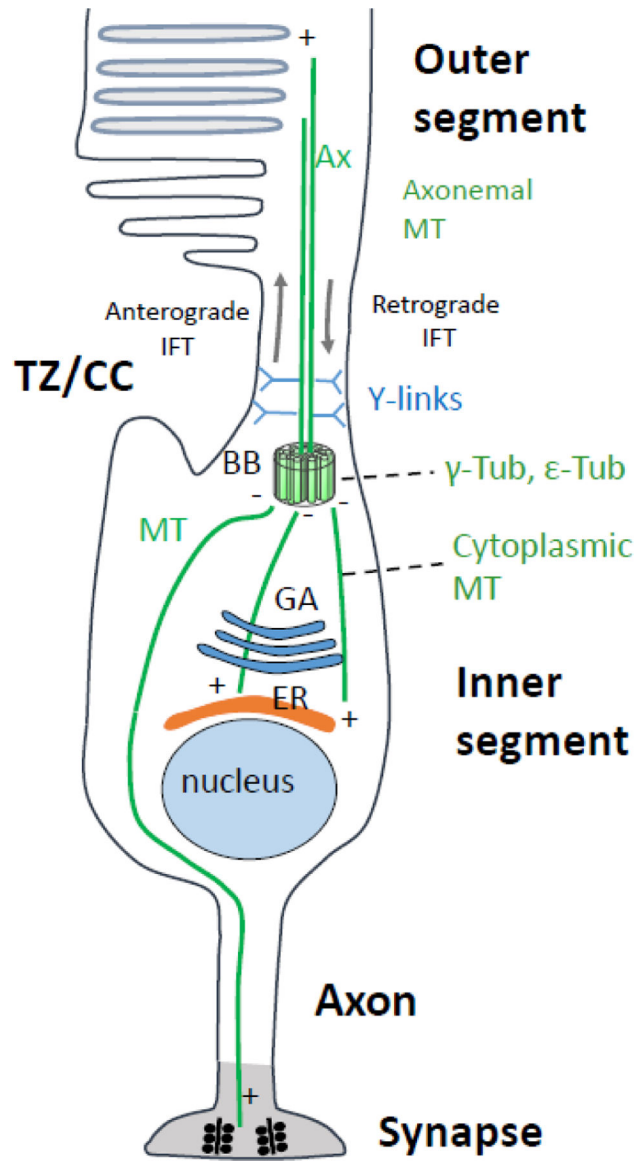


Figure 10.

Schematic of rod microtubule organization. Microtubules (green lines) radiate from the basal body (BB, or MTOC) to the photoreceptor periphery, i.e., the outer segment or alternatively, synaptic terminal. Microtubule (–) ends are located at the BB, (+) ends at the periphery. Plus-end directed kinesin-2 and minus-end directed cytoplasmic dynein transport “cargo” (vesicles loaded with membrane protein) to the appropriate destinations. Kinesin-2, an anterograde molecular motor, transports cargo through the TZ/CC to maintain the axoneme in the face of daily turnover of outer segment (OS) components. Cytoplasmic dynein-2 is the motor for retrograde intraflagellar transport (IFT). Y-links and ciliary proteins at the TZ/CC (CEP290) base have been proposed to form a gate controlling access to the OS, but a functional gate has not been shown to exist in photoreceptors. TZ/CC, transition zone/ connecting cilium; Ax, axoneme; BB, basal body; GA, Golgi apparatus; ER, endoplasmic reticulum; MT, microtubules.

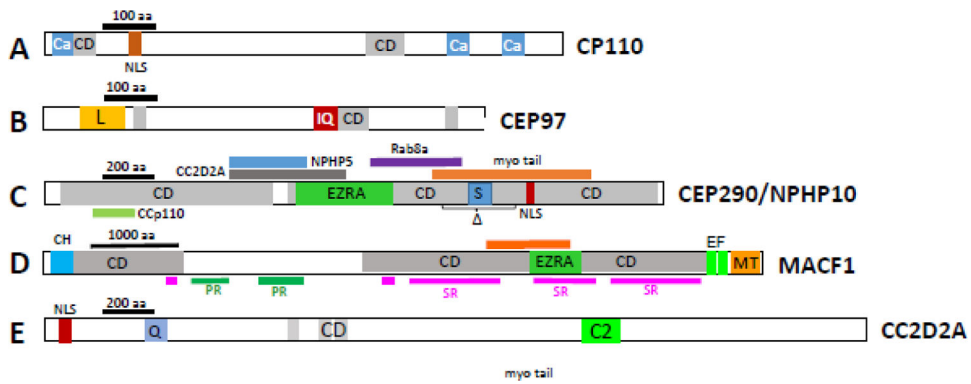


Figure 11.

Distal centriole and proximal TZ protein domain structures. A, CP110; B, CEP97; C, CEP290; D, MACF1; E, CC2D2A. Ca, calmodulin- and centrin-interacting sites (Tsang, 2006); CD, coiled-coil domains; NLS, nuclear localization signal. L, leucine-rich domain; IQ, IQ calmodulin binding motif. EZRA, EZRA (bacterial scaffolding protein) domain; myo, myosin tail domain; colored bars above and below denote interaction sites with indicated proteins; Δ , area of in-frame deletion of exons 36–39 in *rd16*, a CEP290 mutant. S, serine-rich domain. C2, Ca^{2+} -binding domain, a β -sandwich composed of 8 β -strands that co-ordinates two or three Ca^{2+} ions; Q, glutamine-rich domain. (microtubule-actin crosslinking factor 1). PR, plectin domain; SR, spectrin domain; EF, high-affinity Ca^{2+} -binding site; CH, calponin-homology (actin-binding) domain; MT, microtubule-interacting region.

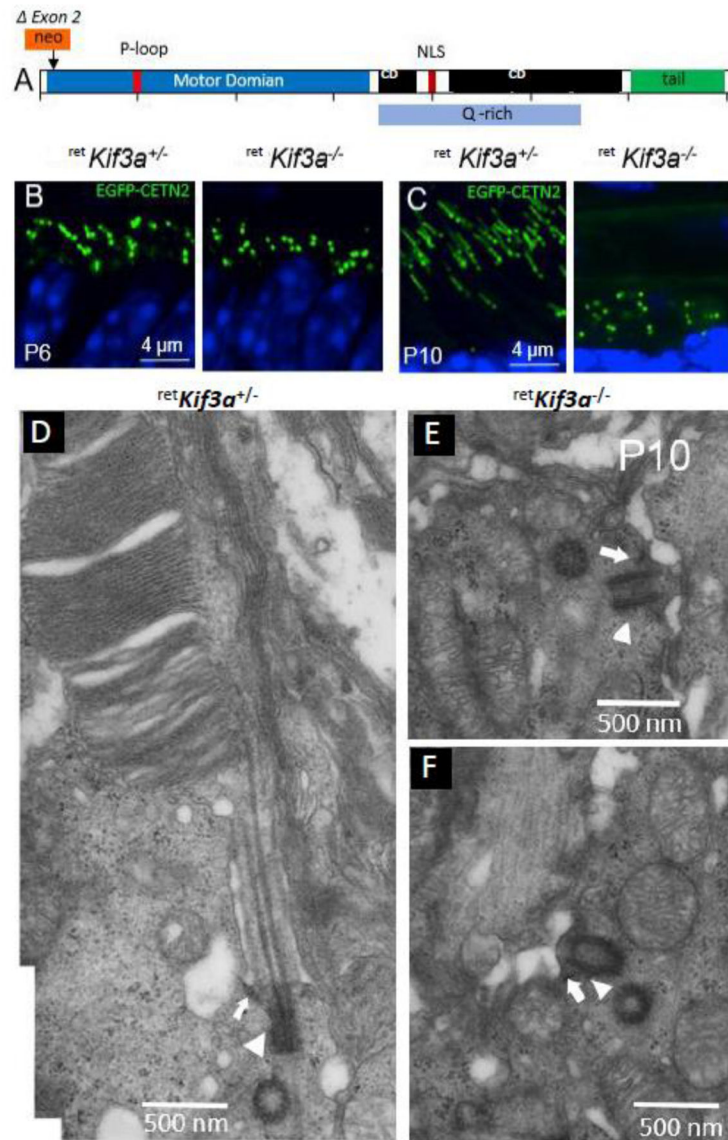


Figure 12.

Retina-specific deletion of *Kif3a* in photoreceptors (*ret Kif3a^{-/-}*). A, KIF3A domain schematic. Six3-Cre expression excises exon 2, thereby truncating the protein after exon 1. B, C, connecting cilium formation in *ret Kif3a^{+/-}* (left) and *ret Kif3a^{-/-}* (right) photoreceptors expressing the centriole marker, EGFP-CENT2, at P6 (B) and P10 (C). In C, CCs appear as 1 μ m-long streaks resembling shooting stars; despite presence of centrioles in the knockouts, CCs are absent. D-F, *ret Kif3a^{+/-}* (D) and *ret Kif3a^{-/-}* (E, F) photoreceptor ultrastructure. P10 *ret Kif3a^{+/-}* photoreceptor with stacks of membrane discs forming at the connecting cilium distal portion (D). E,F, mother centrioles of P10 *ret Kif3a^{-/-}* photoreceptors dock to the cortex normally but are devoid of CCs and outer segments. Mother centriole subdistal (arrow) and distal (arrowhead) appendages are indicated.

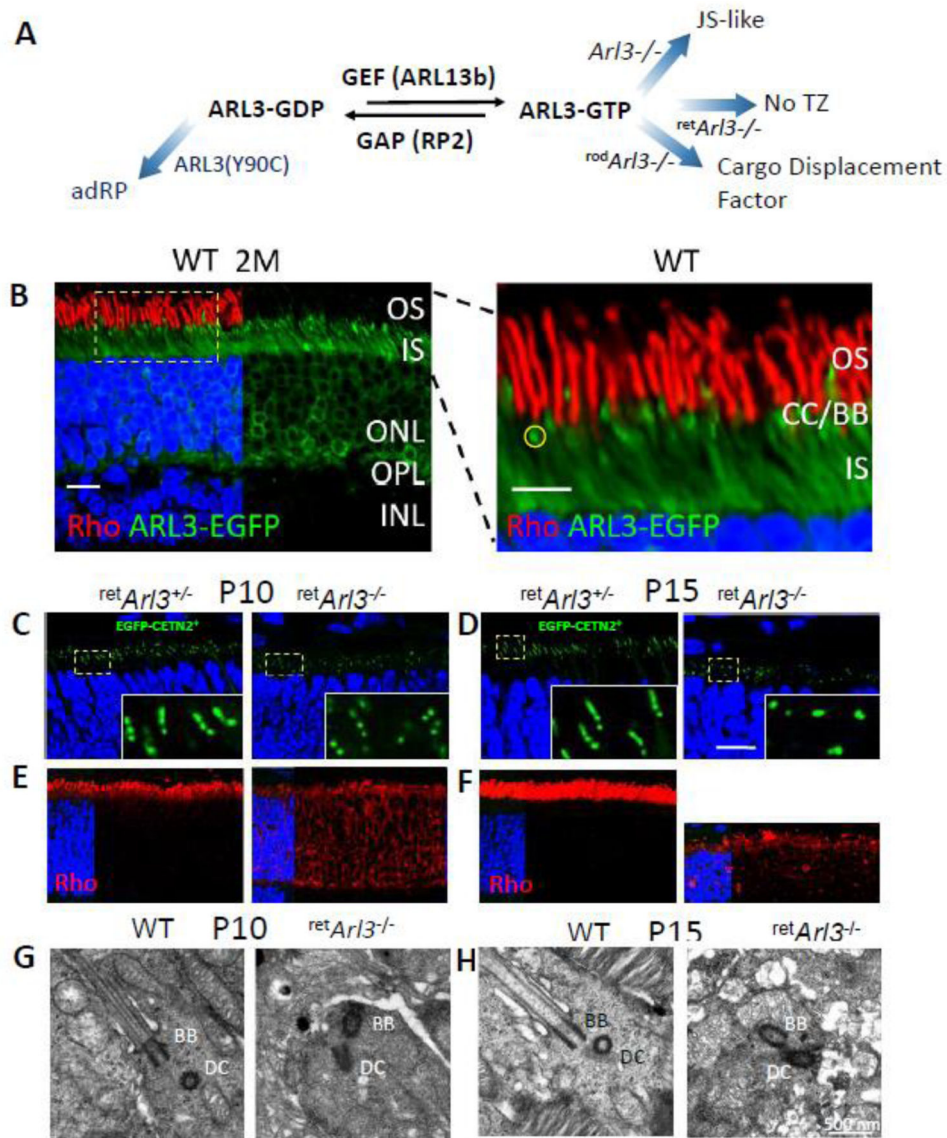


Figure 13.

ARL3 distribution and function in photoreceptors. A, ARL3 activation by its GEF (ARL13b) and inactivation by its GAP (RP2) schematized. B, virally-expressed ARL3-EGFP localizes to the CC/BB area (identified by a yellow circle), inner segment (IS) and outer nuclear layer (ONL) of WT photoreceptors. Rhodopsin (red) is identified with polyclonal antibody directed against the mouse rhodopsin N-terminus (VPP-rho). Scale bar, 10 μ m. Enlargement of dotted area, right; scale, 5 μ m. C-F, ONL immunohistochemistry at P10 (C,E) and P15 (D,F). EGFP-CETN2 fluorescence (C,D), or anti-rhodopsin labeling (E,F) are illustrated. C,D (left panels) show controls with normal transition zones. C, D (right) are retina-specific knockouts with stunted or absent transition zones. Rhodopsin localizes normally to ROS (E,F left panels); rhodopsin mislocalizes to the outer nuclear layer (E,F, right). DAPI (blue) identifies extent of outer nuclear layer. Scale bar, 10 μ m. G, H, Ultrastructure of *retArl3*^{-/-} retina. Transition zone ultrastructure of P10 (G) and P15 (H) WT

and mutant retinas. Controls (G,H left panels) demonstrate intact CC, BB and DC. CCs are absent in each knockout (right). Scale bar, 500 nm.

Author Manuscript

Author Manuscript

Author Manuscript

Author Manuscript

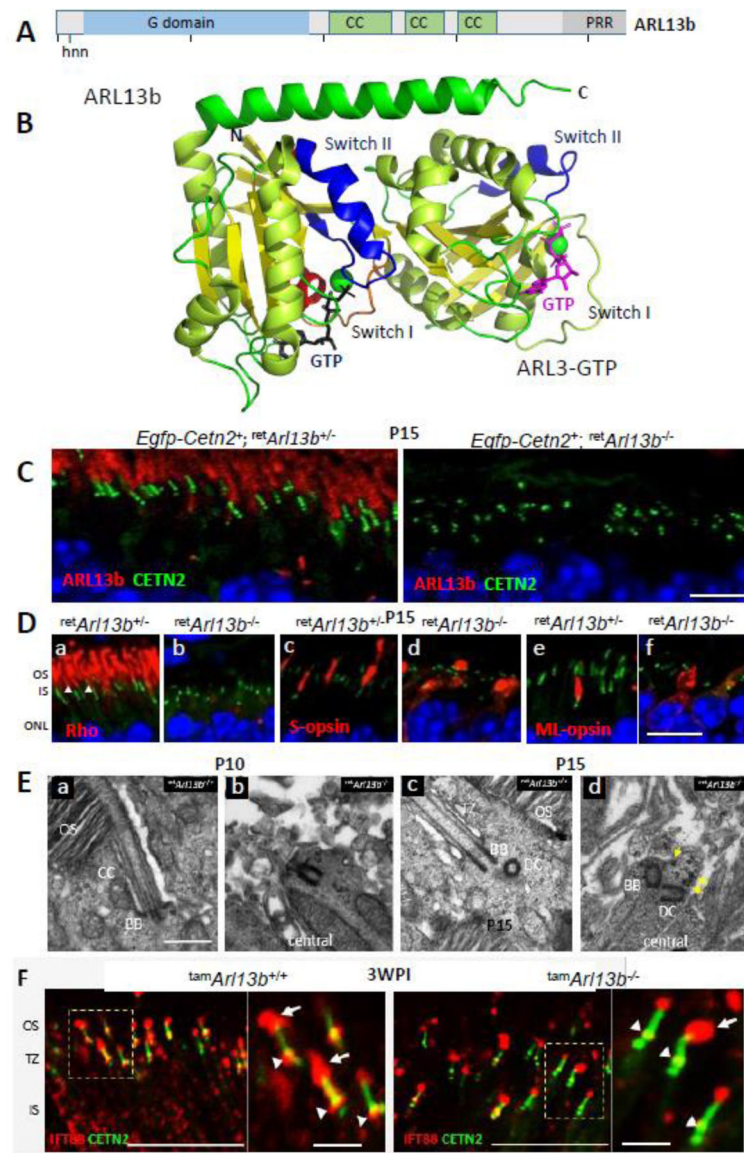


Figure 14.

Deletion of *Arl13b* in retina. A, ARL13b domains: hnn, hennin truncation mutation in mouse; PRR, proline-rich domain; CD, coiled-coil domain; G-domain, a canonical switch motif ('on' with GTP bound, 'off' with GDP bound). B, Co-crystal structure of *C. reinhardtii* ARL13b (residues 17–220, left) and ARL3 (residues 16–180, right) G-domains. Green circle, Mg^{2+} bound to GTP. C-terminal helix and switch II of ARL13B mediate GEF activity. C, Arl13b (red) immunolocalization in control (left panel) and knockout (right) photoreceptors; note, CCs of the heterozygous control are absent in the knockout. D, *Egfp-Cetn2⁺;retArl13b^{+/-}* (a, c, e) and *Egfp-Cetn2⁺;retArl13b^{-/-}* (b, d, f) P15 mouse retina cryosections were labeled with antibodies directed against rhodopsin (a, b), S-opsin (c, d) and ML-opsin (e, f) (red). *retArl13b^{+/-}* photoreceptors develop transition zones (a, white arrowheads), while formation of the CC and OS in *retArl13b^{-/-}* photoreceptors (b, d, f) is impaired. Scale bar, 5 μ m. E, Ultrastructure of P10 (a, b) and P15 (c, d) WT and mutant

photoreceptors. Controls (a, c) develop a CC and OS, while knockouts do not (b, d). Scale bar, 500 nm. F, tamoxifen-induced depletion of ARL13b, assayed 3 weeks post-injection (3WPI). Immunohistochemistry of 3WPI $^{tam}Arl13b^{+/+}$ (left) and $^{tam}Arl13b^{-/-}$ (right) cryosections with anti-IFT88 antibody. Proximal OSs (arrows) and basal bodies (arrowheads) are indicated. Enlargements, IFT88 (red) accumulates at the basal body, CC and proximal OS of control photoreceptors, while IFT88 appears predominantly restricted to the proximal OS of Arl13b-depleted cells. Scale bar, 10 μm ; enlargements, 3 μm .

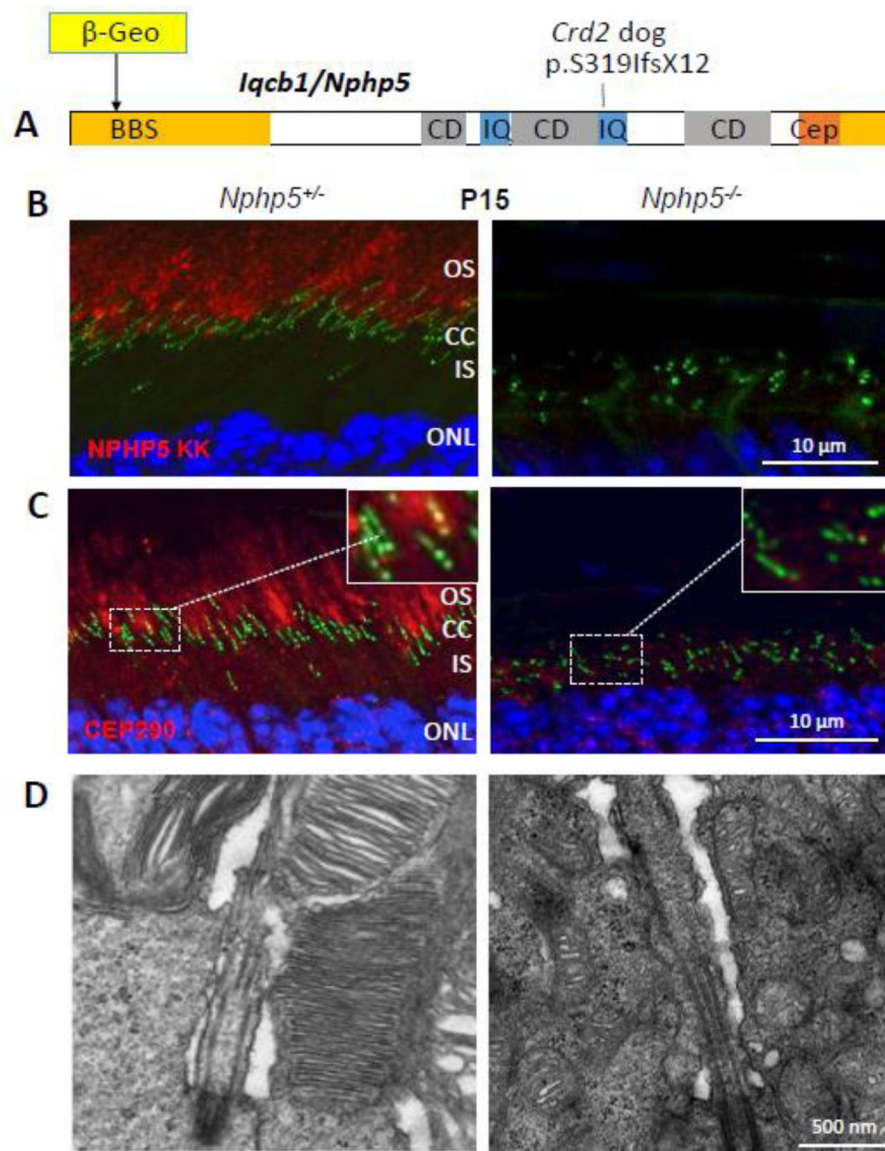


Figure 15.

IQCB1/NPHP5 domain structure and photoreceptor localization. A, IQCB1/NPHP5 functional domains. BBS, BBSome interaction site; CD, coiled-coil domains; IQ, IQ calmodulin-binding motifs; Cep, CEP290-binding site. *Crd2 dog*, position of frameshift mutation in exon 12 associated with SLS. β-GEO identifies the approximate position of truncation in the *Iqcb1* germline knockout. B, IQCB1/NPHP5 immunolocalization in P15 control (left) and *Iqcb1/Nphp5*^{-/-} cryosections. Centrioles/CCs are identified by transgenic expression of EGFP-CETN2. Note, germline *Iqcb1/Nphp5* knockout mice have photoreceptors that are unable to form OS. C, retina cryosections probed with anti-CEP290 antibody. CEP290 is unstable and degraded in the absence of IQCB1/NPHP5. D, P10 control (left) and *Iqcb1/Nphp5*^{-/-} (right) ultrastructure showing photoreceptor transition zones.

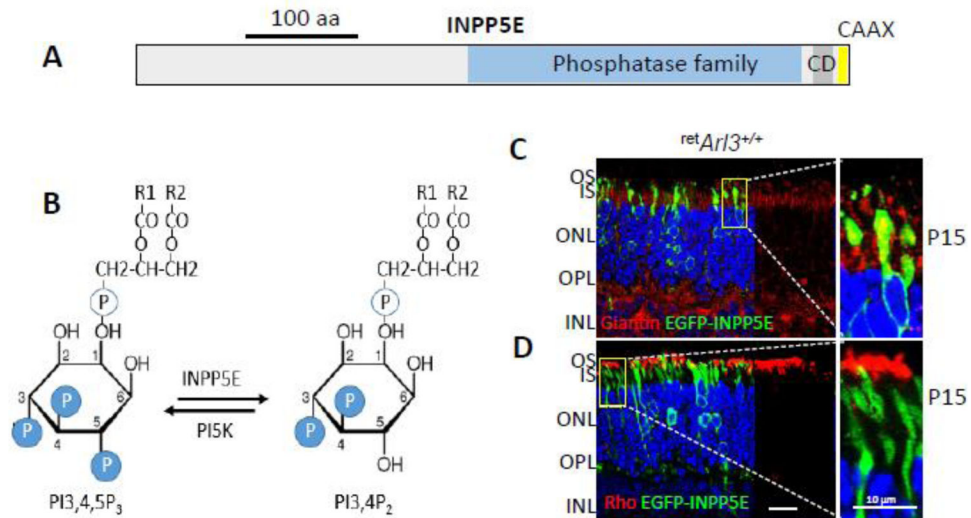


Figure 16.

INPP5E and phosphoinositides. A, INPP5E domain structure. An inositide polyphosphate phosphatase, INPP5E bears a coiled-coil domain at its C-terminal region and a CAAX motif signaling farnesylation. B, INPP5E enzymatically removes a 5'-phosphate at the inositol ring of PI(3,4,5)P₃; side chains R1 and R2 are acyl esters attached to glycerol. PI(3,4,5)P₃ is a key secondary messenger in photoreceptors and other cells. C, virally-expressed EGFP-INPP5E (green) distributes to the Golgi apparatus of the inner segment and colocalizes partially with the Golgi marker, giantin (red). INPP5E is also found associated with the perinuclear endoplasmic reticulum (ER). D, Anti-rhodopsin labels the rod outer segments where EGFP-INPP5E is undetectable.

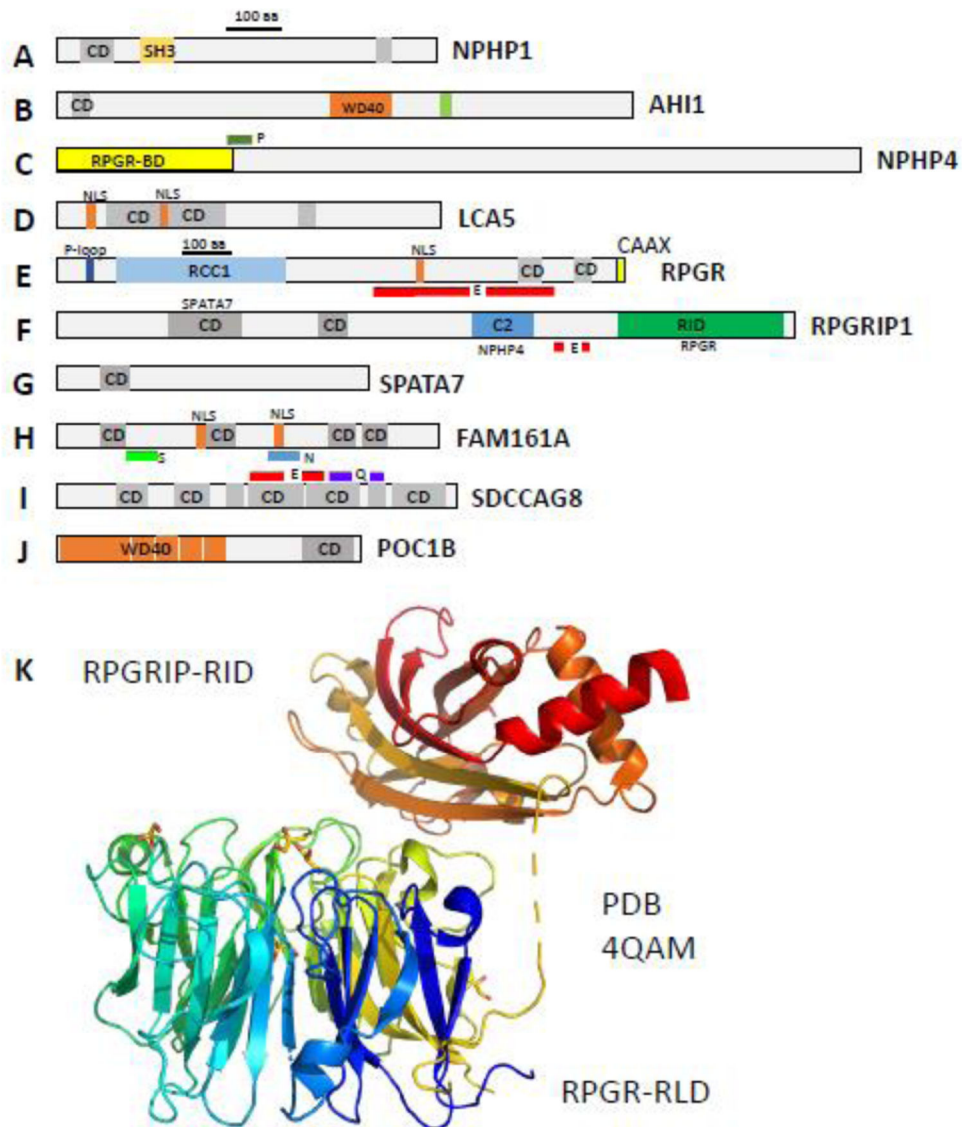


Figure 17.

Domain structures of A, NPHP1, B, AHI1 (jouberin); C, NPHP4; D, lebercilin (LCA5); E, RPGR (RP3); F, RPGRIP1; G, SPATA7; H, TMEM67 (meckelin); I, FAM161A; J, SDCCAG8; K, POC1b. CD, coiled-coil domain; SH3, Src homology 3 domain; WD40, WD40 repeat (40 amino acids flanked by W and D); RPGR-BD, RPGR binding domain; P' proline-rich domain; NLS, nuclear localization signal; P-loop, phosphate binding loop for interaction with ATP/GTP; RCC1, Regulator of Chromosome Condensation 1; E, glutamic acid-rich region; RID, RPGR-interacting domain; C2, β -sandwich structure that coordinates Ca^{2+} ions; TM, predicted transmembrane domain; S, serine-rich domain; N, asparagine-rich domain; Q- glutamine-rich domain. J, co-crystal structure of RPGR RCC1-like domain (RLD) and the RPGR-interacting domain (RID) of RPGRIP1. RPGR-RLD forms a seven-bladed propeller, each consisting of four anti-parallel β -strands (Waetzlich et al. 2013).

RPGRIP1-RID consists of an eight-stranded antiparallel β -sandwich. Several mutations associated with XLRP are located at the RLD interface with RID (Remans et al., 2014).

Author Manuscript

Author Manuscript

Author Manuscript

Author Manuscript